TAMPEREEN TEKNILLINEN YLIOPISTO
TAMPERE UNIVERSITY OF TECHNOLOGY

JONI GRÖNHOLM

EQUAL CODED DIGITAL HYDRAULICS IN LOW TEMPERATURES USING WATER-GLYCOL SOLUTION

MSc. Thesis

Examinor: Adjunct Professor Matti Linjama
Examinor and topic approved by the Dean of the Faculty of Engineering Sciences on 2nd of May 2018

ABSTRACT

JONI GRÖNHOLM: Equal coded digital hydraulics in low temperatures using water-glycol solution

Tampere University of Technology
Master of Science Thesis, 93 pages, 2 Appendix pages
September 2018
Master's Degree Programme in Automation Technology
Major: Fluid Power Automation
Examiner: Adjunct Professor Matti Linjama

Keywords: equal coded digital hydraulics, water-glycol, propylene glycol, arctic temperatures, multi-valve pulse width modulation, multi-valve pulse frequency modulation

In this thesis work, effects of arctic temperatures for digital hydraulic system was researched. Hydraulic medium was environmentally friendly and additive free 50 wt% water-glycol solution. Dynamics of on/off valves, steady-state properties of on/off valves and system's hydraulic natural frequency were qualities under inspection. These qualities were chosen as they are key qualities for digital hydraulics. On the other hand, this research was conducted to determine usability of commercially available on/off valves, when controller applying multi-valve pulse modulation and multi-valve pulse frequency modulation is used. Another objective was to find out, which method might be preferable to compensate the changing properties of system to accuracy of control.

Research was conducted as simulation and experimental study. Simulations were minor part of the research and were performed to validate the implemented controller. Experimental study was done using a hydraulic system that composed of equal coded digital valve system and a hydraulic cylinder that was used to move a mass in horizontal direction. Experimental research can be separated to two different parts. In first part, changes in system properties were investigated in temperature interval of -20°C…30°C. Second part of the experimental research was testing the controller in different temperatures. Controller was tested with three different cylinder strokes (15 mm, 150 mm and 300 mm) in three different temperatures (-20°C, 0°C and 30°C).

Results of this research indicate that dynamics of on/off valves slows down and volume flow in steady-state conditions decrease in low temperatures. Hydraulic natural frequency of the system increased in low temperatures. Results attained using the controller were comparable to results achieved in reference study. This indicates that commercially available valves are usable in multi-valve modulation control. In addition, results attained in low temperature using the controller suggest that correct way to increase control accuracy in low temperatures is to compensate slowing dynamics of valves.

TIIVISTELMÄ

Joni Grönholm: Equal coded digital hydraulics in low temperatures using water-glycol solution
Tampereen teknillinen yliopisto
Diplomityö, 93 sivua, 2 liitesivua
Syyskuu 2018
Automaatiotekniikan diplomi-insinöörin tutkinto-ohjelma
Pääaine: Fluid Power Automation
Tarkastaja: dosentti Matti Linjama

Avainsanat: tasakoodattu digitaalihydrauliikka, vesiglykoli, propyleeniglykoli, pakkaslämpötila, moniventtiilipulssinleveysmodulointi, moniventtiilipulssintaajuusmodulointi

Diplomityössä tutkittiin muutoksia digitaalihydraulisessa järjestelmässä pakkaslämpötiloissa. Hydraulinesteenä käytettiin ympäristöystävällistä ja lisäaineetonta 50 m-% vesiglykoli seosta. Tarkkailtavat ominaisuudet olivat on/off-venttiilien avautumis- ja sulkeutumisdynamiikka, vakiintuneen tilan virtausominaisuudet ja järjestelmän hydraulisen ominaistaajuus. Tarkkailtavat ominaisuudet määrittyivät digitaalihydrauliikalle tärkeimpien ominaisuuksien perusteella. Toisaalta työssä tutkittiin myös kaupallisesti saatavien on/off-venttiilien sopivuutta moniventtiilipulssinleveysmodulointi- ja -taajuusmodulointiin perustuvaan säätöön. Tavoitteena oli myös selvittää miten lämpötilasta johtuvia muutoksia olisi järkevintä yrittää kompensoida järjestelmän säätötarkkuuden parantamiseksi.

Tutkimus koostui simulointi ja kokeellisesta tutkimuksesta. Järjestelmän mallintamisen ja simuloinnin tavoite oli todentaa järjestelmän säätimen toiminnallisuus. Kokeelliset tutkimukset tehtiin hydraulijärjestelmällä, joka käytännössä koostui tasakoodatusta digitaaliventtiilistöstä ja hydraulisylinteristä, jolla liikutettiin massaa vaakatasossa. Kokeellinen tutkimus voidaan jakaa kahteen osaan. Ensimmäisessä osassa tutkittiin aikaisemmin mainittujen järjestelmän ominaisuuksien muutoksia lämpötilavälillä -20°C…30°C. Toinen osa kokeellista tutkimusta oli moniventtiilimodulointiin perustuvan säätimen testaus eri lämpötiloissa. Säädintä testattiin kolmella eri sylinterin iskunpituudella (15 mm, 150 mm ja 300 mm) sekä kolmessa eri lämpötilassa (-20°C, 0°C ja 30°C).

On/off-venttiilien dynamiikka hidastui ja virtaus venttiilin läpi pieneni lämpötilan laskiessa. Hydraulijärjestelmän ominaistaajuus nousi matalissa lämpötiloissa. Säätimellä saadut tulokset 30°C olivat täysin vertailukelpoisia referenssinä käytettyyn tulokseen. Tämä viittaa siihen, että kaupallisesti saatavat on/off-venttiilit ovat käyttökelpoisia moniventtiilimodulointiohjauksessa. Lisäksi matalissa lämpötiloissa tehtyjen säätimen testien perusteella, paras tapa parantaa säätötarkkuutta vaikuttaa olevan hidastuvan dynamiikan huomioonottaminen.

FOREWORDS

Study conducted in this thesis work was made for Laboratory of Automation and Hydraulics in Tampere University of Technology. Appreciations to Matti Linjama and Lauri Siivonen for giving this opportunity and for their effort in executing this thesis work. Neither should be forgotten Miika Paloniitty, who gave his valuable time to debug the controller. Nor should be underestimated the valuable advices during experimental work given to me by Jyrki Tammisto. Also, the effort made by the staff of heavy laboratory 3 should be noted to troubleshoot the never-ending problems of the experimental system. Learnings while conducting this study gave me a lot for the future. Likely, there would not have been any better place to conduct this research and finishing up my Master of Science thesis. Eventually, everything ends and so did this thesis work.

In Tampere, 25.9.2018

Joni Grönholm

CONTENTS

TABLE OF FIGURES

1. INTRODUCTION

Mineral oil has been firmly associated with hydraulic power transmission for hundred years. Mineral oil has many good qualities like high viscosity, anti-corrosiveness and relative cheapness, which explain its wide usage as a hydraulic medium. To balance its good qualities, mineral oil also has its drawbacks. Main drawbacks of mineral oil are that it provides fire hazard and is an environmental waste. In these times of environmental concern, drawbacks of mineral oil impose a demand for cleaner alternatives.

Self-evident environmentally friendly alternative fluid is water. Water is cheap, widely available and non-flammable. Naturally, water has its drawbacks as hydraulic medium when compared to mineral oil. Perhaps main drawbacks are low viscosity, corrosiveness and its ability to sustain microorganisms. Water and water-based hydraulic fluids have been used in industry to provide fire resistance and non-toxicity, but drawbacks mentioned earlier set extra challenges for the system itself and maintaining it. These challenges have prevented water to become widely used hydraulic medium except for specific fields. Although, water might make its breakthrough as common hydraulic medium as environmental aspects become more vital.

For this research, one of water drawbacks is raised to center of attention. Water has high freezing point, which prevents water hydraulics to be used in areas where subzero temperatures are in concern. This is especially problematic for mobile hydraulics, which are not only used but, in many cases, also stored in subzero temperatures. Therefore, a water-glycol solution is interesting alternative to pure water as glycol lowers freezing point of the solution and, if the glycol is chosen carefully, should not impose environmental hazard. Propylene glycol is relatively non-toxic and biodegradable, which makes it interesting fluid in environmental point of view.

Digital fluid power or digital hydraulics is an interesting alternative to more traditional analogues hydraulics. Aim behind digital hydraulics is to simplify physical hydraulic system and transfer complexity to control software (Linjama et al. 2003). For example, analogues proportional or servo valves are replaced with simple on/off valves that are connected in parallel. Now, rather than controlling volume flow through valve with spool displacement, volume flow is controlled with opening and closing valves. Digitalization of hydraulics can be applied to every area of hydraulics, but in this research, interest lies in valves. An interesting question arouses from the sizing of the parallelly connected valves. Two extreme sizing methods, that all the integer multiplications of smallest volume flow are still realizable, are sizing valves in binary series or equally. Sizing valves in binary series utilizes least number of valves while sizing equally utilizes the greatest

number of valves. Sizing valves equally is in many ways superior in performance compared to binary sizing but need for large number of valves consumes space and increase expenses. This was at least the case with traditional way of controlling digital valve systems. A new control method might prove the need for large number of valves in equal sized valve systems to be an overestimation.

Paloniitty & Linjama (2018) introduced multi-valve pulse width modulation control method for equally sized digital valve system. Idea is to open and close valves during a control cycle to realize decimal values of opened valves rather than just even numbers. They also used multi-valve pulse frequency modulation to improve controller's performance in low control values. Obtained results were reported to be considerably better than using traditional control or in reference study using binary sized valve system.

This research investigates the effects of low temperatures to a digital water hydraulic system. To be able to conduct the research in arctic temperatures pure water cannot be used as hydraulic medium. Water is mixed with propylene glycol to decrease freezing point enough for hydraulic medium to be usable in arctic temperatures. Siivonen et al. (2005) researched effects of low temperatures on digital valve system and proportional valve, although they used mineral oil as hydraulic medium. They observed decrease in flow rates and slowing in valves' dynamics in arctic temperatures. These results are most likely something to be observed also when water-glycol solution is used as hydraulic medium. Simultaneously this research observes the usability of water-glycol solution without additives while using parts intended for water hydraulics. Additives are used in commercially available water-glycol hydraulic fluids to alter their properties closer to mineral oil.

Second interest of this research is in the control method of Paloniitty & Linjama (2018). The research was conducted using fast protype valves, which are not commercially available. This leaves question open if the control method is applicable to slower but commercially more available on/off valves. In this research, slower and commercially available on/off valves are used to determine feasibility of the new control method. Results of Linjama & Vilenius (2005) are used as reference in evaluating the performance. Linjama & Vilenius used in their research a binary coded digital valve system with same on/off valves that are used in this research. Simultaneously, effects of low temperature on performance of the control method is investigated. Aim is to identify if the changing properties of system could be compensated and performance increased in low temperatures.

This thesis work is structured in following way: In second chapter, first a look to the field of water hydraulic is given. Then a closer look to the water, propylene glycol and water-propylene glycol solution concentrating in their physical and chemical properties is taken. Third chapter presents the field of digital fluid power concentrating on digital valve systems. Fourth chapter explains theory behind this study. Physical phenomenon and equations governing the experimental system and controller are explained in theoretical level.

Fifth chapter introduces to the simulation model that was implemented using equations of fourth chapter. Simulation model was implemented for testing of controller and some simulations to prove the implementation's validity are given. Sixth chapter presents experimental system used in the measurements. Measurements of the characteristics of the system are in seventh chapter. These measurements include hydraulic natural frequency of the system, on/off valves' dynamics and steady state flow characteristics in different temperatures. Eight chapter contains trajectory measurements of the experimental system using the controller introduced by Paloniitty & Linjama. Also, these measurements were done in multiple temperatures. This is followed by the concluding conclusion of this thesis work.

2. WATER AND WATER-GLYCOL AS HYDRAULIC MEDIUMS

The main motivation for using water based hydraulic fluids in industry has been fire resistance (Koskinen & Aaltonen 2014). Water based hydraulic mediums can be separated to three different categories determined by International Organization for Standardization (ISO): HFA, HFB and HFC (Trostmann 1996). HFA or oil-in-water emulsion that typically contains over 80% of water, while rest of the emulsion is mineral oil and additives. HFB or water-in-oil emulsion, in which mineral oil and other flammable ingredients typically comprise 60% of solution and rest of the emulsion is water. HFC or water-glycol solution that typically consists of about 35% water and rest of the solution is some glycol and additives. Fourth brand, although not categorized by ISO, is pure water as hydraulic medium. Naturally, water can be further divided to tap, sea, distilled and de-ionised water. In this research, interest lies in tap water.

Interest of this work is in sustainable fluids. Therefore, HFA and HFB fluids are not in interest of this research as they contain mineral oil and are used to improve fire resistance rather than for environmental reasons. Pure tap water is interesting choice for environmentally sustainable hydraulic medium but has some physical properties that decrease its value as such. For this research, the main downfall is the high freezing point, which prevents the usage of water in sub-zero temperatures. This leads to the conclusion to use water-glycol solution for this research. A pure mixture of tap water and a glycol was decided to be used, because commercially available HFC fluids contain additives. Additives were seen to hide a risk of environmental unfriendliness and increase uncertainty in generalizing results of the research. Propylene glycol was chosen to be used as glycol in solution, because of its non-toxicity and biodegradability, which are dealt more closely later. Additionally, Trostmann (1996) lists non-water based environmentally friendly hydraulic fluids such as HPG (polyglycols), HTG (vegetable oils) and HE (synthetic esters), which might have been interesting alternatives for this research. These fluids were rejected, because a decision to limit the research to water-based fluids was done.

Next, closer look to water hydraulics and water's physical properties compared to oil is given. This is followed by inspection of propylene glycol's physical properties and motivation of the selection of it as glycol for this research. Last part of this chapter is examination of physical properties of water-propylene glycol solution.

2.1 Water as hydraulic medium

Trostmann (1996) lists as main benefits of water as a hydraulic medium low pressure losses, availability, low cost and leakages or disposal of used fluid do not present fire

hazard or pollution. Koskinen & Aaltonen (2014) adds to this list overall energy and cost efficiency of total supply chain of tap water when compared to supply chain of mineral oil. As main disadvantages Trostmann gives corrosiveness, poor lubrication quality and limited range of working temperatures. Additionally, scarce supply of water hydraulic parts seems to be a major limiting effector for water hydraulics. Koskinen & Aaltonen complain about the lack of wide variety of variable-displacement axial-piston pumps, while Paloniitty (2016) comes to the conclusion that water hydraulic control valves are not common in the market. Benefits and disadvantages can be explained through examination of physical and chemical properties of water.

Density of water is 1000 kg/m^3 in temperature of 0°C and it decreases to 955 kg/m^3, when temperature increases to 100°C. Previous statement is true with atmospheric pressure. Increase in pressure has also an effect to density. Increase is 4%, when pressure rises from atmospheric pressure to 1000*atm and water temperature is 50°C. If the density of water is compared to mineral oil's (Shell Tellus S3 M 32 - Tuotetiedot) density 855 kg/m^3, when oil is in temperature of 15°C, it is evident that water is more dense than mineral oil. Higher density is a disadvantage, because higher density results in higher pressure peaks and flow friction losses. Although, flow friction losses for water are minor compared to mineral oil, because of considerably lower viscosity.

Kinematic viscosity or internal friction of water stays close to constant in temperature interval 0°C …100°C. Kinematic viscosity decreases from 1.7 cSt to 0.3 cSt (Trostmann 1996), while mineral oil (Shell Tellus S3 M 32 - Tuotetiedot) has drastic change from 324 cSt to 5.5 cSt in the same temperature interval. Therefore, water can be stated to have considerably lower viscosity than mineral oil. Kinematic viscosity changes also as a function of pressure, but similarly to temperature the change is rather minor for water. In pressure interval of 1…1000*atm the kinematic viscosity changes from 0.6 cSt to 1.1 cSt, when water temperature stays constant at 50°C (Trostmann 1996). The low viscosity of water has multiple effects from hydraulic point of view. Lower kinematic viscosity that water flows with less friction, which means lower pressure losses in pipe flow. This allows usage of higher flow velocities or in other words smaller pipes and hoses than with oil hydraulics. Downside of the lower kinematic viscosity is that water leaks through smaller gaps than oil. Conrad (2005) claims that gaps in water hydraulic system should be sized with factor of 0.32 to reduce leakage flow to same level as with oil hydraulics. Another downside of the low viscosity is the poor lubrication qualities of water. Poor lubrication requires smooth surfaces to prevent excessive wear.

Bulk modulus of water behaves rather strangely as a function of temperature, according to Koskinen (2004). Bulk modulus is 2 GPa at temperature of 0°C. Bulk modulus increases until to temperature of 50°C peaking in value 2.4 GPa. After this bulk modulus decreases as temperature increases ending back to value 2 GPa in temperature of 100°C. According to Koskinen mineral oil behaves differently starting from value 2.7 GPa and decreasing to value 0.3 GPa in the same temperature interval of 0…100°C. Pressure has

slight effect on bulk modulus. In pressure interval of 1…700*atm, bulk modulus of water increases form 2.2 GPa to 2.25 GPa, when water temperature is 20°C. Similar change happens to mineral oil. Water has higher bulk modulus than mineral oil in operating temperatures. This makes water hydraulic system stiffer, which allows faster control but increases pressure peaks.

Thermal conductivity of water is 5-6 times that of mineral oil (Koskinen 2004). In addition, thermal conductivity of water slightly increases as temperature increases while mineral oil's thermal conductivity stays constant. Higher thermal conductivity is an advantage, because it improves cooling of the system. Furthermore, water's specific heat is twice the value of mineral oil's specific heat (Conrad 2005). This is yet another advantage as water can absorb more heat than mineral oil, which reduces warming problem.

Cavitation can occur by two different ways: Either air bubbles dissolved to fluid or vapor bubbles of fluid itself are formed after pressure drop. Air dissolves to water poorly compared to mineral oil, because of higher density (Trostmann 1996). Therefore, air bubbles as reason for cavitation is not as much of a problem as is the case for mineral oil. Cavitation risk comes from water vapor, because water has high vapor pressure. This practically limits the maximum temperature of water to 50°C in hydraulic applications (Trostmann 1996). In this temperature, water's vapor pressure is 0.12 bar, which is high compared to vapor pressure of mineral oil's value 10^{-8} bar.

Chemical properties of tap water, mainly corrosiveness, is something to consider also. Hydrogen-ion concentration or pH value should be above 6.5 (Trostmann 1996) as lower values are symptom of acid formation and might cause corrosion. Although, also higher minimum pH values are presented. Skoog (2016) claims that minimum value pH 8 should be maintained with water-based hydraulic fluids. Chloride-ion content should not be above 200 mg/l, because it might cause corrosion even to stainless steel (Trostmann 1996). Hardness of water should stay in interval of 5…10 °d to prevent lime formation (Trostmann 1996). Lime starts to form in walls of pipes in temperatures above 50°C, which is another reason not exceed the temperature limit imposed by cavitation risk.

Microorganisms poses a unique problem for water hydraulics compared to mineral oil hydraulics. Microorganisms has negative effects to environment through leakages and to hydraulic system itself by coating the inner parts of the hydraulic system causing corrosion (Trostmann 1996). Risk of microorganisms can be reduced by preventing contamination particles and nutrition entering to the system.

2.2 Propylene glycol

Propylene glycol or 1,2-propanediol is organic substance that is composed of chain of three carbon atoms and two hydroxyl groups that are attached to carbons 1 and 2. It is colorless, odorless and fully soluble to water.

Main motivation to use glycol in this research is to decrease the freezing point of pure tap water to allow water-based hydraulics to be used in sub-zero temperatures. Motivation to use propylene glycol rather than any other glycol comes from its non-toxicity (Fiume et al. 2012), biodegradability (Goode 1998; Toscano et al. 2013; Toscano et al. 2014), wide usage as an deicer and in industry. Although, contaminating groundwater with propylene glycol has a recognized risk of depleting oxygen, because biodegradation of propylene glycol demands excessive amounts of oxygen (Goode 1998; Toscano et al. 2013). Another risk from biodegradability is that decomposition products include acids (Veltman et al. 1998), which might advance corrosion in hydraulic system. In addition to lower freezing point, physical properties of propylene glycol have some further benefits and downsides, which are described next.

Density of propylene glycol is 1033 kg/m^3 at 25°C (Curme 1952). Density of propylene glycol is therefore higher than of water. This is a disadvantage of hydraulic point of view as stated earlier. Although, the difference is only few percent and not a drastic one.

Kinematic viscosity of propylene glycol is 1640 cSt at -20°C (Curme 1952), 230 cSt at 0°C (Curme 1952) and 7 cSt at 65°C (George & Sastry 2003). Both references (Curme 1952; George & Sastry 2003) state only absolute viscosities, but kinematic viscosity can be calculated from it by dividing it by density. Kinematic viscosity of propylene glycol can therefore be stated to be higher, which is advantageous from hydraulic point of view.

Bulk modulus of propylene glycol is 2.3 GPa at 25°C (George & Sastry 2003). One must consider that reference (George & Sastry 2003) does not include information of bulk modulus but value of speed of sound in propylene glycol. Speed of sound and density can be used to calculate bulk modulus using equation (17), which is introduced in chapter (4.2.2). Bulk modulus is on the same level as of water. Although, the bulk modulus behavior is like mineral oil in that it decreases as a temperature increases rather than increases.

Thermal conductivity of propylene glycol is about third and specific heat is about half of that of water (Curme 1952). This is disadvantageous as propylene glycol is worse medium in aspect of warming control.

Vapor pressure of propylene glycol is 0.99 mmHG or 0.0013 bar at 50°C (Curme 1952). This is considerably lower than vapor pressure of water at the same temperature. Therefore, propylene glycol should be cavitation resistant fluid for hydraulic use. Especially, when this is combined with the higher density of propylene glycol.

2.3 Water-glycol as hydraulic medium

Water-glycol or HFC fluids emerged as hydraulic fluids in the 1940's after concerns of fire hazard of mineral oil (Totten 2012). HFC fluids are commonly used in industry as

fire resistant hydraulic medium and even in some cases as hydraulic medium for mobile machinery for environmental reasons (Conrad 2005). Commercially available HFC fluids contain thickeners, antiwear additives and corrosion inhibitors to improve physical and chemical qualities for hydraulic use. This left some concerns for usage of pure water-glycol compound, because material compatibility charts were done for commercial HFC fluids. For example, in reference (Totten 2012) water-glycol is claimed to be compatible with multiple different metals but only when corrosion inhibitor is properly maintained. On the other hand, information from propylene glycol manufacturer The DOW Chemical Company was contradictory. In (Engineering and Operating Guide, 2008) DOW reports of corrosion test, in which corrosion to copper and brass imposed by water and separately by propylene glycol are similar. Materials are commonly used in water hydraulics. This is contradicted by DOW in (Guide to Glycols, 2003), in which DOW do not recommend usage of copper or brass with propylene glycol. In this research, parts intended for water hydraulic use were solely used.

Because the main motivator for using glycol in this research was to decrease freezing point of water below arctic temperatures, glycol to water ratio to be used was determined through freezing point. Testing infrastructure limited the arctic temperature to roughly -20°C. Therefore, propylene glycol content was decided to be 50 wt%. Freezing point of the solution is -31.7°. Next physical properties of 50 wt% water-glycol solution are given.

Density of 50 wt% water-glycol solution is 1038 kg/m^3 at 25°C (Curme 1952), which is higher than density of pure propylene glycol. In fact, density of aqueous propylene glycol solution peaks at around 70 wt% propylene content.

Kinematic viscosity of 50 wt% water-glycol solution is 73.0 cSt -20°C (Curme 1952), 17.3 cSt at 0°C (Curme 1952) and 1.74 cSt at 65°C (George & Sastry 2003). Both references (Curme 1952; George & Sastry 2003) state only absolute viscosities. From the values it is certain that properties of water dominate in viscosity, but viscosity is still considerably higher than with pure water.

Bulk modulus of 50 wt% water-glycol solution is 3.0 GPa at 25°C (George & Sastry 2003). One must consider that reference (George & Sastry 2003) does not include information of bulk modulus but value of speed of sound in propylene glycol. Bulk modulus is considerably higher than ones of water and propylene glycol.

Thermal conductivity of 50 wt% water-glycol solution is about half and specific heat is reduced about 15 % of that of water (Curme 1952).

Vapor pressure of 50 wt% water-glycol solution is 72 mmHG or 0.096 bar at 50°C (Curme 1952). Although, vapor pressure is lower than that of water, the reduction is rather small and does not able the usage of higher temperatures.

3. DIGITAL FLUID POWER

This section constitutes of introduction to digital fluid power, its history and main principles. Focus of the introduction is to the branch of digital valve systems. A closer look to different flow control techniques is given after the initial introduction.

Digital fluid power can be defined as hydraulic or pneumatic system with discrete valued components actively controlling an output of the system (Linjama 2011). This definition leaves some vague instances. Such as the so-called bang-bang control, as is implied by Linjama (2011), but definition seems to be good as it makes clear distinction between traditional and digital fluid power. Traditional fluid power components' values are continuous compared to digital fluid power, in which they are discrete.

The digitalization of hydraulics can be applied to all branches of hydraulics. Digital pump and motor systems can be applied by parallel connected pumps/motors (Heitzig et al. 2012) or by controlling individual pressure chambers of a pump/motor (Rampen 1992). These enable control of effective displacement of the pump/motor unit by changing the number of pumps/motors or number of pressure chambers connected to a system. Digital cylinders are realised by multi-chamber cylinders, in which cylinder consists of 3 or more chambers. Chamber pressures, inflows and outflows are controlled separately (Huova et al. 2010). Digital flow control is applied by parallel connected on/off valves or by a switching valve (Linjama et al. 2003). With parallel connected valves, flow is dependent on number of opened valves. In switching control, flow is controlled by opening and closing valve in high frequency. Basic concepts of controlling fluid flow through a valve are by controlling opening time of a valve or by controlling frequency of openings of a valve when the opening time is kept constant. Former control method is known as pulse width modulation (PWM) and latter one is known as pulse frequency modulation (PFM). Linjama (2011) also mentions digital hydraulic power management systems and linear transformers as digital hydraulic applications.

Linjama (2011) claims that main benefits of the digital fluid power compared to analogue fluid power to be more robust, simpler and reliable components, better performance due to faster valves, higher degree of programmability, unification of components due to characteristics' dependence on software rather than physical aspects and higher efficiency in pump, motor and transformer functions. On the other hand, downsides of digital fluid power are listed as noise and pressure fluctuation, durability of fast switching valves, physical size and prize of parallel connected systems and complicated control.

Digital fluid power using parallel connections is a rather new field of study of interest starting from the early years of 2000, although the principle is old. Linjama (2011) gives an example from late 19th century, in which multi-engine hydraulic power distribution

system's output power was managed by adjusting speed of the engines and by selecting the number of engines running concurrently. Bower (1961) introduced first real digital valve system that utilized parallel connected on/off valves. In his concept, fluid flow was controlled by opening right amount of parallel connected on/off valves, which were sized by binary number series. This fluid flow control method is nowadays known as pulse code modulation (PCM). What prevented adoption of the parallel connection principle at this time was the difficulty to effectively apply it without computers and on the other hand, inventions of analogues components namely servo and proportional valves and variable displacement pumps and motors (Linjama 2011). As the renewed interest in parallel connected on/off valves emerged in early 2000's, interest laid first in PCM (Linjama et al. 2003). Soon ideas of different kind of modulation occurred, namely pulse number modulation (PNM), in which parallel valves are sized equally (Linjama & Vilenius 2007).

Around the same time as first parallel connected digital fluid power system was introduced, research for switching or pulsation technologies emerged (Pollard 1963). Although, basic ideas of switching control were introduced and applied already in 18th and 19th centuries (Scheidl et al. 2005). The research of Pollard was motivated by innovations in the field of electronics and the aim was to produce hydraulic equivalents to electrical components. According to Scheidl et al. (2013) a fast switching valve is a hydraulic equivalent to an electrical transistor. Unlike parallel connection techniques, switching techniques were easier to implement, even with relay control (Scheidl et al. 2005). Therefore, industry applied switching techniques rather quickly. Automotive industry applied hydraulic switching techniques in anti-lock braking systems and in electrical fuel injection already in 1970's (Linjama 2011). Motivation for automotive industry at this point was fast response, robustness and low price compared to analogues valves. Anti-lock braking systems and electrical fuel injection systems are systems of low energy and small flow rates. Research for systems that are more traditional with higher energies and flow rates emerged in 90's (Scheidl et al. 2005). Research has since gone from mere fast switching valves to implementation of hydraulic converters that are equivalent to electrical converters (Scheidl et al. 2013).

For both branches of digital fluid power flow control technologies referred here, the same fact applies: wide acceptance and utilisation of them in industry has not yet happened. Some exceptions exist in addition to automotive industry and its usage of switching technology in low flow rate systems. For example, digital fluid power has been applied to train tilting systems (Fischer et al. 2015) and in multinip calender systems in paper industry (Digital Hydraulics 2016).

3.1 Flow control technologies' characteristics

Target is to give clear picture of different phenomena and different control techniques there are, concentrating on subjects that are in greater concern from point of view of this research.

First basic characteristics and practical solutions of switching technology is given, followed by parallel connection technology. After those, a look to some control techniques utilizing both is given ending up to control technique used in this research.

3.1.1 Switching technology

Switching technology bases on fast switching valves. Fluid flow through valve is controlled with quick opening and closing of a valve. This presents demand for the valve to be fast, which practically means that opening time of valve should be in order of milliseconds as is the case with anti-lock braking systems or even faster as is case with fuel injection systems (Scheidl et al. 2005). Perhaps the greatest characteristic of switching control is pulsation of volume flow through valve and pressure. These phenomena are depicted in figure (1)

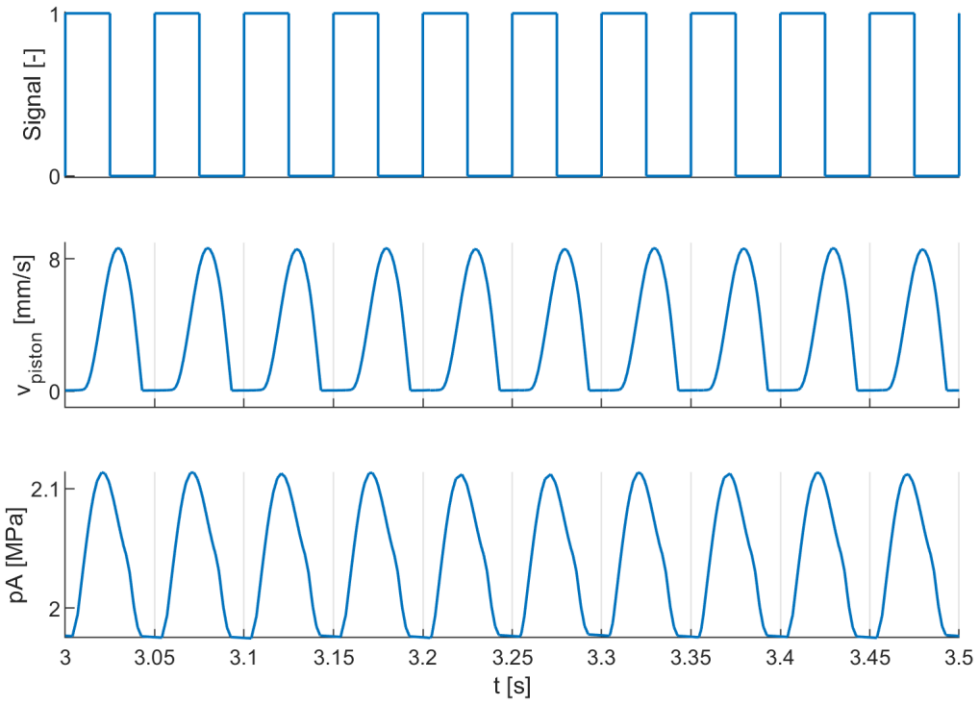

Figure 1. *Characteristical behaviour of switching control from a simulation of a cylinder system in which a switching valve is used to control volume flow to chamber A.*

Scheidl et al. (2013) claims that advantages of switching control, when compared to analogues control are simple components, easier control, better energy efficiency when using converter applications and generation of fast motions with relatively high loads. As challenges, he lists lack of suitable instruments, pulsation and noise as valve is constantly changing its state and developing control algorithms that give good control results, but that cope with pulsation phenomenon.

Different modulation methods for control signal of valve exist. Basic modulation methods are PWM and PFM. Schepers (2012) also lists inverted pulse frequency modulation

(invPFM), duty cycle frequency method (DFM) and optimized pulse modulation (OPM). All the modulation methods are applying in different ways equation of control period

$$T = t_i + t_p, \tag{1}$$

in which t_i is duration of pulse and t_p is duration of pause. For PWM, duration of period is constant. For PFM, duration of pulse is constant. For invPFM, duration of pause is constant. For DFM, duty cycle or t_i/T is constant and for OPM, duration of pulse is dependent on duration of pulse. OPM takes to account valve dynamics or varying closing time of valve with different pulse durations or widths. Valve opening and closing dynamics are examined more thoroughly in chapter (4.1.2). Interest of this research are PWM and PFM methods. Therefore, in figure (2) are depicted their behaviour as reference or duty cycle value changes.

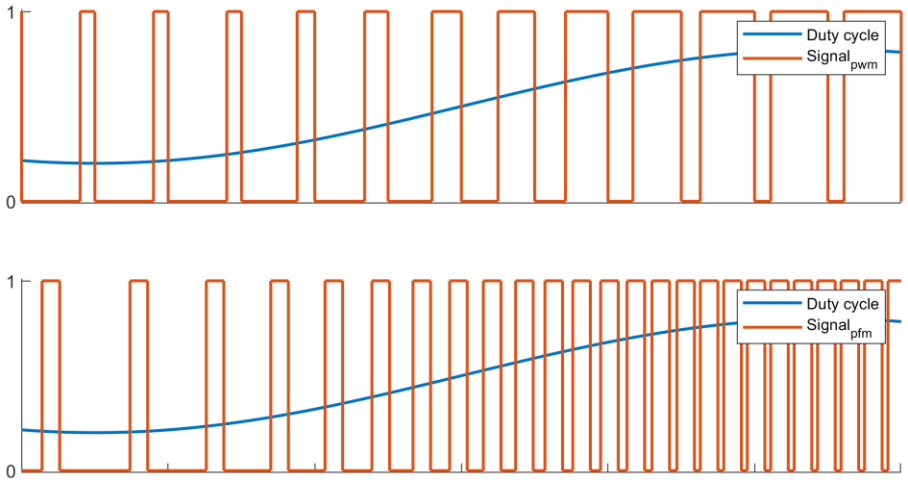

Figure 2. *PWM and PFM.*

One can see from figure (2) that as reference increases, pulse duration increases, but control period stays the same. In practice, PWM cannot be used in small or high reference values or duty cycle values, because valves have lag in opening and closing. Therefore, valve will not have time to react to changing signal values and stays either fully closed or fully opened. With PFM, pulse duration stays constant, but as reference increases duration of period decreases. In practice, PFM has also some limitation. With small duty cycles, the output becomes more unbalanced as duration of pause widens considerably longer than duration of pulse. With high duty cycles the same problem with valve's closing lag occurs that was limitation for PWM. Although, invPFM can be used to resolve this.

Practical solutions of switching control can be separated to two fields: Elementary switching and switching converters (Scheidl et al. 2013). There are no other components between switching valve(s) and actuator in elementary switching. For elementary switching the dominating parameter of performance is switching frequency, because of the lack of

extra dampers for pulsation. Elementary switching can be used at least in two modes. In one-way mode, either pressure line valve or tank line valve is switching depending on the desired fluid flow direction. In two-way mode, valves in both lines are switching, but in crosswise fashion. Two-way mode can be more energy efficient, if tank valve is scheduled to be open, when oscillation of actuator and pressure fluctuation allows medium to be sucked from tank line.

Switching converters have some extra components between valve(s) and actuator. Components between valve(s) and actuator are there to damp fluctuation and/or increase energy efficiency. Scheidl et al. (2013) lists four experimented converters: Wave converter, resonance converter, buck converter and motor converter. Pan & Plummer (2018) adds also flow booster and pressure booster. Because converters are not in interest of this research, more thorough investigation is not given.

3.1.2 Parallel connection technology

Parallel connected digital flow control bases on parallel connected on/off valves. One entity of parallel connected valves is called digital fluid control unit (DFCU). Number of opened valves determine fluid flow through a DFCU. Linjama (2011) describes DFCU to be equivalent to traditional two-way proportional valve with quantized output or flow rate. One DFCU is used to control one flow boundary. Therefore, multiple DFCUs are needed to successfully control actuator. A four-way proportional valve is realized with four DFCUs, which is depicted in figure (3).

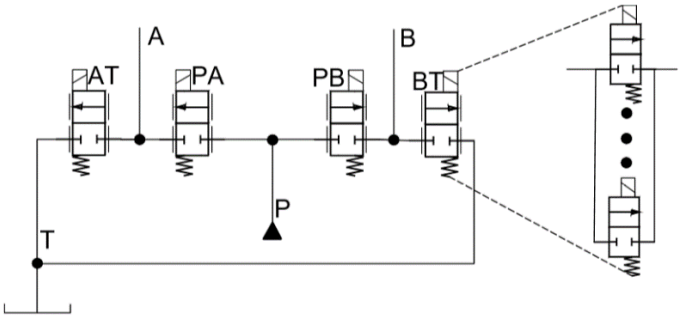

Figure 3. *Four-way digital valve system.*

Although, figure (3) depicts usage of four DFCUs, the number may differ depending on desired control boundaries. For example, Huova (2015) examined usage of fifth DFCU between actuator lines to improve energy efficiency of a cylinder system. Independent control of DFCUs allows control of not only flow rates but also pressure levels of chambers. Distributed nature of control allows different control modes. Different control modes differ from each other by which DFCUs are controlled. If two DFCUs are controlled in four-way digital valve, then modes are inflow/outflow and differential modes. In inflow/outflow mode pressure line is open to either of the actuator lines and other actuator line is opened to tank. In differential mode both pressure side DFCUs are opened

to allow flow between actuator lines. This improves energy efficiency, because need of flow from pump diminish. More modes can be applied with two DFCU control if suction from tank line is considered. Another way to add more modes is to control third DFCU. This allows sum flow control. Sum flow control is in interest of this research, because it was used by Linjama & Vilenius (2005), and the results of their research is used as reference in this research. In sum flow control inflow/outflow mode is altered that also DFCU between tank line and actuator line that is opened to pressure line is controlled. This results in crossflow, which means that part of the fluid flow from pressure line to actuator line flows straight to tank. This decreases energy efficiency but increases resolution of the four-way digital valve, especially in small control values. Resolution is ratio of total nominal flow rate of valve to largest step in nominal flow rates between states. Larger resolution means better controllability of valve.

Traditional way to control parallel connected digital hydraulic cylinder system is presented by Linjama (2007). Controller can be applied to both PCM and PNM control. The control method might be described to be a way to find an optimal opening combination of valves with PCM control or optimal number of opened valves with PNM control in a control cycle. Time of a control cycle is in vicinity of tens of milliseconds. First, motion controller is used to define closed loop velocity reference. Closed loop velocity reference composes of feedforwarded velocity reference and P-controlled position error reference. Other inputs of the controller are pressures of chambers and supply pressure. Chamber pressures are used to count steady state load force. Closed loop velocity reference, steady state load force and supply pressure are used to select the best mode to use in control cycle. Mode selection also determines pressure references. Mode and pressure references are used to determine search base for optimal control combination of valves. Model-based controller is used to numerically count steady state values of chamber pressures and velocity of cylinder for the control combinations of determined search base. Optimal control combination for opened valves is determined with cost function. Cost function can consider at least control combinations error between close loop velocity reference and steady state velocity, error between reference pressures and steady state pressures, power losses and switching of valves between different control cycles. The opening combination which has the lowest cost is the optimal control combination. This control method is computationally heavy, because different valve opening combinations for four-way digital valve that has five valves in each DFCU is over million. Search base determination reduces computational heaviness, because not all control combinations' steady state and cost calculations are done. Perhaps another problem with this control method is weighing of cost function components. There is no real analytic method to do it and leaves the weighing to be done by testing.

Two extreme coding methods of DFCU are binary and equal coding. Binary coding is applied by sizing valves of a DFCU in binary series (1:2:4:8…). This means that, if first valve's nominal flow rate is Q_n, then second valve's nominal flow rate is $2*Q_n$ and third

valve's is 4*Q_n and so on. Binary coding is extreme in that it utilizes least number of valves, but all the nominal flow rates that are integer multiplications of Q_n until to the maximum nominal flow rate of DFCU are realizable with different opening combinations Number of different states of binary coded DFCU is 2^n-1, in which n is the number of valves in DFCU. For example, DFCU with five valves has 31 states. Resolution is equal to state amount, because the maximum nominal flow rate is 31*Q_n and smallest flow rate step between states is Q_n. Disadvantage of binary coding is bad state transitions, which lead to pressure peaks (Laamanen et al. 2005). In bad state transition simultaneous opening and closing of valves occur. In ideal case this is not problematic, but with varying opening and closing times of valves transitions happen in different times. This creates uncertainty of effecting opening of the DFCU during transitions. In worst case scenario, transition to state of higher flow rate might even result for zero flow rate during transition. This creates unwanted pressure peaks. Pressure peaks can be avoided by using dampers, taken the bad state transitions to account in controller as a component in cost function or changing the coding method.

Equal coding is applied by sizing valves of a DFCU equally. Equal coding is extreme in a sense that it utilizes the greatest number of valves to gain certain amount of states and resolution. Number of different states and ideal resolution equals to number of valves. This means that to gain same controllability more valves are needed when compared to binary coding. For example, to get 31 states 31 valves are needed in an equal sized DFCU, when only five valves were needed with binary coding. Although, seemingly disadvantageous with the large number of valves, equal coding has some benefits over binary coding. Bad state transition can be avoided with equal coding, because change in flow rate is done by either opening or closing individual valves but never both simultaneously. Switching of valves, and therefore wear, can be distributed evenly between identical valves. Equal coding allows usage of PNM-control with traditional controller. Because PNM uses number of opened valves rather than opening combinations, which is the case with PCM-control used with binary coding, computational heaviness of traditional controller can be reduced. A concept of microhydraulics was introduced (Linjama & Vilenius 2007) to surpass the disadvantage of seeming need of large quantities of valves. Idea was to develop miniaturized valve that would have been simple and mass producible. Miniaturization would have made the valve small and mass production would make valve cheap. Therefore, large quantities of valves would not occupy too much space and would be monetarily cost-effective. Prototypes of miniaturized valves have been produced (Paloniitty et al. 2014). Although, results of equal coding with a new control method (Paloniitty & Linjama 2018) that combines parallel connection and switching control suggest that need of large quantities of valves in equal coding might be overestimation.

3.1.3 Combination of switching and parallel connection technologies

Digital hydraulic valve systems utilizing both parallel connections and switching have been researched (Huova & Plöckinger 2010; Paloniitty et al. 2015; Paloniitty & Linjama 2018). Aim of these researches have been to increase resolution of the system compared to pure PCM or PNM control. Although, resolution of pure PCM or PNM can be enhanced with crossflow, increase in energy consumption and computational heaviness makes alternative solutions intriguing.

Huova & Plöckinger (2010) researched improving resolution of binary coded four-way digital valve with four valves in a DFCU. Research combined PWM to PCM control. First the coding was modified from pure binary series to series of 1.25:2.5:3.75:7.5. This coding was better suited for intended control method. DFCU composed of two fast switching valves with 2 ms opening time and two slower valves with 10-12 ms opening times. Fast switching valves were sized to be the smaller ones in the series. Slower and larger valves were PCM controlled and other one of the fast switching valves was controlled with PWM and another with PCM depending desired opening of DFCU. Because PWM control method is not suitable for small or large duty cycles the resolution was further improved with crossflow. Reported result of the research was that ratio of maximum and minimum velocity of cylinder controlled with the digital valve was 350. This was compared to the result of Linjama & Laamanen (2005), with another 4x4 digital valve system utilizing PCM control with crossflow. The reported ratio was about 50. Therefore, PWM-PCM control was deemed to be promising way to increase control resolution. Although, this PWM-PCM control method has the same problem with computational heaviness, caused by numerical steady state calculations, as pure PCM control has.

Paloniitty et al. (2015) researched feasibility of PFM control for equally coded digital valve system to increase controllability in low velocities of an actuator. Digital valve was two-way and a DFCU had eight equally sized valves. Opening response time of valves were 1.5 ms. Control method was to open valves in turns using PFM signal. This would allow controllability in the whole DFCU opening range, because PFM signals to individual valves could overlap. Opening frequency was controllable parameter and it was determined using model-based controller. PFM was utilized only in small velocities and after certain frequency threshold controller utilized PNM control. The results of this control method were compared to results of pure PNM control with same system. Result was that maximum error with smallest stroke of cylinder decreased about 74%, but with larger strokes no significant change was noticed. (Paloniitty et al. 2015) Although, integrated square error (ISE) values decreased also with longer strokes, because PFM-PNM control allowed more accurate positioning of cylinder. Advantage of combined PFM-PNM was that increase in controllability was achieved without crossflow. On the other hand, fast

switching was distributed to multiple valves, which decrease wear of an individual valve, when compared to traditional switching control using only one valve.

Paloniitty & Linjama (2018) researched a way to improve resolution of equally coded digital hydraulic valve system using multi-valve PFM and PWM control, similarly to PFM control researched in PFM-PNM control depicted earlier. Multi-valve PWM was the main control method and the whole control range of DFCU was controllable with overlapping control pulses of individual valves. PFM control was utilized in small control values, because limitations of PWM in small duty cycles. PFM was used until control frequency increased to control frequency of PWM control. Model-based controller was utilized to determine desired opening of DFCU and the opening was then converted to PFM or PWM pulse. Digital valve was two-way, and it had eight equally coded valves in a DFCU. Results of the research were compared to PNM control with the same system. Results indicated clear increase in controllability of the system when multi-valve PFM-PWM control was used. Maximum position errors of cylinder with PNM control were over 0.7 mm with all three trajectories measured, but with multi-valve PFM-PWM control maximum position errors drop below 0.2 mm in all trajectories. Results were also compared to results of Linjama & Vilenius (2005), in which PCM control was used with crossflow for 4x4 valve system. Used performance indicator was ratio of maximum position error and maximum velocity of cylinder. Smaller number indicates better control performance. Paloniitty & Linjama claimed ratio of 1.7 (ms), and when it is compared to ratio of 5.3 (ms) of Linjama & Vilenius, the control method of multi-valve PFM-PWM seems promising. Advantageous of this control method is that computational heaviness of more traditional PCM/PNM is overcome, because numerical steady-state calculations are not utilized. Also, this control method indicates that good controllability with equal coding is attainable without enormous quantities of valves. This control method is utilized in this research. Paloniitty & Linjama used fast valves with opening response time of 2 ms. Interest in this research in multi-valve PFM-PWM control point of view is to examine feasibility of commercially more available slower on/off valves. More thorough investigation of controller is in chapter (4.5) and implementation of the controller using Matlab/Simulink is in chapter (5.1).

4. THEORETICAL BACKGROUND

In this section, a look to the theoretical background and physical equations governing the research are given. Physical aspects of this research are determined through properties of on/off valve and hydraulic cylinder and how their properties affect a hydraulic system. Third part of theoretical study to be conducted is the controller, which is utilizing physical properties of valves and cylinder.

Implementation of these equations and theories in modelling are explained deeper in chapter (5.2). Measurements done to explore some of the parameters and values of the test system are examined in chapter (7).

4.1 On/off valve

On/off valves have two states: open and closed or 1 and 0. This makes them simpler when compared them to servo or proportional valves, which have continuous values for states between −1…1. Although simple, they can be used to accomplish complicated and exact control, when used parallel or by implementing switching techniques, as depicted earlier.

Different types of on/off valves exist. Different types differ amongst other thing between flow rate and swiftness of opening. Needle valves were used in this research. Needle valves have a needle or rather a piston inside a cylinder that blocks flow orifice, when in closed position. Needle stays in place, because a returning spring pushes it to close position. When needle moves inside the cylinder to open position, flow orifice is opened, and fluid is free to flow through the valve.

Opening of valve is done with a coil, which is located around the cylinder. As current goes through the coil, a magnetic field emerges that projects a force to the needle. Therefore, the growth of current, as electric potential implements over the coil, has great impact on opening time of a valve. The growth of current can be made faster by using booster electronics. Booster's working principle is to use higher voltage at the start of implementation of electric potential. Therefore, the current in coil grows more rapidly and on the other hand, the magnetic force projected to needle grows more rapidly. Booster changes to the nominal voltage level of the coil after certain time interval concludes.

As mentioned earlier, on/off valves have two states. Interest lies in transition between these states and in the open state. Therefore, a closer look to flow model of orifice and opening and closing characteristics is next.

4.1.1 Flow model

Volume flow of fluid through valve is determined by viscosity and density of fluid, pressure differential over the valve and shape and size of the orifice of the valve. Further, phenomenon of cavitation choking occurs if outlet pressure is considerably smaller than inlet pressure in ratio. Effect of the phenomenon is that volume flow stays constant even if the outlet pressure decreases. Cavitation choking occurs only in valves that have long dominating orifice (Linjama et al. 2012).

In practical terms, flow through valve can be treated as flow through orifice. Basic equation for volume flow through orifice is

$$Q = K_v\sqrt{\Delta p}, \tag{2}$$

in which K_v is flow coefficient and Δp is pressure differential over orifice. The equation (2) does not count cavitation choking and in practice exponent of 0.5 of pressure differential is inaccurate. Therefore, more accurate model has been defined, which takes to account cavitation choking and differing exponents. The model is generalized exponent model and its equation group is

$$Q = \begin{cases} K_v(p_{in} - p_{out})^x, & bp_{in} < p_{out} < p_{in} \\ K_v[(1-b)p_{in}]^x, & p_{out} < bp_{in} \end{cases} \text{ (Linjama et al. 2012)}, \tag{3}$$

in which p_{in} is inlet pressure, p_{out} is outlet pressure, x is generalized exponent and b is critical pressure ratio or cavitation choking ratio. The equation (3) is here depicted to only positive volume flows. Equations for negative volume flow are similar, but they are not in interest of this research. Flow coefficient, exponent and cavitation choking ratio are determinable by measurements. Flow coefficient K_v comprises characteristics of fluid and shape and size of valve. Flow coefficient's equation is

$$K_v = \mu A\sqrt{\frac{2}{\rho}}, \tag{4}$$

in which μ is discharge coefficient, A is area of valve's orifice and ρ is density of fluid. Area of valve's orifice A stays constant. Density of fluid ρ changes as function of temperature and pressure but can be handled as constant. Throughflow factor μ in fact consists of two factors:

$$\mu = \varepsilon\varphi \text{ (Basniev et al. 2012)}, \tag{5}$$

in which ε is stream contraction coefficient and φ is velocity coefficient. Stream contraction coefficient ε is ratio of valve's orifice area and constricted fluid stream's smallest cross-section area. Smallest cross-section area of fluid flow locates after the orifice and

is therefore smaller than orifice's area. This is due to inertia of the fluid, which makes the fluid flow constrict even after the orifice (Basniev et al. 2012).

Velocity coefficient is ratio of ideal flow velocity and real flow velocity. Velocity coefficient is determined to be

$$\varphi = \frac{1}{\sqrt{\alpha+\zeta}} \text{ (Basniev et al. 2012),} \quad (6)$$

in which α is correction factor for non-uniform velocity distribution in flow and ζ is local resistivity factor. Velocity coefficient and stream contraction coefficients are not independent from each other and they vary as function of Reynold's number. Basic concept is shown in figure (4).

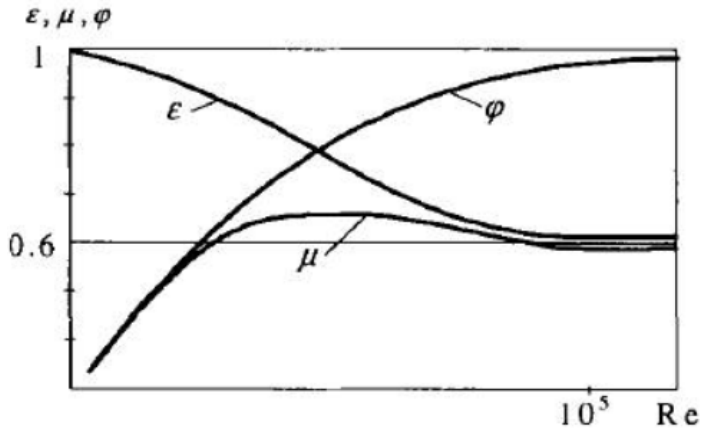

Figure 4. *Discharge, stream contraction and velocity coefficients as function of Reynold's number (Basniev et al. 2012).*

As one can see from figure (4), discharge coefficient is constant in only large Reynold's numbers. As Reynold's number decreases discharge coefficient first gets larger values before starting to decrease towards zero. Reynold's number is defined with equation

$$Re = \frac{v_f L}{\nu}, \quad (7)$$

in which v_f is velocity of fluid flow, L is characteristic linear dimension and ν is kinematic viscosity. From equation (7), one can see that discharge coefficient is dependent on velocity of fluid flow and viscosity of fluid, if characteristic linear dimension is presumed to stay unchanged.

Although, flow coefficient K_v of valve is not tuneable, the flow through valve is tuneable by placing an external orifice in series with the valve. When an external orifice is set in series with valve the new flow coefficient $K_{v,tot}$ can be counted from equation.

$$K_{v,tot} = \frac{K_{v,1}K_{v,2}}{\sqrt{K_{v,1}^2+K_{v,2}^2}}, \quad (8)$$

in which $K_{v,1}$ and $K_{v,2}$ are flow coefficients of valve and orifice.

4.1.2 Opening and closing dynamics

Transition dynamics from open state to closed state or vice-versa is dividable to three phases: Lag, piston motion and settling (Schepers et al. 2011). The concept is illustrated in figure (5).

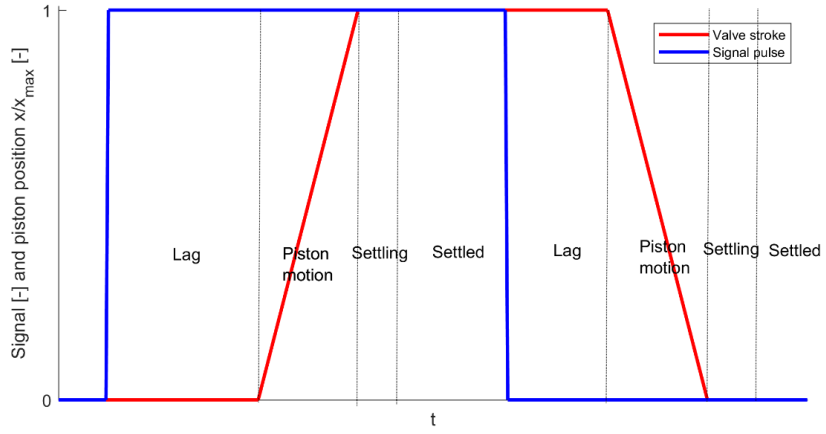

Figure 5. *Simplified concept of valve opening*

In figure (5), transitions from open to close and vice-versa are depicted to be symmetrical, but they can be asymmetrical. In addition, acceleration of piston is not visible. Time scale is in tens of milliseconds.

Lag of transition is the time that valve takes to react to opening or closing signal. No reaction in valve state is detectable, if signal pulse is shorter than the lag time.

In piston motion phase, piston moves from fully closed to fully open state or vice-versa. If signal pulse is shorter than the time it takes valve fully transition, but longer than lag time, the valve is in ballistic mode. In ballistic mode, change of volume flow through valve is nonlinear, if pulse width is altered. This is observable from figure (5), because if piston motion turns to other direction during motion, the area drawn between piston position and time axis is triangle. The area of triangle, if motions to both directions are symmetrical, can be counted from equation

$$A = t_b^2 \tan(\alpha), \tag{9}$$

in which t_b is time of signal during motion or t_{signal}-t_{lag}, and α is the angle between motion line and time axis. Equation (9) shows that area is function of pulse width in second order and therefore, change in pulse width effects to nonlinear change in area. Volume passed through valve is proportional to area between piston position and time.

Valve has fully opened or closed in settling phase but has not fully stuck or settled to its state. This makes the lag time of opposite movement to vary, if pulse width changes. This makes the change in volume flow to be nonlinear.

When valve has fully settled, the change in pulse width affects only to the wideness of quadrangle part of trapezium, without an effect to opening or closing phases. Therefore, change in volume flow through valve is linear, if pulse width changes. Linearity of volume flow is of interest as predicting behaviour in nonlinear zone is harder and more prone to changing situations.

To model the dynamics, Schepers et al. (2011) proposed a model that uses virtual ranges to model effects of lag and settling. The concept is depicted in figure (6).

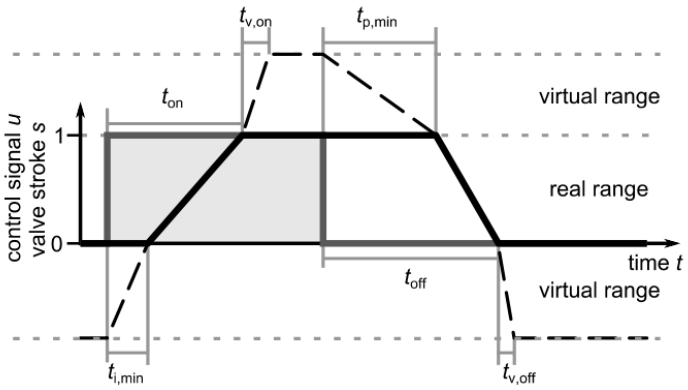

Figure 6. *Concept of model for valve dynamics (Schepers et al. 2011).*

Different times t are depicting times of same phenomena lag, piston motion and settling that were in figure (5). As one can see from figure (6), rather than modelling valve opening between 0…1 the model has values between −1…2. Naturally, only values between 0…1 are used as valve's state output. In practice, this can be done by integrating inverse number of time of phase. Which time of phase to use, depends on signal value and range, in which the integrated value is currently. Algorithm goes as follows:

1. If signal is 1 and
    a. If valve state is in virtual range -1…0, integrate inverse number of time of opening lag.
    b. If valve state is in real range 0…1, integrate inverse number of time of opening motion of piston.
    c. If valve state is in virtual range 1…2, integrate inverse number of time of settling of opening.
2. If signal is 0 and
    a. If valve state is in virtual range -1…0, integrate inverse number of complement of time of settling of closing.
    b. If valve state is in real range 0…1, integrate inverse number of compliment of time of closing motion of piston.
    c. If valve state is in virtual range 1…2, integrate inverse number of compliment of time of closing lag.

Output or value of real valve state is kept between values 0…1 by saturating the integrated virtual value to interval in question.

4.2 Cylinder

Cylinder is a hydraulic or a pneumatic actuator that transforms flow of medium to linear movement of a piston. Basic composition of a cylinder is that there are two chambers separated by a piston. Chambers are called A-chamber and B-chamber. A load is connected to the piston with a piston rod, which goes through the B-chamber. Therefore, as the piston moves the load moves. In the context of this research, cylinder is considered, as addressed above, to have two chambers, to be asymmetrical as piston rod is one sided and to be controllable to both directions of movement. One must consider that in other context a cylinder might be symmetrical, controllable to only one direction or have more than two chambers.

Cylinder can be used to create rotational movements by placing a cylinder between two separate links and connecting links with a rotational joint or by a gear that is rotated by the linear movement of a piston. The basic concepts of cylinder use are illustrated in figure (7).

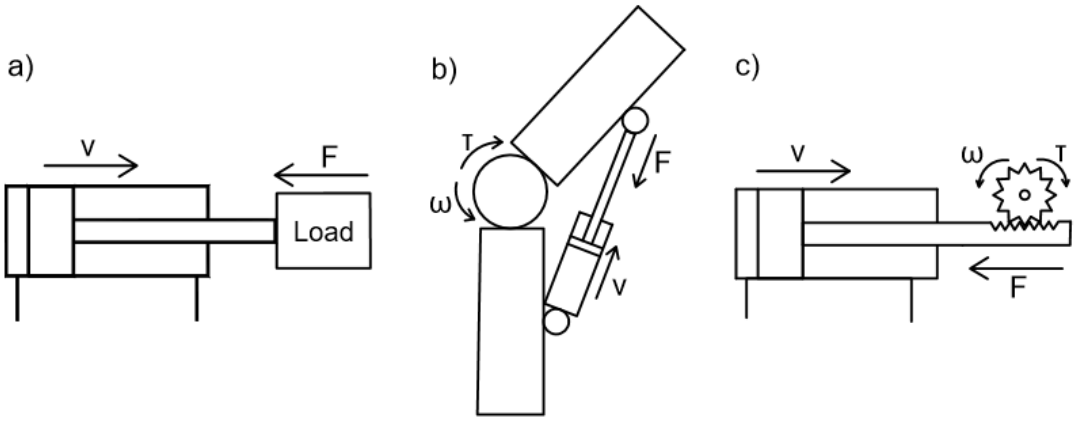

Figure 7. *Basic cylinder usage concepts. A) linear movement, b) rotational movement with two links and c) rotational movement with gear.*

In this research, interest lies in the linear movement depicted in the figure (2a). As can be seen from the figure (2a), the outputs from the system are velocity and force. Velocity is determined by fluid flows to the chambers and chamber pressures determine projected force to the load, then again friction of seals must be taken into account. Next, a closer look to the friction, chamber volume and pressure relation and finally ending up to the projected force equation.

4.2.1 Seal friction

In cylinders, seals are used to provide such film thickness that levels of friction, leakage and transition of contamination are all on acceptable levels (Bustos 1996). Seals are located between piston and cylinder bore and between piston rod and cylinder end. In cylinders, friction can be separated to three regimes: Static friction, boundary lubrication and hydrodynamic lubrication. The realms of these different frictions are determined by the thickness of lubricate layer between piston seal and cylinder bore, which in other hand is determined by relative velocity of the piston in a reference to the cylinder bore. As relative velocity increases thicker lubricate layer is generated between the sliding surfaces. Static friction regime occurs, when the relative velocity is zero, which means that there is no lubricate layer between surfaces. When the relative velocity is increased slightly from zero, a thin, only couple of molecules thick, lubricate layer is generated between the surfaces. This is the regime of boundary lubrication. In boundary lubrication, friction is determined by chemical properties of surfaces and lubricant. As lubricant and surface material contacts, molecular adhesion occurs, and this creates protective layer of lubricant to the surface. Practically, the strength of these bonds determines the friction properties. When the relative velocity is increased more, the film gets thicker. This leads us to the regime of hydrodynamic lubrication. In hydrodynamic lubrication, fluid flow occurs between sliding surfaces, which completely separates the surfaces from each other. Therefore, the friction is determined only from the viscosity or inner friction of the fluid as it flows through the gap between surfaces. The different friction regimes are illustrated in figure (8).

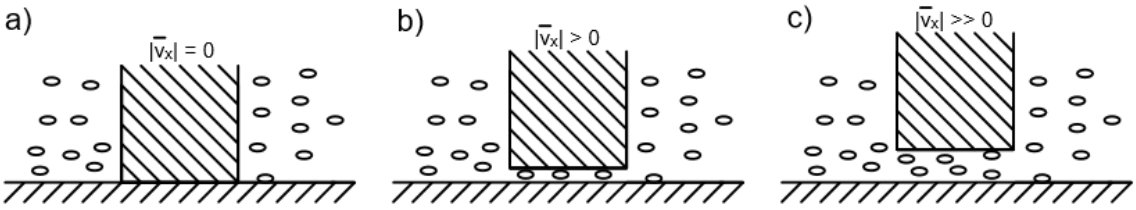

Figure 8. *Friction regimes. A) Static friction, b) boundary lubrication, c) hydrodynamic lubrication.*

Mathematically the friction force occurring between seal and cylinder bore can be expressed with an equation

$$F_\mu = \Psi * sign(v) * \left(F_c + (F_s - F_c) e^{-\left(\frac{v}{v_s}\right)^2} \right) + bv \text{ (Hyvönen 2015),} \qquad (10)$$

in which Ψ is pressure dependency, v is velocity of the piston, F_c is the Coulomb friction force, F_s is the static friction force, v_s is the Stribeck velocity or velocity of lowest friction force and b is the viscous friction coefficient. In the equation (10), first factor represents friction regimes of static friction and boundary lubrication, and the second factor represents regime of hydrodynamic lubrication. A plot of the equation (10) is in figure (9).

Used variables are arbitrary, but figure (9) illustrates the different regimes of friction as function of velocity. Only positive velocities and friction forces are shown. Therefore, one must consider that similar curve would emerge with negative velocities, but with complement friction force values.

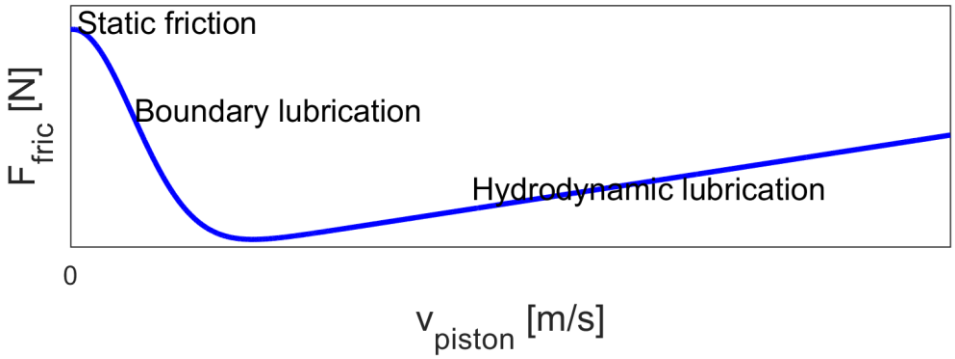

Figure 9. *Plot of friction force as a function of velocity.*

To get better model of friction occurring in cylinder, also bending of the seal must be considered. When a force that is smaller than static friction force is applied to the piston, it bends the seal, but the seal does not move in relation to the cylinder bore. When the applied force gets larger than static friction force, the seal is fully bended and starts to move in relation to the cylinder. The model is called dynamic friction model and it originates from study of friction between two surfaces (C. Canudas de Wit et al. 1995). In microscopic level, friction force between two surfaces can be modelled as bristles. When tangential force is applied to the them, they start to bend, until they are fully bended, and the surfaces starts to move in relation to each other. This model is here applied in macro level for seals. The dynamic model for friction is

$$F_\mu = \sigma_0 z + \sigma_1 \dot{z} + bv \text{ (Hyvönen 2015)}, \tag{11}$$

in which σ_0 is spring constant of the seal, σ_1 is damping coefficient of the seal, z is the bending of the seal and $\dot{z}$ is velocity of the bending of the seal.

New parameters can be either counted, measured or approximated. Value for spring constant σ_0 can be counted by either measuring or approximating maximum bending of the seal z_{max}. Now the spring constant is

$$\sigma_0 = \frac{F_S}{z_{max}}. \tag{12}$$

Damping coefficient can be either measured or approximated with formula

$$\sigma_1 = k * (\sigma_0 m)^{0.5}, \tag{13}$$

In which k is coefficient of value 0.5…2 and m is the inertial load of the cylinder. Velocity of the bending of the seal $\dot{z}$ can be counted with equation

$$\dot{z} = v - \frac{\sigma_0 |v|}{F_\mu^*} z, \tag{14}$$

in which $F_\mu{}^*$ is the friction force determined in equation (10), but without the viscous friction force factor bv.

4.2.2 Effective bulk modulus

Bulk modulus represents elasticity of fluid and mechanical parts under pressure. Elasticity of the system has a degrading effect on position and velocity control, because it causes resonance (Fonselius et al. 2006). The effective bulk modulus represents elasticity of a whole system. In it, elasticity of fluid and mechanical parts is considered by lumping them together by weighing the bulk modules of different elastic parts of the system with volume. Formula for effective bulk modulus is

$$\beta_e = \left(\sum_i^n \frac{V_i}{V_{tot}} * \frac{1}{\beta_i} \right)^{-1}, \tag{15}$$

in which n is the total amount of different elastic parts of the system, V_i is the volume of the part under inspection, V_{tot} is the total volume of the system and β_i is the bulk modulus of the part under inspection.

Although, the equation (15) is straightforward, one must consider that suspended air bubbles in the fluid and other uncertainties seems to make theoretical effective bulk modulus to be rather large. Trostmann (1996) gives as a rule of thumb, that estimated effective bulk modulus of the system equals to half of the calculated one.

The change volume because of elasticity of the system can be determined, as the effective bulk modulus is known. Formula of the change of volume because of elasticity of the system as a function of pressure differential is

$$\Delta V = \frac{V}{\beta_e} \Delta p, \tag{16}$$

in which V is the mean volume of compression and Δp is the pressure differential.

The effective bulk modulus has also connection to speed of sound of fluid in the system. Formula for speed of sound of the fluid of the system is

$$c = \sqrt{\beta_e / \rho}, \tag{17}$$

in which ρ is density of fluid. This formula is one way to clarify effective bulk modulus of a system or bulk modulus of a liquid, if the effect of the system to the effective bulk modulus is minimal.

4.2.3 Chamber volume and pressure

Chamber volumes of cylinder determines the location of a piston and the change of the volumes determine velocity of the piston. Naturally, this can be thought other way around. Change of the volume is determined by in and out flows of volume flow of fluid. If volume flow is larger than the change of chamber volume, then the fluid compresses or in other words, pressure rises. Therefore, state of equation for chamber volume can be written as

$$Q_{in} - Q_{out} = \frac{dV}{dt} + \frac{V}{\beta_e}\frac{dp}{dt}, \tag{18}$$

In which Q_{in} is volume flow of fluid into the chamber, Q_{out} is volume flow of fluid out of the chamber, V is the chamber volume, p is the chamber pressure and β_e is the effective bulk modulus. The equation (18) is rather simple to understand: if volume flow is larger into the chamber than out of it, then volume of the chamber grows. If the growth of volume is not as large as the volume flow of fluid, then pressure rises. For later use, the equation (18) can be rearranged to form of

$$\frac{dp}{dt} = \frac{\beta_e}{V}\left(\sum Q - \frac{dV}{dt}\right), \tag{19}$$

as the pressure differential is more interesting, because its integrated value leads to the force projected by the chamber.

4.2.4 Force equation of cylinder

Five forces are present when piston moves in cylinder: Force projected by pressure of A-chamber F_a, which always works towards positive direction. Force projected by pressure of B-chamber F_b, which always works towards negative direction. Friction force F_μ, which always works against direction of piston velocity. Load inertia F_{load}, which always works against acceleration. Fifth force is gravitational force of load, which is not interest of this research of horizontal trajectories. Therefore, it is neglected from this point onwards. Friction force was already defined earlier in equation (10) to be a function of velocity and pressures. Forces projected by chambers follows basic pressure formula

$$F = pA, \tag{20}$$

in which p is the pressure of the chamber and A being the area of piston. As was stated earlier, pressure differential in chamber follows equation (19) and pressure is got from it by integration.

Force projected by the inertia of the load follows the Newton's second law of motion

$$F = ma, \tag{21}$$

in which m is mass of load and a is acceleration of load.

The forces present in cylinder and their directions, when velocity is positive, are illustrated in figure (10).

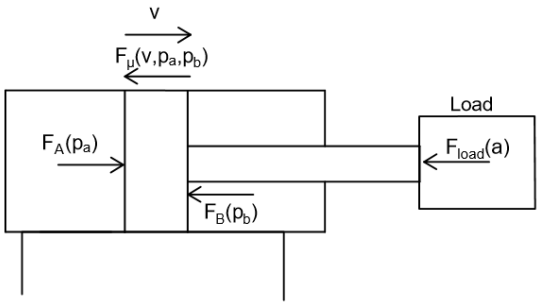

Figure 10. *Forces present in cylinder system when velocity is positive.*

The force equation of a cylinder can be written

$$F_A(p_A) - F_B(p_B) - F_\mu(v, p_A, p_B) = F_{load}(a), \tag{22}$$

and if equations (20) and (21) are placed

$$p_A A_A - p_B A_B - F_\mu(v, p_A, p_B) = m_{load} a, \tag{23}$$

On the other hand, formula (23) can be rewritten in form of

$$\frac{p_A A_A - p_B A_B - F_\mu(v, p_A, p_B)}{m_{load}} = a, \tag{24}$$

which reveals the true value of interest – acceleration of piston. Acceleration is quantity of interest, because its integrated value is velocity and velocity's integrated value is position. Equation (24) is defined as a function of piston velocity and chamber pressures. Now, one gets piston velocity by integrating the equation (24) itself and chamber pressures by integrating the equation (19), as was already stated earlier.

4.3 Hydraulic natural frequency

Hydraulic cylinder system corresponds to a mass that is connected to fixed points, in both sides of the mass, via springs. Mass reflects piston and load it is holding. Springs reflect compressible fluid columns in cylinder chambers and in hoses. The equivalence is depicted in figure (11), in which (11a) shows basic cylinder system and (11b) shows equivalent mass-spring system.

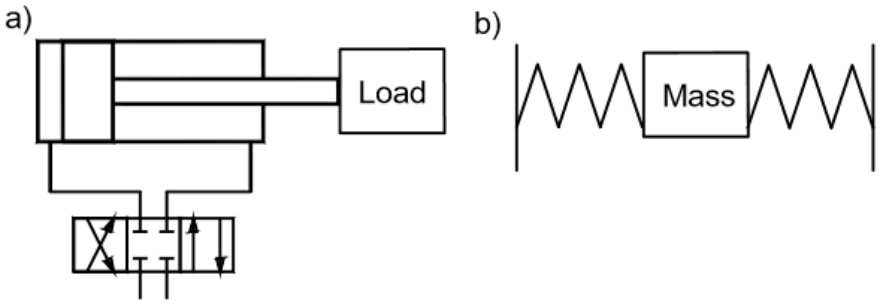

Figure 11. *Cylinder system's equivalence to mass-spring system.*

Hydraulic natural frequency is defined to be

$$\omega_h = \sqrt{\frac{k_{h,tot}}{m}} \text{ (Linjama 1996),} \tag{25}$$

in which $k_{h,tot}$ is a hydraulic spring constant of the system and m is a load of the system. One can predict from figure (11b), that in fact hydraulic spring composes of two springs in series: Fluid column in A-side of the cylinder and fluid column of B-side of the cylinder. Therefore, hydraulic spring constant of the system $k_{h,tot}$ can be written as sum of spring constants of separate sides

$$k_{h,tot} = k_{h,A} + k_{h,B}. \tag{26}$$

Spring constant of a hydraulic spring is defined by formula

$$k_h = \frac{\beta_e * A^2}{V}, \tag{27}$$

in which β_e is the effective bulk modulus of the system half under inspection, A is the piston area of the system half under inspection and V is the volume of the system half under inspection. If volume consists of cylinder's volume and volume of hoses, then the equation (27) can be rewritten

$$k_h = \frac{\beta_e * A^2}{xA + V_{hose}}, \tag{28}$$

In which x is the position of piston and V_{hose} is the volume of hose. One has to consider that equation's (28) volume of cylinder xA is only valid for A-side and for B-side the valid volume of cylinder is $(L\text{-}x)A$, in which L is the maximum stroke of the cylinder. Equation (28) can be now written to form of

$$\omega_h = \sqrt{\frac{\beta_{e,A} * A_A^2}{(xA_A + V_{hose,A})m} + \frac{\beta_{e,B} * A_B^2}{\big((L-x)A_B + V_{hose,B}\big)m}}. \tag{29}$$

Equation (29) is plotted for an asymmetrical cylinder in figure (12) as a function of piston position. Used parameters for figure (12) were arbitrarily chosen and figure (12) is merely depicting principle of changing value of hydraulic natural frequency.

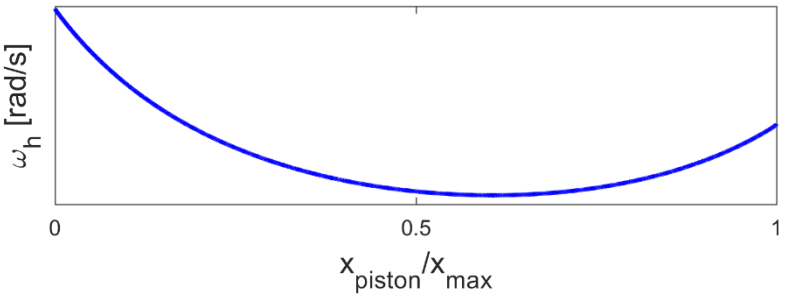

Figure 12. *Hydraulic natural frequency as a function of piston position.*

Figure (12) reveals that minimum hydraulic natural frequency seems to be slightly over half of the maximum stroke of the cylinder. Minimum value is interesting, because it is used in tuning of filtered P-controller.

4.4 Filtered P-controller

Filtered P-control is used to improve properties of conventional P-control by limiting high frequency gain using low-pass filter (Linjama 1998). Tuneable parameters are proportional gain K_p and time constant of filter τ. Low-pass filter is supposed to decrease gain near lowest natural frequency. This is achieved, if criterion $\tau >> 1/\omega_h$ is satisfied. Linjama (1998) gives as a rule of thumb that coefficient of 2…3 is a good compromise to satisfy the criterion, but not to slow down response of the system too much. Therefore, desired time constant can be determined from equation

$$\tau = \frac{3}{\omega_h}. \tag{30}$$

If the criterion defined earlier is satisfied, dynamics of the cylinder can be neglected. Open loop transfer function is approximately

$$G_{sys}(s) = \frac{K_p}{s(s\tau+1)}. \tag{31}$$

The unity feedback around $G_{sys}(s)$ produces a second order transfer function with a closed loop natural frequency

$$\omega_c = \sqrt{\frac{K_p}{\tau}}, \tag{32}$$

and damping factor

$\xi_c = \frac{1}{(2\sqrt{K_p \tau})}$ (Linjama 1998). (33)

A good value for damping factor to step-wise references is 0.7, but for smoother references, a lower value is suitable (Linjama 1998). For example, Paloniitty & Linjama (2018) used 0.58 as value for closed loop damping factor.

4.5 Equal coded multi-valve switching controller

Paloniitty & Linjama (2018) introduced digital hydraulic equal coded multi-valve switching controller. Controller utilizes mainly multi-valve PWM (MVPWM) control, but with small control values multi-valve PFM (MVPFM) is used. Block diagram of the controller is in figure (13).

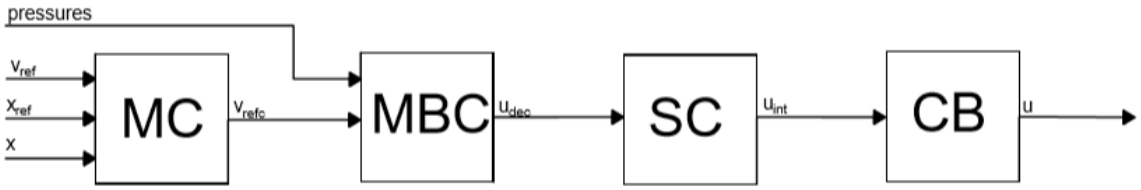

Figure 13. *Block diagram of controller*

In figure (13), MC stands for motion controller, MBC for model-based controller, SC for switching controller and CB for circular buffer. Controller inputs are pressures, position of actuator and trajectory reference of velocity and trajectory reference of position. Output of the controller is opening combination of valves of DFCUs. Controller is similar to traditional PNM controller. Both controllers utilize model-based controller to determine desired opening of DFCU. Dissimilarity comes from the fact that PNM numerically counts steady-state values of different states and is only able to determine integer values of DFCU states for control cycle. Multi-valve switching does not use numerical steady-state calculations and cost function, but rather calculates one steady-state calculation and transforms it to frequency or pulse width. Therefore, control values between integer values are also possible to realize with accuracy that depends on the sample time of the controller.

4.5.1 Motion Controller

Motion controller applies closed loop position control and open loop velocity control. Use of this kind of a motion controller in parallel connected digital hydraulics seems to be established and is used already by Linjama & Vilenius (2005). No clear explanation for this cannot be found, but feedforwarded velocity reference could be justified by the fact that velocity is the quantity under control and proportional position control improves accuracy. On the other hand, P-control of position is established control method with proportional and servo valves (Linjama 1996).

Motion controller's inputs are cylinder trajectory's position reference x_{ref} and trajectory's velocity reference v_{ref} and measured position of cylinder x. Output of the motion controller is closed loop velocity reference v_{refc}. Closed loop velocity reference is sum of velocity reference and position error Δx multiplied by proportional gain K_p. Position error is difference between trajectory's position reference and measured position. Therefore, closed loop velocity reference can be written to form of

$$v_{refc} = v_{ref} + K_p(x_{ref} - x). \tag{34}$$

If filtered P-controller is applied, then position error is low-pass filtered and equation (34) changes to form of

$$v_{refc} = v_{ref} + \frac{K_p}{\tau s+1}(x_{ref} - x). \tag{35}$$

Tuning of the parameters proportional gain K_p and time constant τ of low pass filter were introduced earlier in chapter (4.4).

4.5.2 Model-based velocity controller

Model-based controller's inputs are measured port pressures and closed loop velocity reference v_{refc}. Output of the controller is floating-point control value of desired DFCU openings. Controller's sample time is equal to duration of control cycle. Controller utilizes the flow model equation (3). In a control cycle, measured pressures are used as inputs for flow model to calculate prediction of flow rate through one valve and this is transformed to cylinder velocity by division with piston area. Then ratio between close loop velocity reference and predicted steady-state velocity is taken. This ratio is floating point control value or the decimal value of desired DFCU opening in a control cycle u_{dec}. Therefore, the floating-point control value can be written to be

$$u_{dec} = \frac{v_{refc}A_{cyl}}{Q_{ss}(p_{in},p_{out})}, \tag{36}$$

in which the A_{cyl} is piston area of A-chamber or B-chamber depending on which DFCU is under inspection. The floating point may have value from 0 to number of valves in DFCU. Parameters of flow model ergo flow coefficient K_v, exponent x and cavitation choking ratio b vary between individual valves of DFCU, but average parameter values of DFCU valves can be used to keep computational demand low. On the other hand, the logic to use multiple valves in row should diminish the effects of slight differences between individual valves.

One must consider that steady state calculation can be done only to DFCU of boundary of dominating chamber. This lowers the computational demand even more. Dominating chamber is the one which load force is projected. The floating-point control value of DFCU controlling recessive chamber can be calculated from control value of dominating

chamber by multiplication of piston area ratio of chambers. Alternating this ratio might be usable in controlling pressure levels of the system during motion.

4.5.3 Switching controller

Switching controller's inputs is the floating-point control value determined in model-based controller. Output is number of opened valves in DFCUs. Controller's sample time should be considerably smaller than duration of control cycle, because sample time of the controller ultimately determines resolution of system. Aim of the controller is to realize the floating-point control value using changing integer value during a control cycle. To accomplish that a virtual pulse width w_v that is the sum of time individual valves of a DFCU are open during a control cycle. Virtual pulse width can be calculated from frequency or period of control cycle

$$w_v = \frac{u_{dec}}{f_c} = u_{dec}T, \tag{37}$$

in which f_c is frequency of control cycle and T being period of control cycle. Equation (37) is valid only in case of symmetrical opening and closing of valve. Real valves have asymmetrical opening and closing. When closing takes longer, the realised pulse width would be longer than the virtual pulse width. The difference between closing and opening times is considered by using compensation parameter t_c. Compensation parameter can be determined with pulsation test of a valve. Compensation parameter t_c is positive, when closing takes longer. The virtual pulse width with compensation can be written in form of

$$w_v = \frac{u_{dec}}{f_c} - t_c = u_{dec}T - t_c. \tag{38}$$

The virtual pulse width and floating-point control value are used to determine two other parameters. Number of opened valves at the beginning of control cycle n_s and time of state transition of DFCU during control cycle t_i. State transition during control cycle is practically closing a valve of a DFCU to realize the decimal of the floating-point control value. Time of state transition during control cycle follows equation

$$t_i = w_v \, mod(T). \tag{39}$$

Number of opened valves at the start of control cycle is determined by Paloniitty & Linjama (2018) to be

$$n_s = floor(u_{dec}) + 1. \tag{40}$$

Problem with the equation (40) is that it does not take compensation for closing time t_c into account. Perhaps more generalized equation that includes compensation for closing time could be

$$n_s = floor\left(\frac{w_v}{T}\right)+1. \tag{41}$$

The concept and how the control values mentioned above behave are illustrated in figure (14) for two different control cycles. One must consider that u_{dec} is marked as u.

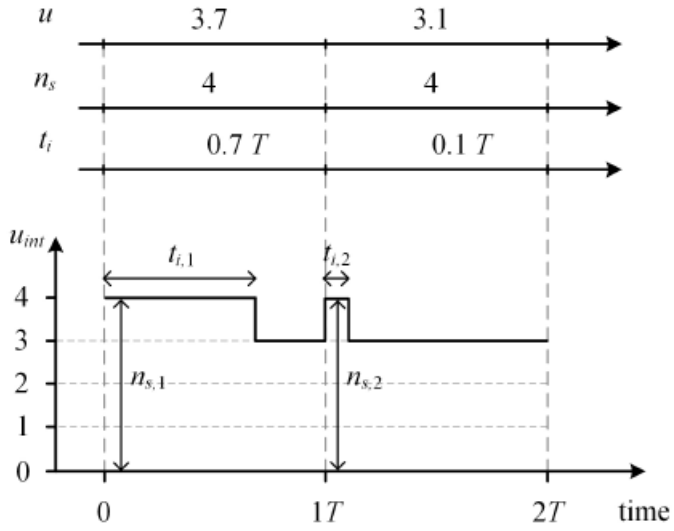

Figure 14. *Multi-valve PWM control example (Paloniitty & Linjama 2018).*

Compensation for longer closing is not regarded in figure (14). Further, one must acknowledge that the u_{int} value is number of opened valves and does not determine which valves are open. For example, in time $1T$ a valve is opened and after interval of $t_{i.2}$ another valve is closed. One must notice that opening and closing happen to different valves.

Above method for multi-valve PWM was adopted from Paloniitty & Linjama. Slight variation of it was used in this research. Rather than compensating the virtual pulse width w_v, compensation was made to state transition time parameter t_i

$$t_i = w_v \, mod(T) - t_c, \tag{42}$$

in which w_v is the uncompensated virtual pulse width of equation (37). In case $t_i > 0$ no change to former method is evident, but if $t_i < 0$ controller behaves differently. The pulse is reversed. This means that at the absolute value of state change interval a valve is opened rather than closed. Therefore, the number of opened valves at the start of control cycle can be written as:

$$n_s = \begin{cases} floor(u_{dec}) + 1, \; t_i > 0 \\ floor(u_{dec}) - 1, \; t_i < 0 \end{cases}. \tag{43}$$

After absolute value of state transition time parameter is due u_{int} value is set to $floor(u_{dec})$ for the rest of the control cycle. Benefit of this way to use multi-valve PWM is that real valve state transitions happen closer to time table of uncompensated symmetrical opening and closing. Downside is the method's slightly higher complexity.

Either of the methods cannot carry out simultaneous switching as such. Simultaneous switching should occur when $t_i = 0$ with accuracy of resolution. This needs to be considered separately in controller. In this research, an extra output is added, which is called vice-versa switch.

Multi-valve PFM is utilized with low control values, because of the dead band in PFM control. Pulse width of PFM w_f is set to same value as is the smallest pulse width of PFM. Desired frequency, in which closing time compensation is applied, of the multi-valve PFM is determined using equation

$$f_{PFM} = \frac{u_{dec}}{w_f + t_c}. \tag{44}$$

Equation (44) is compensated for slower opening. Change from PFM to PWM is done when PFM frequency f_{PFM} is equal to frequency of control cycle. The control value, in which the change between control methods is done can be determined using equation

$$u_{PFMtoPWM} = f_c(w_c + t_c) = \frac{w_c + t_c}{T}. \tag{45}$$

Dead band in PWM control exists also in high control values. In high control values multi-valve invPFM can be utilized. InvPFM works as reflection of PFM. In normal PFM pulse controls opening of a valve, which means that during pulse control value u_{int} is increased from 0 to1. In invPFM pulse controls closing of a valve, which means that during pulse control value u_{int} is decreased from maximum value of N to N - 1. Therefore, the pulse is in fact negative or pulse can be thought as anti-pulse. Pulse width is set to $w_f + t_c$. Desired invPFM frequency is

$$f_{invPFM} = \frac{u_{dec}}{w_f}. \tag{46}$$

One should notice that the pulse width of PFM and denominator of equation (44) have switched places in invPFM control. The float point control value in which PWM changes to invPFM is

$$u_{PWMtoInvPFM} = N - f_c(w_c + t_c) = N - \frac{w_c + t_c}{T}, \tag{47}$$

in which N is the maximum control value that is equal to number of valves in a DFCU.

4.5.4 Circular buffer

Circular buffer's input is number of opened valves in a DFCU. Output of the buffer is opening combination of a DFCU. Therefore, circular buffer's objective is to determine which valves are open. Principle of buffer is to open valve that has been longest time closed and to close a valve that has been longest time open. This principle distributes openings, and therefore wear, evenly between valves. On the other hand, circular buffer

is crucial in successful switching, because it points desired opening for a valve that is most confidently closed and vice-versa. Concept of circular buffer for a DFCU of 8 valves is shown in figure (15).

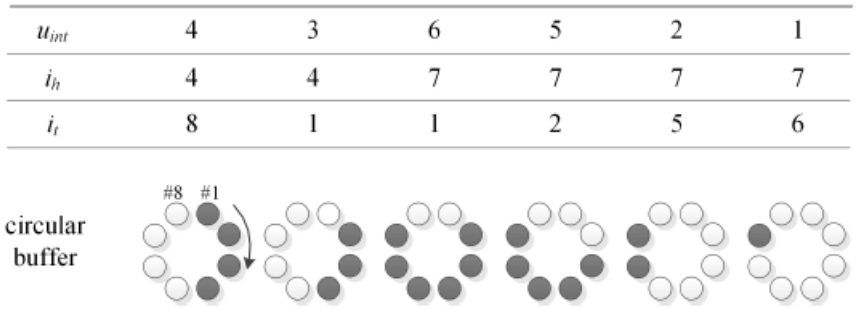

Figure 15. *Concept of circular buffer (Paloniitty & Linjama 2018).*

In figure (15), grey dots present opened valve and white dots closed ones. Index i_h is index of a valve that was lastly opened and index i_t is index of lastly closed valve. Two indexes are essential parameters, because ultimately circular buffer works by changing them according to changes in u_{int} value. When u_{int} decreases index i_t increases and when u_{int} increases index i_h increases. The indexes mentioned here are not only possible ones. Other usable indexes could be index of next valve to open or index of next valve to close.

5. CONTROLLER IMPLEMENTATION AND SIMULATION MODEL

Controller and simulation model were implemented using MATLAB R2017b and its add on Simulink 9.0. Main motivation for doing simulation model was to test the controller. First, implemented controller is presented. Simulation model that was used to validate controller is presented afterwards. Simulation model consists of four-way digital hydraulic valve and a horizontal cylinder. Controller and model system were done for DFCU's with 5 equal sized valves, which sometimes is not visible in following presentation.

5.1 Implementation of controller

In this chapter implemented controller is depicted using figures of Simulink mode. MATLAB-codes of implemented functions are presented in appendix A. Implemented controller's high level is presented in figure (16).

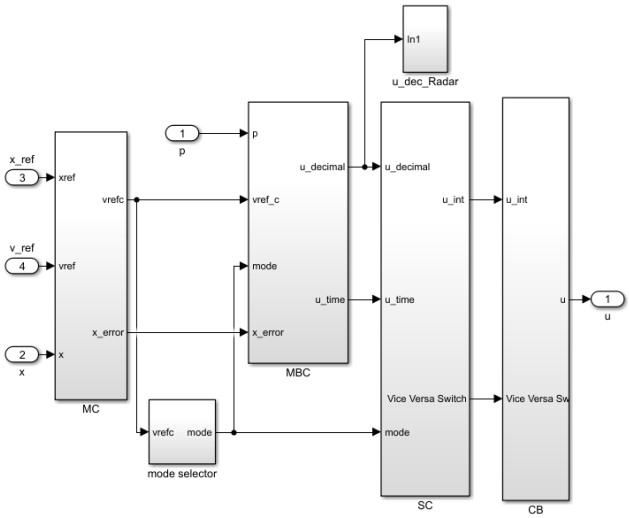

Figure 16. *Implemented controller.*

Figure (16) shows that implemented controller fulfils the principles introduced earlier in chapter (4.5). Slight modifications are made that are visible in high level. First, controller uses modes. Three modes of zero velocity/fine tuning, retracting and extracting cylinder exist. MBC has an extra output *u_time*. This is used in fine tuning of position. Sub-model u_dec_Radar is merely saving u_{dec} values and has no other objectives.

5.1.1 Motion controller & mode selector

Implemented motion controller applies equation (35) and is depicted in figure (17).

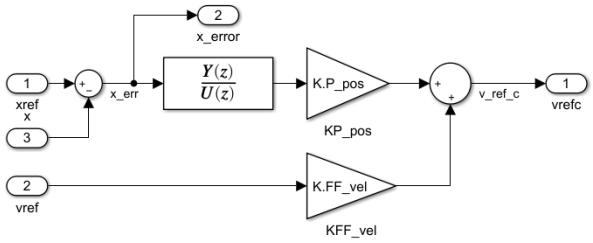

Figure 17. *Motion controller.*

Motion controller has an extra output of position error, which acts as input for fine tuner of position. Mode selector is depicted in figure (18).

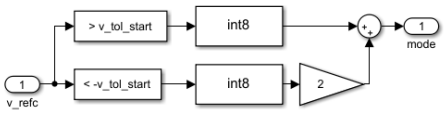

Figure 18. *Mode selector.*

Used mode selector is simple and uses only closed loop velocity reference v_{refc} and tolerance v_{tol} to determine mode. In mode 0, v_{refc} is inside of interval determined by tolerance value. Controller keeps DFCUs closed or uses fine tuning in mode 0. In mode 1, v_{refc} is over positive tolerance value. Mode 1 is extraction of piston and controller opens PA- and BT-DFCUs. In mode 2, v_{refc} is smaller than negative tolerance. Mode 2 is retraction of piston and controller opens PB- and AT-DFCUs.

5.1.2 Model-based controller

Model-based controller consists of model-based controllers for extraction and retraction modes. Also, model-based controller for fine tuning of position, but it will be presented later in chapter (5.1.5). Model-based controller is applying equation (36). Model-based controller for extraction is in figure (19).

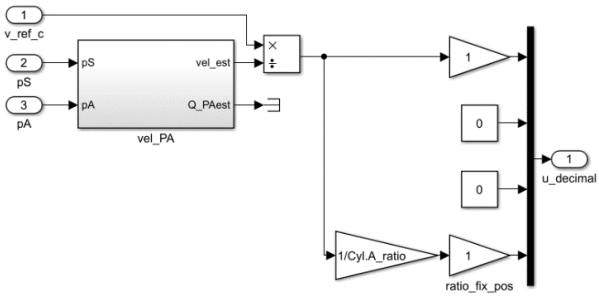

Figure 19. *Model-based controller for extracting motion.*

Model-based controller for extraction calculates steady state velocity estimation v_{ss} of cylinder, when one valve of PA-DFCU is open. Floating-point control value u_{dec} of PA-DFCU is then determined by dividing v_{refc} with v_{ss}. Floating-point control value of BT-DFCU is got by multiplying floating-point control value of PA-DFCU with area ratio of

cylinder piston. *Ratio_fix_pos* gain, visible in figure (19), can be used to control behaviour of system, but this was not thoroughly explored in this research. Floating point control values of AT- and PB-DFCUs are constant zeros during extraction. Model-based controller of retraction is like one of extraction, but naturally PB-DFCU replaces PA-DFCU and AT-DFCU replaces BT-DFCU. Subsystem vel_PA holds flow model and is depicted in figure (20).

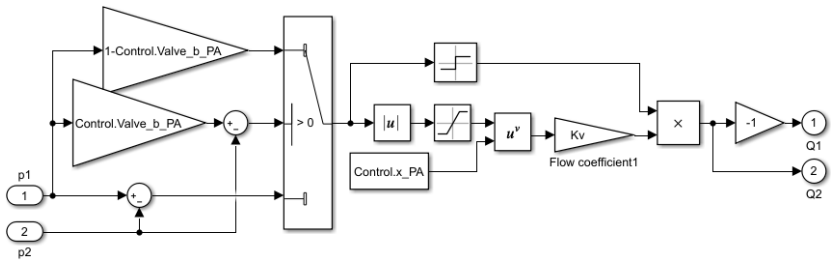

Figure 20. *Model-based controller's flow model.*

Flow model in figure (20) is applying equation group (38). Switch determines if cavitation choking equation is used or not. What is not depicted here is the fact that volume flow is later divided by area of piston to calculate v_{ss}.

5.1.3 Switching controller

Switching controller composes of MVPWM and MVPFM for all four DFCUs. Mode determines which are under active calculation. Switching controller has also switching controller for fine tuning of position, but it will be presented later. MVPWM-controller for PA-DFCU is in figure (21).

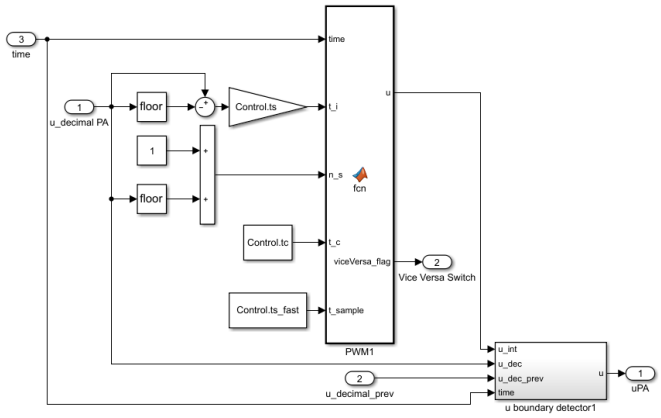

Figure 21. *MVPWM of a DFCU.*

MVPWM-controller in figure is applying equations (39) and (40). *Control.ts* is period of control cycle, *Control.ts_fast* is sample time of switching controller, *Control.tc* is compensation time for longer closing and time is time of control cycle. U boundary detector1 sub-model is controlling control value u_{int} in first control cycles after commencing con-

troller or when control value crosses integer. This is due to asynchronous timing of controller with MVPFM and MVinvPFM controllers. Therefore, the change to MVPWM from them happens, with high probability, during pulse of either of them, which makes the intended control value to be differ from one that is driven. The sub-system has handmade compromises to avoid worst-case scenarios. Controller would work without them, and on the other hand, better way to deal with asynchronization of controllers would be to synchronize them. Function PWM1's m-code is in appendix A. In short, function is applying equations (42) and (43).

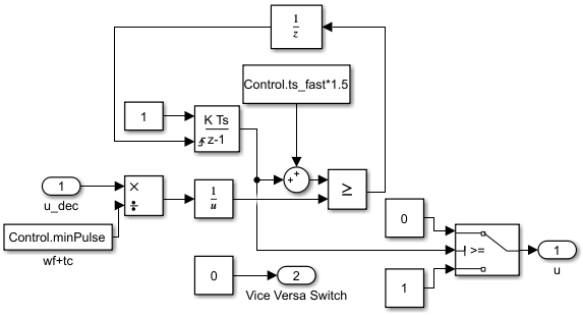

Figure 22. *MVPFM of a DFCU.*

Figure (22), depicts implemented MVPFM-controller for a DFCU. Controller is applying equations (44) and (45). Period of PFM signal is compared to integrator that works as controller's clock. When period of PFM is smaller than time of last pulse a new pulse is created by resetting clock and using switch logic. Compared clock value is compensated for one sample time of switching controller, because of delay of on sample time in resetting. An extra half sample time is added to round the desired PFM period to closest possible alternative. Without this the logic would not round to closest but ceil the desired PFM period.

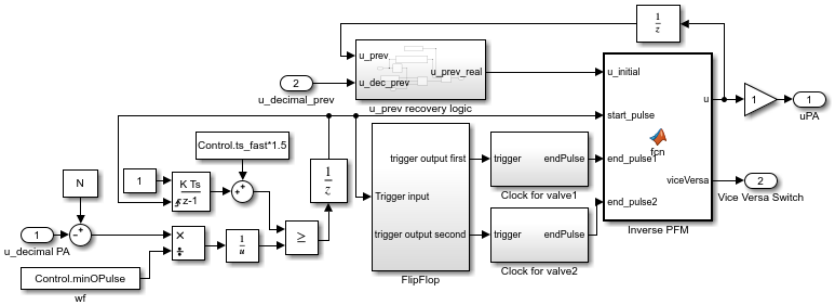

Figure 23. *MVinvPFM of a DFCU.*

MVinvPFM, depicted in figure (23), uses similar clock logic to determine start of the (anti-)pulse as in MVPFM. Similarities end there, because in MVinvPFM individual pulses intersect, which prevents efficient use of simple switches. Inverse PFM function was implemented and m-code of it is in appendix A. In short, function's logic is to decrease u_{int} value when *start_pulse* triggers and increase when *end_pulse* triggers. Two *end_pulse* triggers were implemented to allows intersection of pulses. Clock for valve

sub-models have a clock and simple switch logic to determine when *end_pulse* triggers. Clock is reset with the *start_pulse* signal. FlipFlop sub-model is used to shift in turns between *end_pulse* triggers. U_prev recovery logic sub-model is used in commencing of controller to choose either *N* or *N*-1 to be *u_initial* depending on which direction u_{dec} is coming from. The model implemented only works with control values *N*-1…*N*, for unknown reason. If controller is tried to run with values <*N*-1, output u_{int} drops straight to value *N*-2 and does not recover. Because reason for this was left as a mystery, a handmade switching logic to control values <*N*-1was implemented and is shown in figure (24).

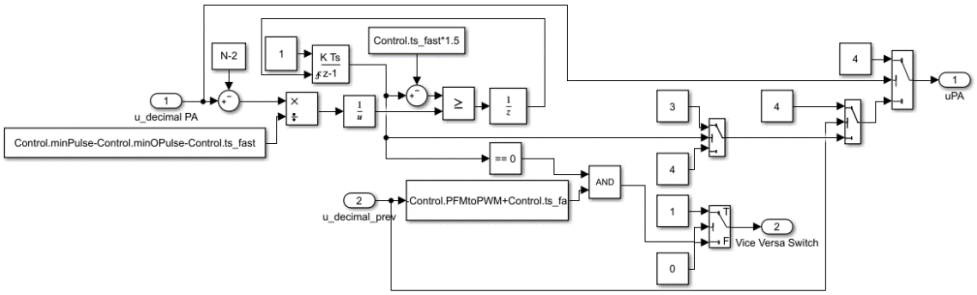

Figure 24. *MVinvPFM of a DFCU when control values <N-1.*

Logic uses simultaneous switching or vice-versa switch when commencing of controller happens from increasing u_{dec} value. If commencing happens from decreasing u_{dec} value, control u_{int} value is kept at *N*-1, which is in figure (24) value 4. In normal, operation pulse is increased from *N*-2 to *N*-1 for two switching controller's sample times, when a pulse is triggered. This solution is far from optimal and should not be used in future.

5.1.4 Circular buffer

Implemented circular buffer consists of the buffer function itself and bittify function to change indexes to opening combinations. Circular buffer is depicted in figure (25).

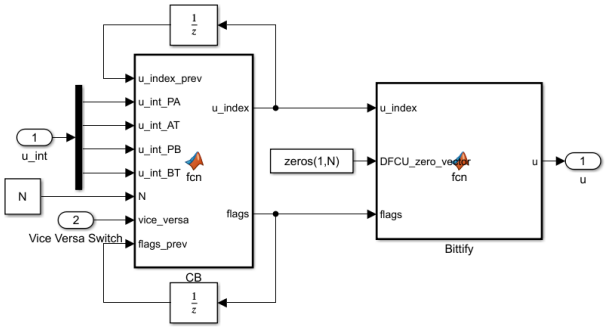

Figure 25. *Circular buffer.*

There is only one circular buffer, in which buffering of all DFCUs are implemented. Circular buffer changes indexes depending on changes in u_{int} values and vice-versa switch value. Indexes used in implementation are previously opened valve and previously closed valve. Problem with the indexes was that the indexes are equal on two occasions: when

all valves are open or closed. To counter this *flags* parameter was introduced to keep track if a valve was opened or closed previously. Bittify function transforms indexes to opening combinations, which are then transmitted to DFCU model in simulations or to a booster in real test system.

5.1.5 Fine tuner of position

Fine tuner of position was implemented to increase positioning accuracy. Although, not central part of controller nor interest of this research a short presentation is given here. Finer tuner is part of mode 0. If position error is over a tolerance value tuner activates. Position error tolerance of was arbitrary 100 µm in this research, although smaller tolerances were usable, except in low temperatures. Logic of the fine tuner was to calculate how much volume should be taken out or added to cylinder chambers to correct error. Crossflow was enabled to allow smaller amounts of volume flows than in pure PFM. One valve of all DFCUs was opened at start. After minimum pulse width secondary DFCUs were closed and primary DFCUs were kept open to allow the estimated optimal volume pass to chamber. Model-based control was utilized and model-based fine-tuning controller to extraction direction is shown in figure (26).

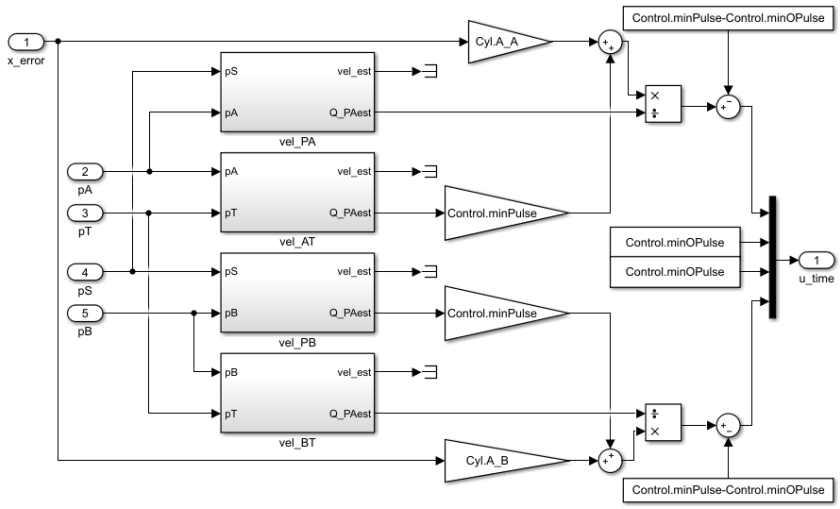

Figure 26. *Model-based fine tuner of extraction.*

In extraction, primary DFCUs are PA and BT. Estimations of volume passed through secondary DFCUs with shortest pulse width were reduced from desired volumes. Primary DFCUs pulse widths were calculated from this value and the last sum is the compensation for longer closing. Output of the model-based fine tuner controller was pulse widths for all DFCUs. Value of pulse widths were transformed to pulses in switching fine tuner controller using simple switching logic, depicted in figure (27).

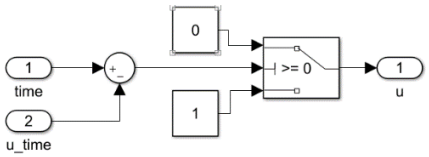

Figure 27. *Switching fine tuner.*

All DFCUs had separate switching finer tuner controller. The pulse was then used as input for circular buffer.

5.2 Simulation model

Simulation model was used to validate the controller. Simulation model consists of the controller depicted above, four-way digital hydraulic valve and a cylinder in horizontal posture. Four-way digital valve consists of four DFCUs and therefore a model for DFCU is presented.

5.2.1 DFCU

Four-way digital valve has four DFCUs. A DFCU can be modelled in two parts: dynamics and flow model. Only one valve model can be utilized for whole DFCU by using matrices. Overlay of valve model is in figure (28).

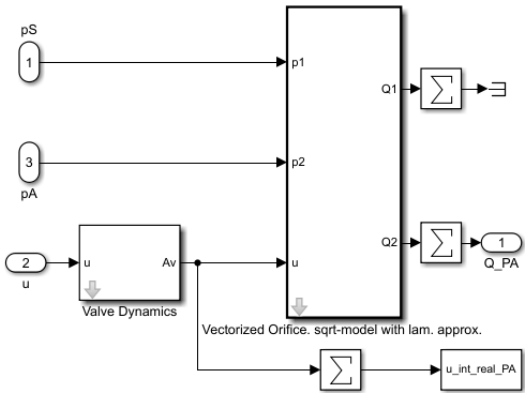

Figure 28. *Valve model.*

Inputs for the model are control combination, inlet and outlet pressures. Valve dynamics sub-model then models openings and closings of valves and the modelled state of valve is then transmitted as input for flow sub-model. Valve dynamics is applying the concept of virtual valve states depicted earlier in chapter (4.1). Valve dynamics sub-model is in figure (29).

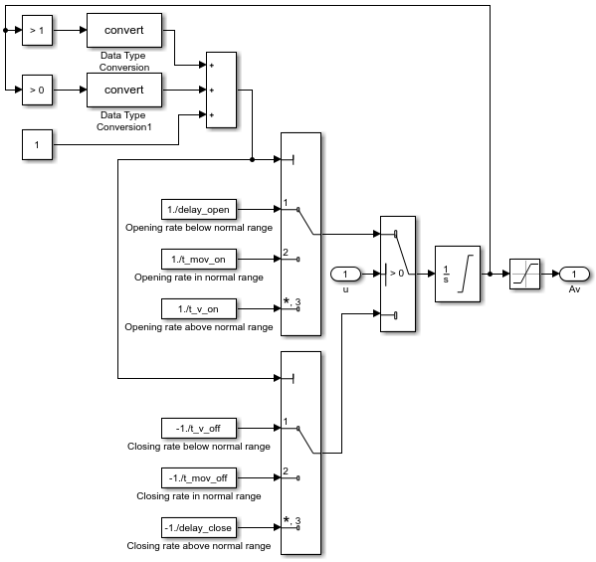

Figure 29. *Valve dynamics.*

In upper left corner of figure (29), the virtual state of a valve is determined. States are numbered 1,2 and 3 and they depict virtual state intervals -1…0, 0…1 and 1…2. Control value of a valve determines if opening or closing and the corresponding reciprocal time value is integrated to initial state value. The model depicted here was got from adj. prof. Matti Linjama.

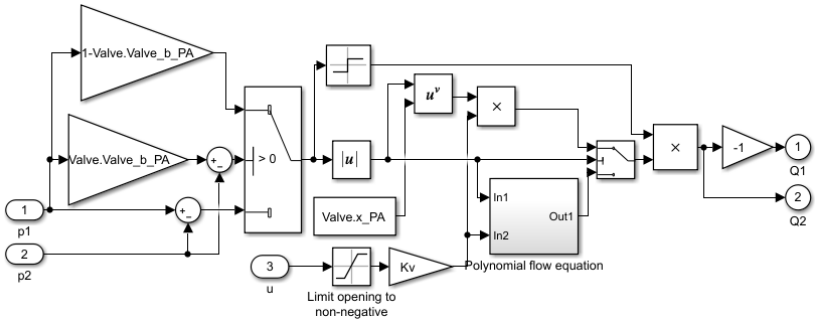

Figure 30. *Valve flow model.*

Figure (30) depicts flow model of a valve. It is like the flow model used in model-based controller. Difference is that transition from positive to negative flow is considered by using polynomial flow equation in small pressure differentials. This prevents singularities during simulation. Sum of volume flows to cylinder chambers are used as input in cylinder model. The model depicted here was got from adj. prof. Matti Linjama, except cavitation choking logic, which was added by the author.

5.2.2 Cylinder

Cylinder model applies wide variety of equations from chapter (4.2). Overlay of cylinder model is depicted in figure (31).

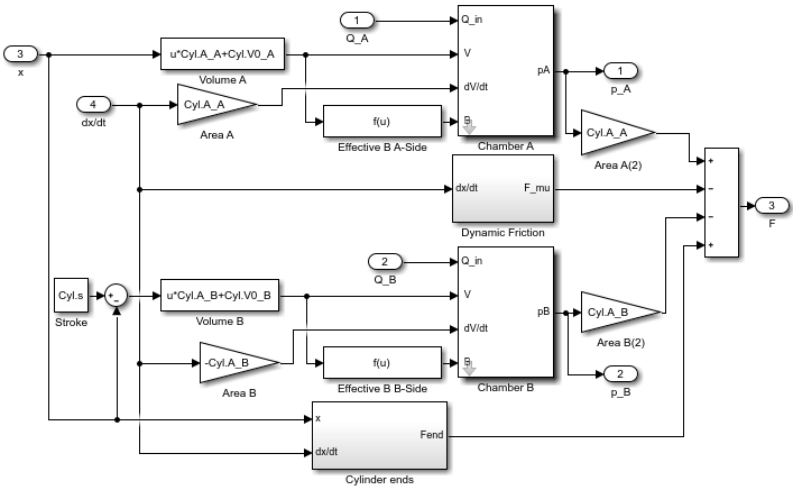

Figure 31. *Cylinder model.*

Cylinder model's inputs are piston position, velocity and net volume flows to chambers. Outputs are chamber pressures and net force projected to external mass. Piston position and velocity are modelled as external mass' position and velocity. Volumes of chambers and effective bulk modules are calculated from piston position. Hoses are considered as part of chamber volume. Sub-models of the cylinder model are chambers, seal friction and cylinder ends.

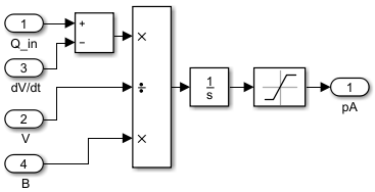

Figure 32. *Chamber model.*

Chamber model, in figure (32), applies state equation (19) of pressure differential. From net volume flow, volume, change in volume and bulk modulus pressure differential is calculated. Pressure in chamber is integral of differential.

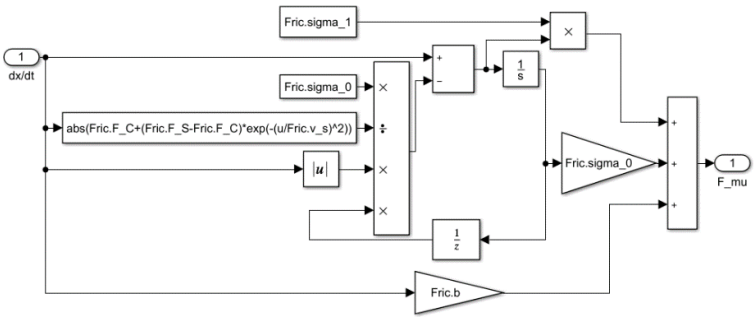

Figure 33. *Friction model.*

Friction model, in figure (33), applies dynamic friction equation (11). Only velocity of piston is needed as input.

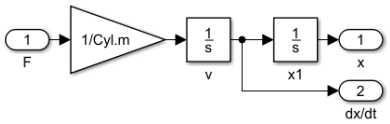

Figure 34. *External mass.*

Net force of cylinder is projected to external mass using model in figure (34). The external mass is modelled as pure inertia, because pose is horizontal rather than vertical. Velocity and position of external mass or piston is achieved by integration. Velocity and position are then feed backed to cylinder model.

5.3 Simulation results

Modelling and simulation of the system was ultimately done to develop and enhance the controller. Second objective was to get estimation of the performance of the real system. The controller and system model were introduced earlier. The used parameters are resembling the real parameters of the system. The experimental system is introduced in chapter (6). Measurements of parameters will be covered in chapter (7). Although, used parameters are resembling those of the real system, modelled system was not fully verified. Especially, friction parameters are based more on assumptions than measurements. This was not seen problematic, because of the set goals of the simulation study. Next, used simulation parameters are revealed. After that simulations of fifth order polynomial trajectories of 15 mm, 150 mm 300 mm. Simulated trajectories are same to those that will be used in measurements of the experimental system in chapter (8). Simulations should prove the operability of the implemented controller and give some rough estimations of the performance.

Parameters of the digital valve system are based on measurements of chapter (7). Parameters used for valve dynamics (figure (29)) and valve model (figure (30)) are presented in table (1). One must consider that there are five valves in each DFCU. Therefore, there are five values for each parameter of a DFCU. One value for every valve. Additionally, cavitation choking ratio parameters b for tank side DFCUs is set to arbitrary 0.001. This is small enough value that in any practical sense model does not model cavitation choking for tank side valves.

Second part of the modelled system is the cylinder. Physical dimensions are following the real experimental system, but especially friction parameters are rather arbitrary. Parameters of cylinder are in table (2).

Table 1. *Valve model parameters*

Parameter	Value
Valve opening delay [ms]	4
Valve closing delay [ms]	9
Valve opening time [ms]	3
Valve closing time [ms]	3
K_v, PA-DFCU [$m^3/(s*Pa)$]	(5.665, 5.907, 5.080, 5.583, 5.760)*10^{-8}
K_v, AT-DFCU [$m^3/(s*Pa)$]	(5.301, 5.107, 5.205, 4.901, 5.236)*10^{-8}
K_v, PB-DFCU [$m^3/(s*Pa)$]	(5.821, 5.575, 5.856, 5.819, 5.874)*10^{-8}
K_v, BT-DFCU[$m^3/(s*Pa)$]	(5.259, 5.048, 5.251, 5.220, 4.975)*10^{-8}
x, PA-DFCU [-]	0.4950, 0.5, 0.4950, 0.5, 0.51
x, AT-DFCU [-]	0.43, 0.44, 0.435, 0.43, 0.43
x, PB-DFCU [-]	0.51, 0.51, 0.51, 0.51, 0.51
x, BT-DFCU [-]	0.46, 0.46, 0.465, 0.4650,0.47
b, PA-DFCU [-]	0.2816, 0.2823, 0.2592, 0.2989, 0.2807
b, AT-DFCU [-]	0.001
b, PB-DFCU [-]	0.3116, 0.2956, 0.3077, 0.3049, 0.3185
b, BT-DFCU [-]	0.001
Transition pressure [MPa]	0.1

Table 2. *Parameters of cylinder model.*

Parameter	Value
Cylinder's piston diameter [m]	0.032
Cylinder's piston rod diameter [m]	0.016
Cylinder stroke [m]	0.5
Cylinder's piston area A-side [m^2]	$\pi*0.032^2/4$
Cylinder's piston area B-side [m^2]	$\pi/4*(0.032^2-0.016^2)$
Cylinder ratio of area (A/B) [-]	1.33
Volume of hose of A-side [m^3]	$\pi*0.0095^2*1.6$
Volume of hose of B-side [m^3]	$\pi*0.0095^2*1.3$
Dead volume of chamber A [m^3]	$2*10^{-5}$
Dead volume of chamber B [m^3]	$2*10^{-5}$
Bulk modulus of stainless-steel cylinder [GPa]	210
Bulk modulus of hose [GPa]	0.4
Bulk modulus of water-glycol mixture [GPa]	2.7
Static friction force [N]	600
Coulumb friction force [N]	400
Viscous friction coefficient [Ns/m]	225
Stribeck velocity [m/s]	0.05
Maximum displacement of the seal [m]	$4*10^{-4}$
Spring constant of the seal [N/m]	$600/4*10^{-4}$
Damping coefficient of the seal [$kg\sqrt{(m)}/s$]	$2*\sqrt{(600/4*10^{-4}*20)}$

The last part of the model to parameterize was the controller. Motion controller's parameters should be based on dynamics of the system. In these simulations, the parameters of

the motion controller were based on the dynamics of the real system rather than the modelled one. This was not seen problematic, because of the ultimate reason for simulation tests. Model-based controller's parameters were based on average values of valves parameters of a DFCU. Switching controller parameters are based on the valves' dynamical characteristics. Parameters used in controller are presented in table (3).

Table 3. *Parameters of controller.*

Parameter	Value
Proportional controller gain [s^{-1}]	17
Time constant of position error filter [ms]	44
Feedforward gain [-]	1
Tolerance of closed loop velocity reference error [mm/s]	5
Estimated K_v, PA-DFCU [$m^3/(s*Pa)$]	$5.599*10^{-8}$
Estimated K_v, PB-DFCU [$m^3/(s*Pa)$]	$5.789*10^{-8}$
Estimated x, PA-DFCU [-]	0.50
Estimated x, PB-DFCU [-]	0.51
Estimated b, PA-DFCU [-]	0.2805
Estimated b, PB-DFCU [-]	0.3077
Duration of control cycle [ms]	10
Sample time of controller [ms]	1
Minimum pulse width [ms]	7
Closing time compensation [ms]	5
Transition control value from PFM to PWM [-]	1.3
Transition control value from PWM to invPFM [-]	3.7
Cut-off frequency of pressure filters [Hz]	10

Three different trajectories with strokes of 15 mm, 150 mm and 300 m were simulated. Results of these simulations are presented next.

Figure (35) shows results of the smallest stroke of 15 mm. Controller stays on control area of MWPFM for whole track. Velocity of the piston has high peaks. Pressure pulsation is high, especially in retraction. Although, the pressures shown in figure (35) are unfiltered. Even though, movement of piston is simulated to be jerkily, the simulated position of piston seems to track the position reference value rather well for small trajectory. Position error seems to pulsate from maximum positive error to maximum negative error quite steadily through strokes. The maximum position error simulated in this single simulation is 0.800 mm.

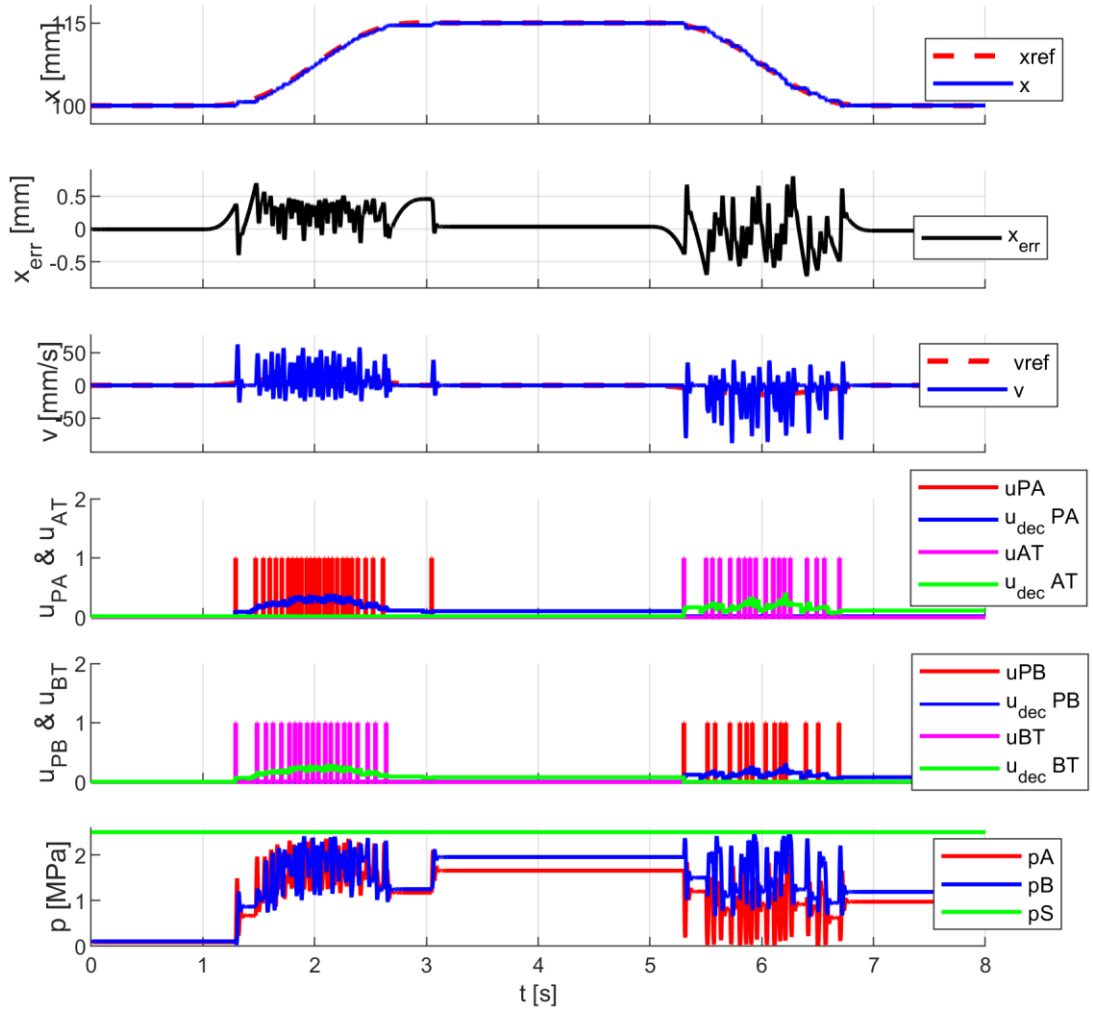

Figure 35. *Simulation results of 15 mm stroke.*

Simulated medium trajectory was with a 150 mm stroke. Results of the simulation are in figure (36). Velocity pulsates only at the start and at the end of the strokes, which is something to expect, as velocity of the piston is now higher compared to stroke of 15 mm. Pressure pulsation is still notable but much smaller. Controller crosses to area of MVPWM control during extraction but stays in MVPFM during retraction. Difference is due to considerably higher pressure levels in extraction. Simulated piston position tracks the position reference well. Similar pulsation in position error is noticeable during jerky motion. After jerky motion, position error behaves much more linearly. Maximum position error in this single simulation is 0.800 mm.

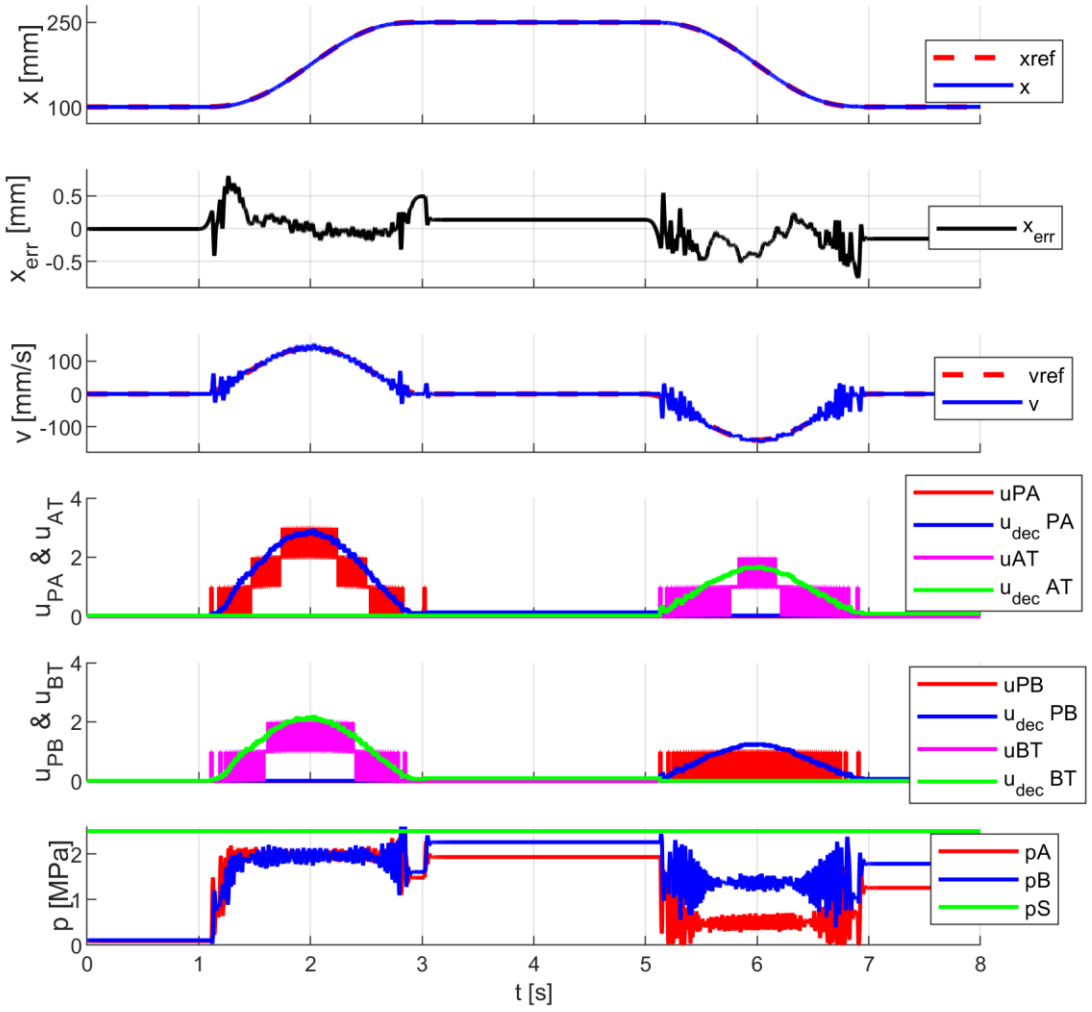

Figure 36. *Simulation results of 150 mm stroke.*

Simulated large trajectory was with a 300 mm stroke. Results of the simulation are in figure (37). Pulsations of velocity and pressures are again smaller than was the case with smaller trajectories. Control goes to MVinvPFM during extraction and to MVPWM during retraction. Simulated piston position follows the reference well during retraction but during extraction, a large position error emerges during the fastest velocity reference. The reason for this can be seen in the control value of PA-DFCU. Control value is over the maximum value of 5. Therefore, simulated piston position falls behind of the position reference. Reason for this is the high pressure level during extraction. Pressure level is controllable through controlling the opening of tank side DFCU. Therefore, an extra simulation with large trajectory was done where the pressure level was kept lower. Maximum position error in this single simulation is 2.652 mm.

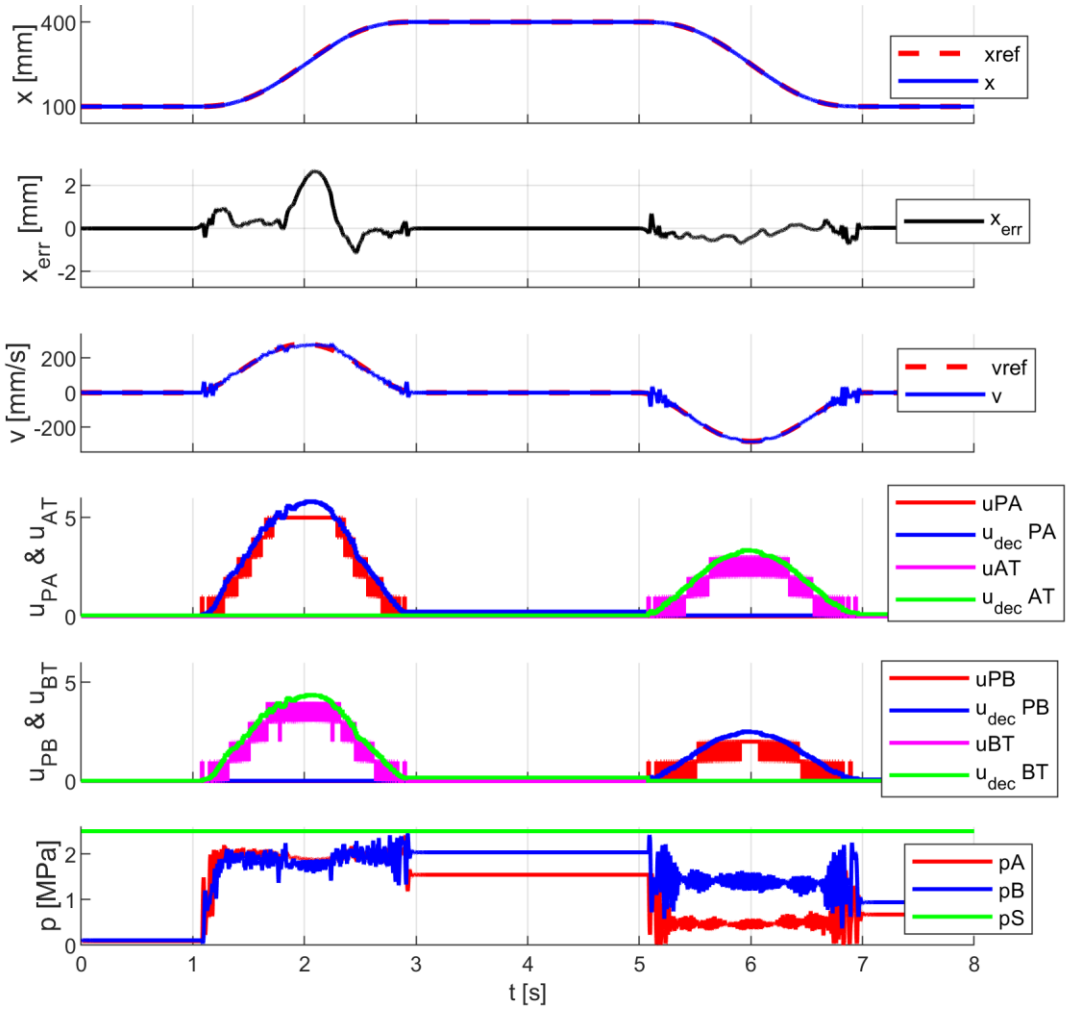

Figure 37. *Simulation results of 300 mm stroke with high pressure levels.*

The extra simulation differed from the earlier simulation in that the opening of the BT-DFCU was multiplied by 2. Results of this simulation with lower pressure levels are in figure (38). Simulation show that in this case control value of BT-DFCU is over the maximum value of 5. The consequence can be seen in pressure levels during extraction. Pressure levels rise as control value is over the maximum value. Control value of PA-DFCU does not go beyond the maximum value, which results in considerably better position error results compared to earlier simulation with stroke of 300 mm. Maximum position error of this single simulation is 0.825 mm.

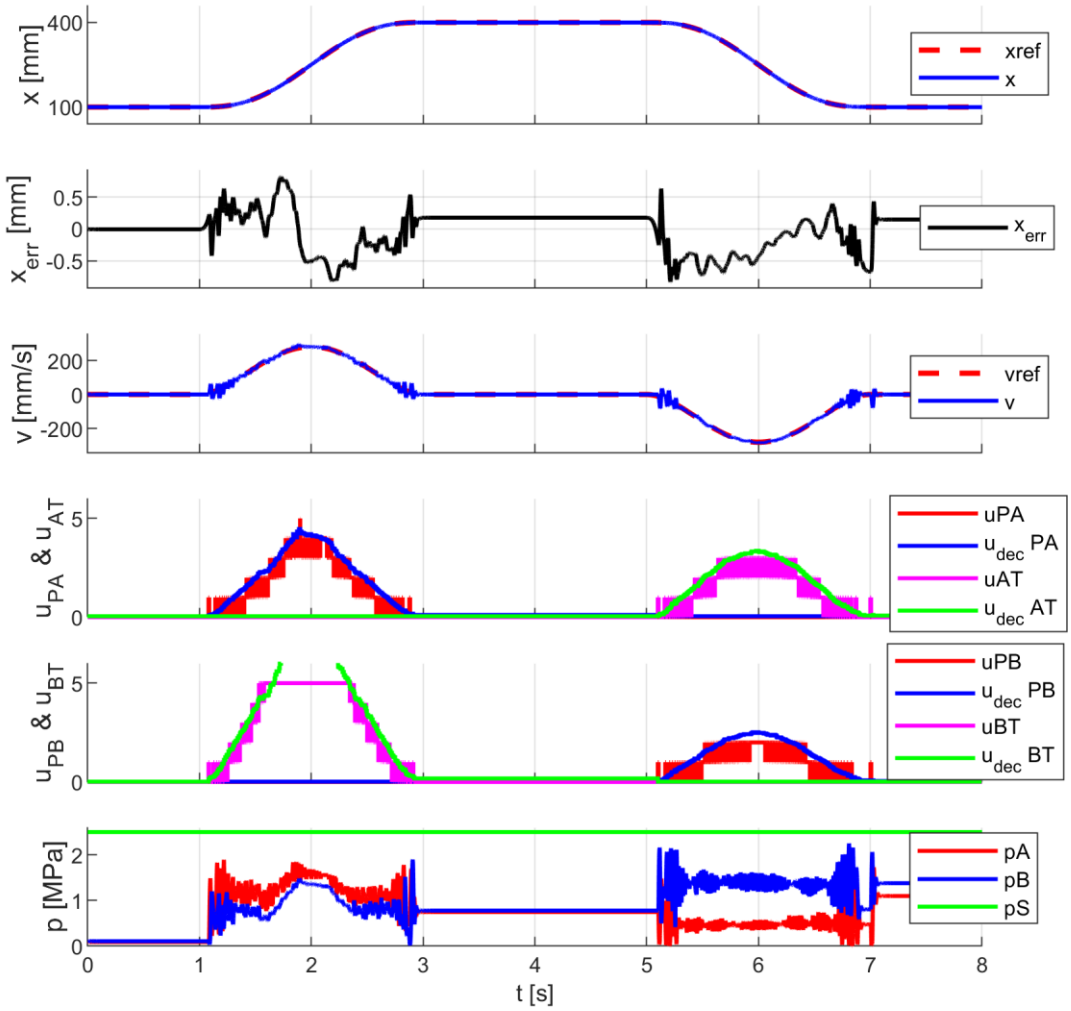

Figure 38. *Simulation results of 300 mm stroke with lower pressure levels.*

Maximum position errors of all simulations are combined to table (4).

Table 4. *Maximum position errors of simulations.*

Stroke [mm]	Maximum position error [mm]
15	0.800
150	0.800
300 (high pressure level)	2.653
300 (low pressure level)	0.825

Table (4) shows that simulated results are indicating that maximum position error to be practically independent from the velocity of the piston. Minor threat is observable from the pressure levels, even though they seem to be controllable through controller, if needed. If the first simulation of 300 mm stroke is excluded, then maximum position error of 0.825 mm would result in maximum position error to maximum velocity ratio of 2.9 (ms), which is a very good results, because reference value from Linjama & Vilenius (2005) is 5.3 (ms). Although, results are promising but one must consider that in these simulations variance in opening and closing times of valves was not considered. Therefore, the results will degrade from the simulated ones. Ultimately, the point of simulations

was to prove the functionality of the controller. Results attained here indicate that controller is working as desired.

6. EXPERIMENTAL TEST SYSTEM

Used real test system is introduced in this chapter. All parts of the system were designed for water hydraulics. System was built inside a freezer. Hydraulic diagram of the system is depicted in figure (39).

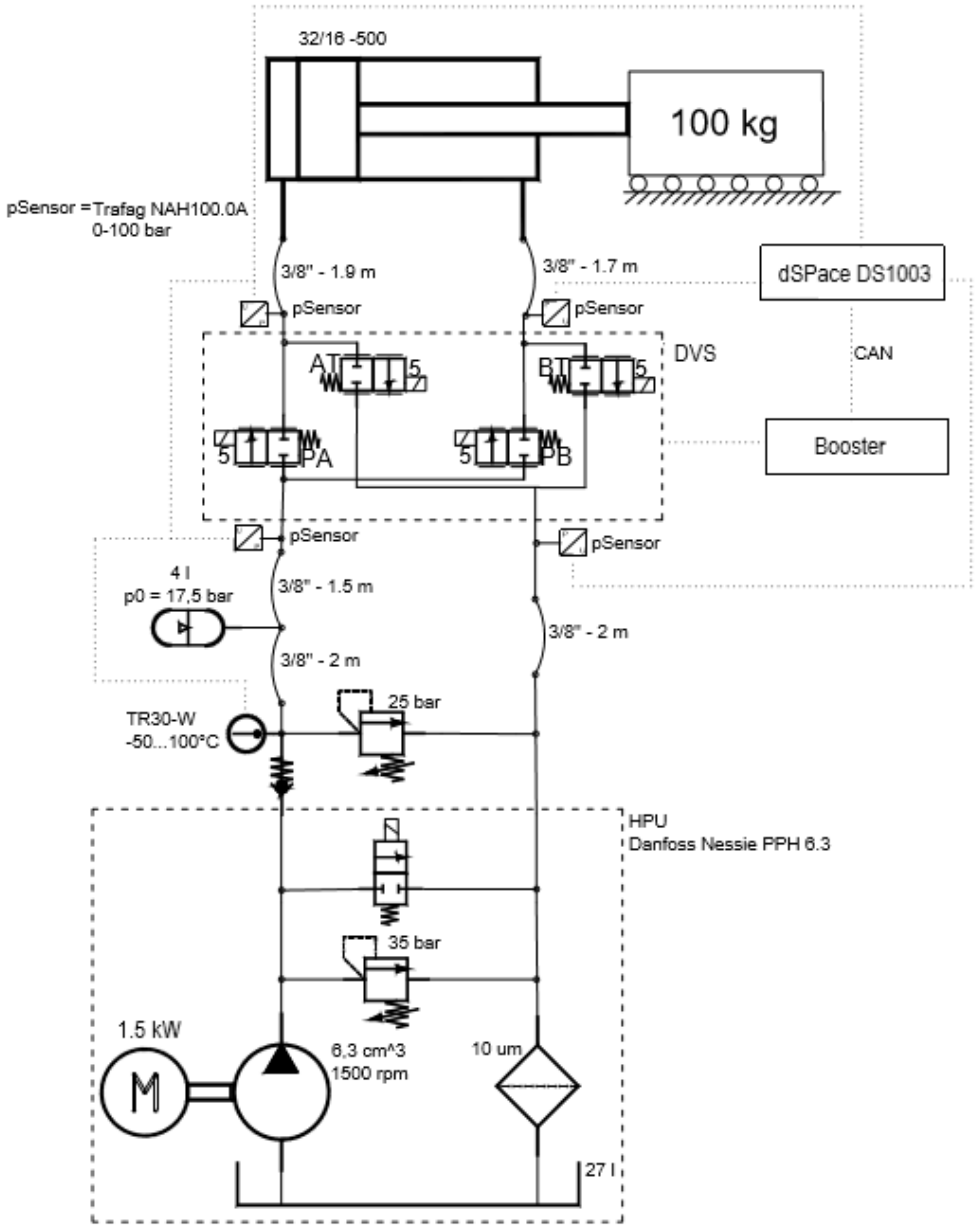

Figure 39. *Hydraulic diagram of the test system.*

Initially, the test system was planned to be simple composing of only hydraulic power unit (HPU), digital valve system (DVS), cylinder, sensors and electronics. Practical reasons forced to use an extra pressure relief valve and an accumulator.

HPU consisted of electrical motor and fixed displacement pump. HPU also had integrated pressure relief valve, by-pass valve, filter and tank. HPU had two shortcomings for intended tests. First, pressure relief valve's lowest pressure level was 35 bar, while the desired pressure level was 25 bar. This was fixed using an external pressure relief valve. Second shortcoming was that pump's output of 8.4 l/min was too low for desired volume flow of about 12.5 l/min. Therefore, accumulator was added to the system to enable desired volume flow.

DVS consisted of manifold and 20 on/off valves - 5 valves for each metering edge. Valve manifold's material was bronze, and valves' material was brass. Size of the DVS after implementation of valves and coils was roughly 210 x 130 x 230 mm. Valves used were Flo Control Q-2RB116 direct operated solenoid valves with spring return. Declared flow coefficient was 1.7 l/min, when pressure differential is 1 bar. Flow coefficient was deemed to be too big. Therefore, orifices of 1.5 mm were added after all valves. Using equation (8), an approximation of new flow coefficient was determined to be about 0.85 l/min. The value presented here was rough estimation, because characteristics of valves were unknown at the time. Assembled and disassembled valves are depicted in figure (40).

Figure 40. *Assembled and disassembled valves*

Cylinder was made of stainless steel. Size of the cylinder and external mass of 100 kg were the same as was used in research of Linjama & Vilenius (2005).

System had six sensors: four pressure sensors, one temperature sensor and a rotary encoder. Pressure sensors were placed close as possible to four metering edges. This allowed as accurate as possible measurements of inlet and outlet pressures of valves. Temperature sensor was placed externally to pressure line to measure temperature of medium leaving the pump. Perhaps more optimal placement would have been after the accumulator, because medium temperature in accumulator might differ from medium coming from pump. Although, this was not deemed to be critical concern. Rotary encoder with belt transmission was used to measure position of piston. Resolution of the rotary encoder was 266060 pulses/m, producing position measuring accuracy of 8 μm.

Controller hardware was dSPACE DS1103 controller board. Controller board connected to valve opening electronics or booster using CAN. Booster used 48 V as boosting voltage during pull time. After pull time voltage was settled to coils' nominal voltage of 24 V.

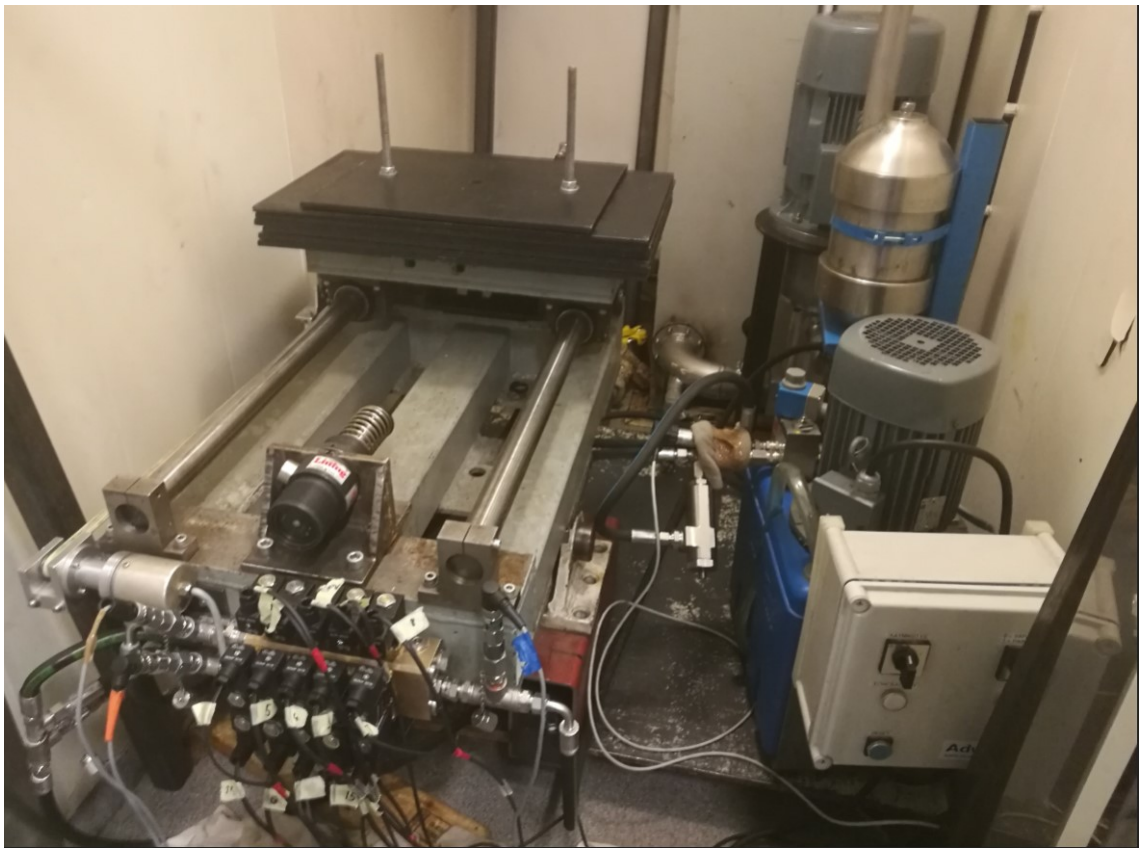

Figure 41. *Test system.*

The assembled system is in figure (41). HPU is in lower right corner and behind it is the accumulator. DVS is in lower left corner attached to the cylinder bench. Cylinder is not visible, because it is behind plates of the external mass seen in opposite side of the cylinder bench. The system sits in a freezer room, which restricted the angle for picture taking seriously. Electric motor behind accumulator is not part of the test system.

7. MEASUREMENTS OF THE CHARACTERISTICS OF THE TEST SYSTEM

In this chapter, results of hydraulic natural frequency, pulsation test and flow coefficient are discussed. Measurements were done in different temperatures to reveal changes in system's characteristics. Basic concept was to make measurements in three different temperatures. Temperatures were -20°C, 0°C and 30°C. In practice, temperature control was rather difficult as measurements took time and running system produced heat. Therefore, the real measurement temperatures varied, and ranges were -20…-13°C, -2…+2°C and 25…40 °C.

Measurement of hydraulic natural frequency is needed for tuning of filtered P-controller, because time constant of filter is based on the value. Pulsation test is done to determine opening time of linear volume flow and time compensation for longer closing time. Measurements of valve parameters is needed for model-based controller. Measurements of valve parameters uncovered values of flow coefficient, exponent and ratio of cavitation choking.

7.1 Hydraulic natural frequency

Hydraulic natural frequency ω_h of the system is necessary to determine for the filtered P-controller, because it is used to determine the time constant of the filter. Hydraulic natural frequency is measurable by oscillation of the system. As was stated earlier, hydraulic natural frequency varies as a function of piston position. Interest of this research is the smallest value of hydraulic natural frequency, which lies close to the middle position of the piston. This was depicted earlier in figure (12).

The measurement for hydraulic natural frequency was started by first driving the piston to zero position. Then all PA-side and BT-side valves were opened, which resulted in positive velocity. Movement was stopped when piston was near the middle of the cylinder. The rapid stopping of movement results in oscillation of the system. The timing of stopping of the movement was done with press button, which resulted differing stopping positions, but all the stopping position where within 10 mm of middle point of cylinder, which was 250 mm. Measurements were done in three different medium temperatures of -19°C, +1°C and +30°C. The results of the measurement are in figure (42).

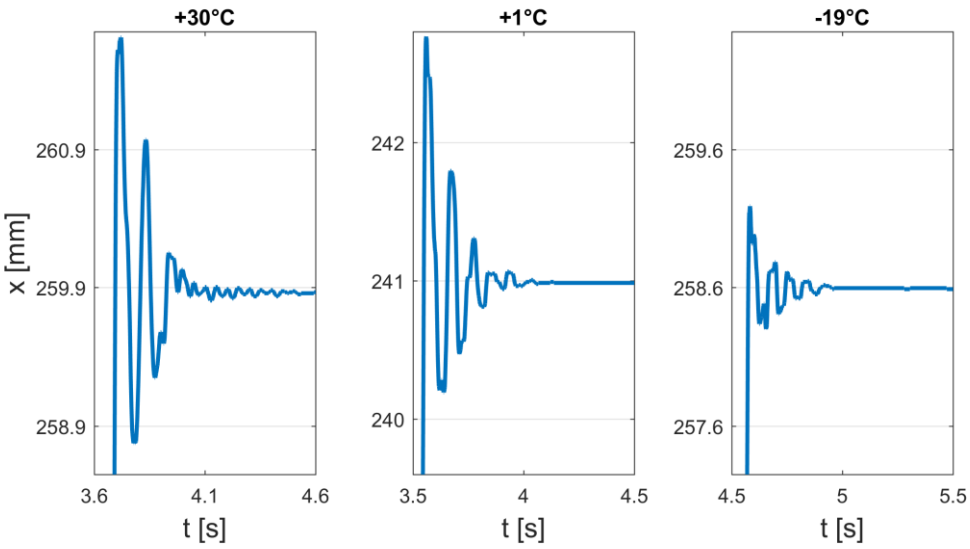

Figure 42. *Hydraulic natural frequency measurement results.*

One must consider that in figure (42) absolute values of times or values of position are not comparable, because they are not synchronous. Because plots are same size, the change of values are comparable. From figure (42) is visible that as temperature decreases, oscillation damps more rapidly. Change in hydraulic natural frequency as temperature changes is not directly visible in figure (42), but it is countable by taking period of the measured sine waves. Frequency (in Hz) is inverse of the period. Angular frequency is frequency (in Hz) multiplied by 2π. Hydraulic natural frequencies of the system in different temperatures are in table (5).

Table 5. *Measured hydraulic natural frequencies*

T [°C]	ω_h [rad/s]
30	64.1
1	70.6
-19	80.6

Table (5) shows that hydraulic natural frequency of the system increases as temperature decreases. Explanation for this phenomenon is in effective bulk modulus of the system. In equation (29) factors of hydraulic natural frequency was determined to be volume, area of piston, load mass and effective bulk modulus. First three of the factors are known to stay constant. Therefore, effective bulk modulus must be the changing factor. On the other hand, from equation (17) effective bulk modulus can be defined to be $\beta_e = c^2\rho$. Since, both speed of sound and density of water-glycol mixture increase as temperature decreases (George & Sastry 2003), bulk modulus of water-glycol fluid increases. Increase in bulk modulus of fluid, naturally increases the effective bulk modulus of the system. It is also possible that the characteristics of different materials change in lower temperatures. Especially easy to imagine is that hoses get stiffer in lower temperatures.

7.2 Pulsation test

Pulsation test was done to determine minimum pulse width that valve has fully opened, and amount of volume flow grows linearly if pulse width is further increased. On the other hand, pulsation test reveals the required compensation for closing time, which differs from opening time. The compensation is determined by continuing the linear volume flow to its theoretical zero value in negative pulse widths. Determined values will be used in multi-valve switching controller.

Pulsation test was done in two different occasions. First time it was made for all valves, without external load. Temperatures of medium varied between 25…40°C. Temperature was not seen to have significance in the first test, because fluids properties do not change drastically in those temperatures. On the other hand, the main purpose to do it for all valves was to make sure that all valves behave in similar manner. In practical terms, even test for one valve had given a picture of desired characteristics of valves. Second time the test was done to one valve of each boundary in three different temperatures. This was done to reveal the effects of temperature to opening times and closing times of valves. External load was on place in these measurements.

Principal method for pulsation test was to make 30 pulses for every valve with every pulse width from 1 ms to 20 ms. Then count average piston movement of pulse width at issue and convert the average piston movement to average volume passed through valve during a pulse of certain width. A valve of opposite side was kept open during measurement. For example, if a valve from PA-side was measured, then a valve from BT-side was kept open. This made pressures to be of similar value between different pulses of certain width and between different pulse widths. In practice, measurements were done only from 4 ms pulse widths onwards, because characteristic of booster. Booster's feature was that minimum pulse width it was capable to drive was set pull time. In preliminary tests, 4 ms pulse width was observed to be in ballistic zone of opening. Therefore, pull time was set to 4 ms, which then acted as the smallest pulse width used in pulse test measurements. The average volumes of flow, with different pulse widths of different valves are presented in figure (43).

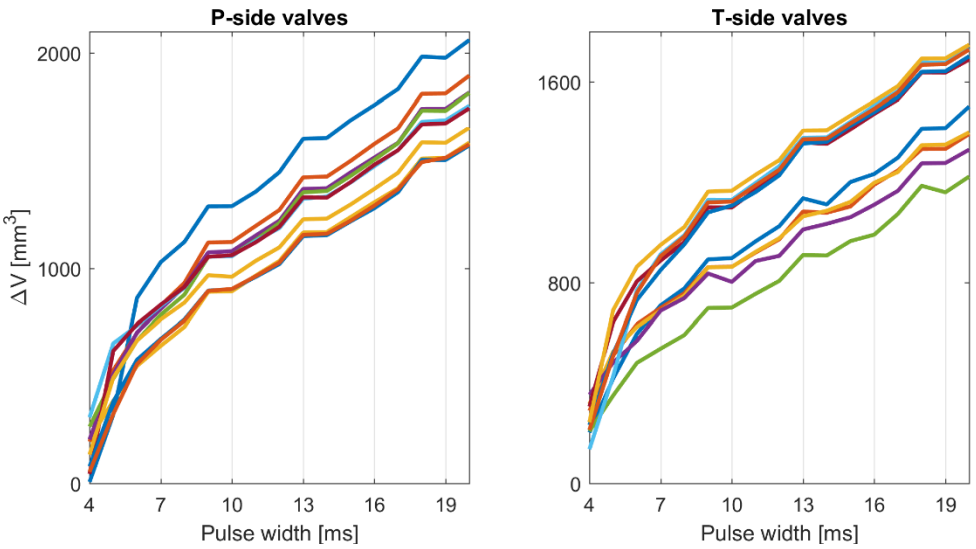

Figure 43. *Pulsation test results.*

One must consider that for P-side valves, the results of figure (43) are directly comparable with each other, because for all valves the pressure differential was over supply pressure to chamber pressure. Supply pressure was kept constant of about 2.6 MPa and chamber pressures were zero. For T-side valves the case is different, because supply pressure was projected through asymmetrical cylinder. This meant that in measurements of AT-side valves the pressure differential was considerably lower of approximately 1.8 MPa. For BT-side measurements the pressure differential was correspondingly higher, approximately 3.2 MPa. This is noticeable in plot of T-side, because the five obviously lower average volumes are results for AT-side valves and the five highest results are for BT-side valves. For opening time, this does not have noticeable effect.

Noticeable phenomenon in figure (43) is spiking in 9 ms, 13 ms and 18 ms pulse widths. Bugs from script that was used to handle measurement data were not found and it is unlikely that the recurring phenomenon was caused by mechanical parts of valves. Therefore, the phenomenon was deemed to be another characteristic of booster. Spiking phenomenon did not disappear or change to different pulse widths as longer pull times were used.

From figure (43), one can notice that all valves are in ballistic zone in 4 ms pulse width. Valves get to linear zone with 6-7 ms pulse widths, some even pulse width of 5 ms. Therefore, it is safe to say that all valves get to linear zone in 7 ms and the value is to be used as minimum pulse width of the system.

Compensation for longer closing time is determined from theoretical zero volume flow of linear zone. This was done with linear regression of volume flows of 7 ms and larger pulse widths of the results of figure (43). Then the regression line was continued to negative pulse widths. Three spiking values of each valve were excluded of this examination,

because they seem to be a disturbance to linearity rather than part of it. Regression lines drawn to negative pulse widths are in figure (44).

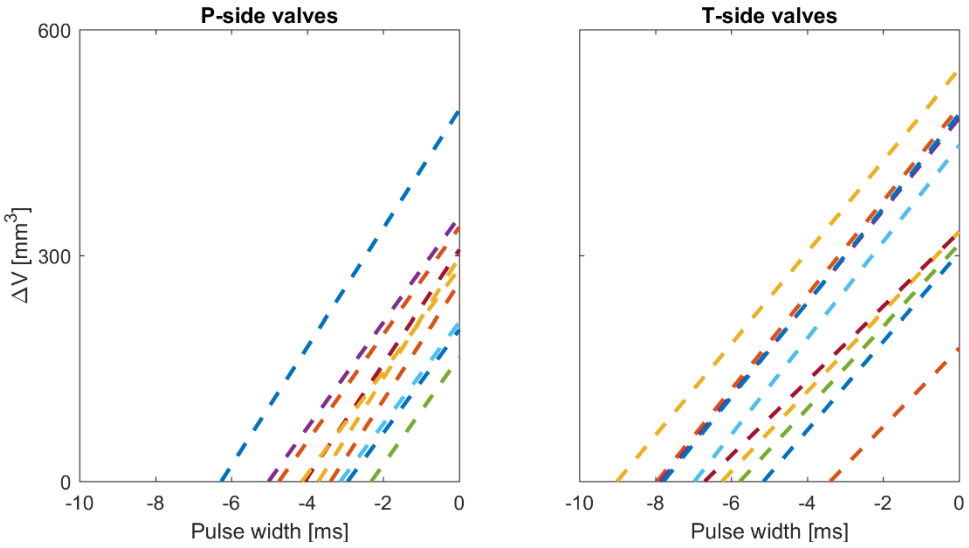

Figure 44. *Theoretical negative pulses*

Closing time lag for pressure side valves seems to be 3…5 ms longer than opening. For tank side valves the closing seems to be notably longer and for the bulk of the valves values is 5-8 ms. Also notable for tank side valves is that BT-side valves seem to take longer to close than AT-side valves. AT-side valves can be distinguished from BT-side valves from figure (44) by values in theoretical 0 ms pulse width. AT-side valves have five lowest values because of lower pressure differential over them. This suggests that closing is dependent on pressure differential over valve. For controller we are more interested in the values of P-side closing time. This is because in horizontal movement, chamber that is connected to pressure line is dominant. Therefore, the desired compensation value should be between values 3…5 ms. Final compensation value will be validated with open loop tests.

Next phase of pulsation tests was research of differing temperature. Pull time of booster was kept as 4 ms, which fixed the shortest pulse width to same as was with the first round of measurements. One valve was measured from every boundary. Selection was made arbitrarily. Warming of system produced a temperature control problem as measurement of one valve took 10…15 minutes. Therefore, in this second phase measurements were done only until pulse width of 12 ms. This was deemed to be enough, because all valves were in linear zone already in pulse width of 7 ms. Another difference in this measurement was that the external load was on place. Temperature varied during measurements, even though time used for one valve for one measurement reduced to about 50 % from first phase. Therefore, different medium temperature measurement zones were −17°C …−13°C, −1°C …1°C and 25°C …30°C. Pulsation tests made in different temperatures for four valves are in figure (45).

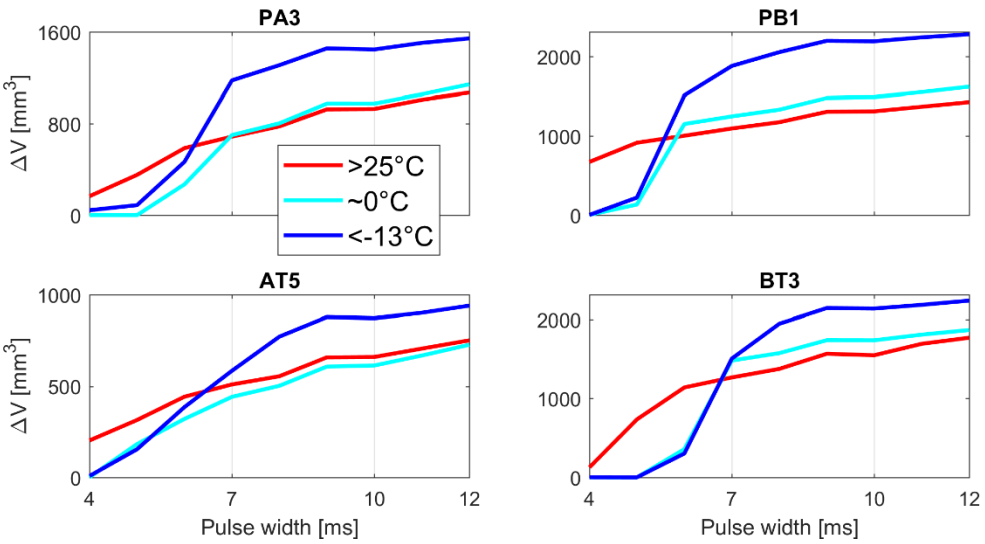

Figure 45. *Pulsation test in different temperatures.*

From figure (45), one can see that adding load seems not make difference in opening time of valves. Valves get to linear zone with pulse widths of 5…6 ms, when medium temperature is over 25°C. This was the case also in earlier measurements without load.

When medium temperature is 0°C, linear zone seems to be achieved with 1 ms longer pulse width. Behaviour in ballistic and settling zones changes also. For medium with temperature over 25°C nonlinear zone seems to be about 3 ms wide of pulse widths, but for medium in 0°C this seems to narrow to 2 ms of pulse widths. Overall, these results show that in medium temperature of 0°C lag of opening increases, time of nonlinear zone decreases and required pulse width for linear zone increases.

When medium temperature decreases further to under −13°C, lag of opening seems not to change when compared to medium temperature of 0°C. What changes is that time of nonlinear zone widens, which further lags the linear zone to wider pulse widths. From the results, it is hard to define, when exactly linear zone is achieved, because of the spiking phenomenon in 9 ms pulse width. Overall, it seems that lag of opening does not increase more than it had already increased with medium temperature 0°C. On the other hand, time of nonlinear zone increases after decreasing in 0°C and this increases pulse width required for linear zone. Also, increase in volume passed through valve in longer pulse widths indicate slower closing of valve.

Negative pulse width examination was also done with the results shown in figure (45). Linear regression was taken from pulse widths of 7 ms onwards, except for tank side results of under −13°C medium temperature, because they are not in linear zone yet. This is also questionable for P-side valves. Pulse width of 9 ms was excluded, because of the spiking phenomenon. Regression lines drawn to negative pulse widths are in figure (46).

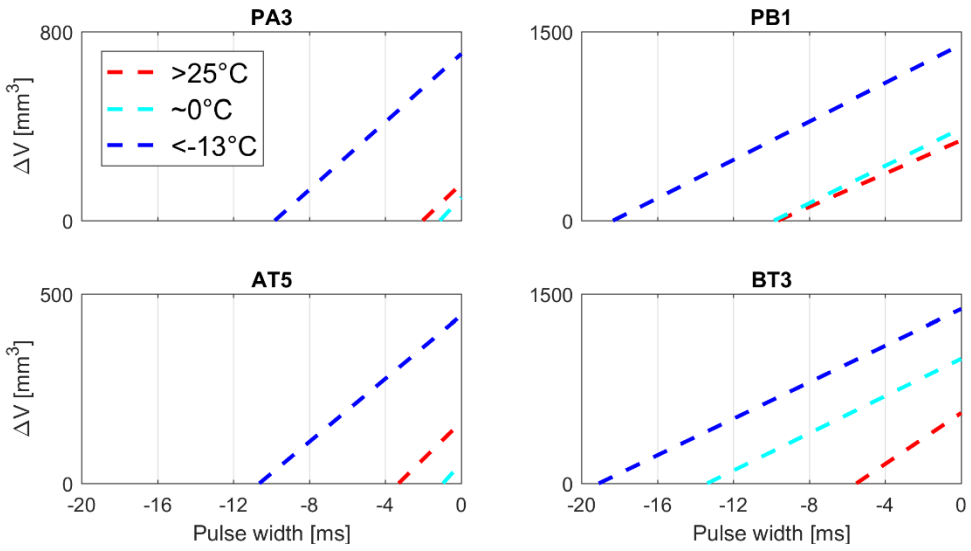

Figure 46. *Theoretical negative pulses in different temperatures.*

One must consider, that regression lines in figure (46) are drawn from fewer samples than regression lines drawn in figure (45). This creates uncertainty to results. Uncertainty is best seen in plot of valve PB1, in which the results indicate compensation of 10 ms for closing but results in figure (45) indicate that largest compensation need for a single P-side valve is about 6 ms.

Comparison between results of medium temperatures of 25°C and 0°C is pointless. Two of the plots of figure (46) indicates decrease in required compensation for closing time, one indicates no change and the last one indicates increase. Therefore, the change in required compensation time for closing from medium temperatures of over 25°C to 0°C remains unsolved.

Results for medium temperature under −13°C are clearer, when compared to either one of the two other medium temperatures. All the plots in figure (46) indicate that compensation for closing time increases considerably. On the other hand, dispersion is large. For valves PA3 and AT5 compensation time is approximately 10 ms, but for valves PB1 and BT3 value is near 19 ms.

Overall, decrease in medium temperature slows down both opening and closing of valve. Reasons for these phenomena most probably is in changing physical properties of medium fluid. As temperature decreases, viscosity of fluid increases, which makes fluid thicker. This increases the work needed from coil to open a valve. Similarly, the returning spring must work towards greater resistance as it closes a valve. It is possible that other phenomena have also influence in this. For example, it is possible that characteristics of returning spring changes in cold temperatures.

7.3 Parameters of valves

Flow coefficient measurement was done to determine factors of flow model or equation group (3). Factors to determine are flow coefficient K_v, exponent of pressure differential x and ratio of cavitation chocking b. Aim is to get average values for all DFCUs PA, AT, BP and BT, therefore examinations are done through average values of DFCU rather than through individual valves. Average values are used in model-based controller to determine desired number of opened valves for corresponding velocity reference.

Measurements were done by opening valves with different combinations. Each combination was driven for one second, and the last half a second of drive was used to determine average pressure levels and velocity of piston. Velocity of piston is directly related to volume flow through valve by formula $Q = Av$. Seven different combinations were used. Some combinations gave sample point to pressure side valves and some to tank side valves. Different combinations are in table (6).

Table 6. *Combinations of opened valves in flow measurements*

Combination	Pressure side	Tank side
1st	1 valve open	1 valve open
2nd	1 valve open	2 valves open
3rd	1 valve open	Crossflow
4th	2 valves open	1 valve open
5th	Crossflow	1 valve open
6th	1 valve open	3 valves open
7th	3 valves open	1 valve open

From table (6), one can notice that valve under inspection is always the single valve open of a side. Exception is first combination that gave samples for both pressure side and tank side valves. One must consider that every combination was driven five time back and forth. For example, first combination was started with valves PA1 and BT1 open, which resulted positive movement. This was followed by opening of valves PB1 and AT1, which resulted in negative movement. After the first back and forth movement was over, a second one followed with combinations of PA2/BT2 and PB2/AT2 and so on. This method resulted in four samples of volume flow in different pressure differentials for each valve.

Four sample points were used to determine parameters K_v and x of equation (3). In addition, parameter b was determined, if cavitation chocking was detected. In practical terms, K_v and x were determined from two samples that were in pressure differentials approximately between 0.5…1.5 MPa. This allowed forming of two equations with two unknowns K_v and x of equation (3). Two parameters were solved from equation group, with basic equation group solving methods.

Measurements were done in six different temperatures of fluid medium. Temperatures were −16°C, −10°C, 1°C, 10°C, 20°C, 30°C. Temperature rose during measurements, but

measured values stayed within boundaries of ±1.5°C of declared ones. Measurements revealed how valves' flow change as temperature drops.

Results of measurements in different medium temperatures for four valves are in figure (47). Measurements were done for all valves, but for readability and space concerns only four are shown here. Valves are from different DFCUs.

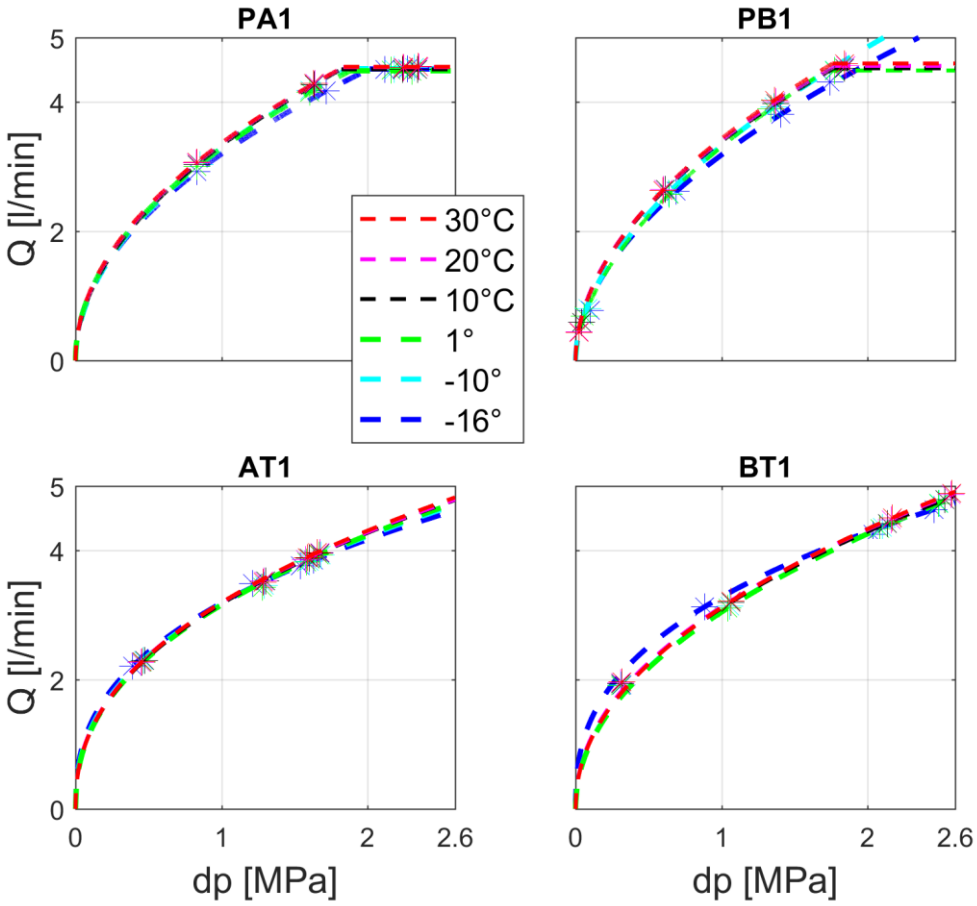

Figure 47. *Diagrams of fluid flow as function of pressure differential for four valves.*

Figure (47) shows, in which pressure differentials sample points were. This justifies the usage of only two data points to curve fitting. For pressure side valves there were only two samples in operational zone of approximately 0.5…1.5 MPa pressure differential. Two of the points were in cavitation area, for PA-DFCU. For PB-DFCU, one sample is in very small pressure differentials and another in cavitation area. This excludes measurements with medium temperatures of −16°C and −10°C, because measured points move out of the cavitation area. Therefore, parameter *b* remained unknown for PB-DFCU valves in those medium temperatures. Change in medium temperature decreases the fluid flow, but effect is not drastic. Tank side valves behave differently, because in practice cavitation chocking is affecting from the start. This is because outlet pressure of valve stays constant and inlet pressure changes. For pressure side valves, this goes the other

way around. Effect of decreased temperature is also visible and seems to be bending of the curve. This will be discussed later more thoroughly. Results for other valves in corresponding boundaries were similar, when compared to the example valves of figure (47). K_v values for all valves in different temperatures are in figure (48).

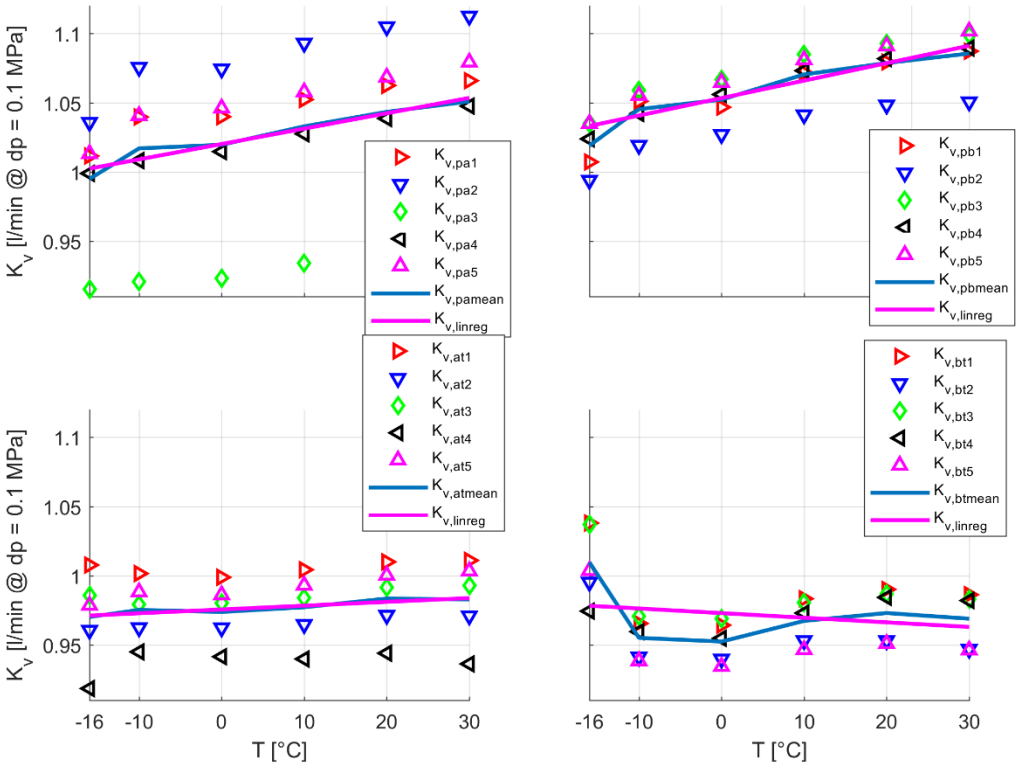

Figure 48. *Flow coefficients as function of temperature.*

Figure (48) shows clear decline trend in lower temperatures for pressure side valves' flow coefficients K_v. Drops are for PA-DFCU 4.9 % and for PB-DFCU 5.3 % in regression line. Trend for AT-DFCU's valves is also decreasing, but the drop is only 1.3 % in regression line. Results are more complicated for BT-boundary's valves. Flow coefficient is clearly decreasing until measurements done in medium temperature of −16°C. Flow coefficient seems to make drastic increase, which makes the total trend of flow coefficient to increase as temperature decreases. The result is contrary to results from other boundaries. The most probable explanation for this will be discussed later, with results of exponent. The increase in regression line is 1.6 %. If measurements on −16°C were excluded from regression line, decrease in flow coefficient would be 2.3 %. This would be similar result as gained from AT-DFCU. Most notable individual valve is PA3, which flow coefficient differs greatly from other pressure side valves. Differing result was not due to bad valve, but misplaced drilling of valve manifold, which created an extra orifice in front of the valve. Results for exponents are in figure (49).

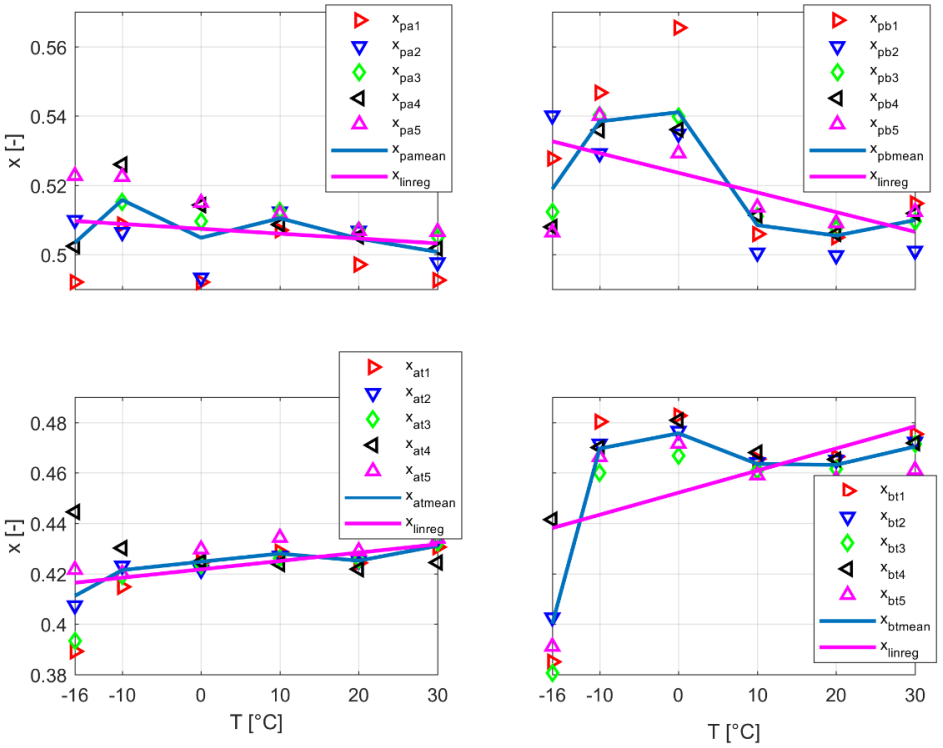

Figure 49. *Exponents as function of temperature.*

Figure (49) shows that for pressure side valves trend of exponent is to increase as temperature decreases. Increase is 1.3 % for PA-DFCU valves and 4.9 % for PB-DFCU valves in regression line, as temperature decreases from 30°C to −16°C. Although, one must consider that for especially PB-DFCU the regression line does not seem to reflect very well the exponents gained from curve fitting.

Exponent of AT-DFCU valves decreases as temperature decreases. The decrease is 3.5 % from 30°C to −16°C in regression line. Results for BT-DFCU valves are again more complicated. The trend is increase of exponent as medium temperature decreases, but from −10°C to −16°C sharp decrease in exponent is evident and this makes the total trend of exponent to decrease as medium temperature decreases. Total trend of decrease in exponent as medium temperature decreases from 30°C to −16°C for BT-DFCU is 8.4 %. If exponent of −16°C is excluded from linear regression, then the exponent would increase 2.4 % as temperature decreases from 30°C to −16°C.

It is evident that examination that is more thorough is needed for BT-DFCU in temperature interval of −10°C to −16°C, when this result is combined with BT-DFCU's flow coefficients' sharp increase in same temperature interval in figure (49). It is unlikely that the characteristics of valves of BT-DFCU would change this drastically, because nothing comparable is seen with other valves of other boundaries. Therefore, it is most likely that characteristic of measured sample point changes, which then has great effect on curve fitting. This was seen in figure (47) for BT1 valve, where the measured sample point of

medium temperature −16°C in about 1 MPa pressure differential is in lower pressure differential but has about the same volume flow as in measurements in other medium temperatures. The point was used in curve fitting and therefore it has drastic effect on exponent and flow coefficient. Reason for the change of characteristic of this one point is most likely found in fact that flow coefficient is constant only in higher Reynold's numbers, as was earlier mentioned in chapter (4.1.1). Fluid's viscosity increases as temperature decreases, which on the other hand decreases Reynold's number when volume flow stays constant. It is likely that the sample point in question moves from constant flow coefficients to area of increased flow coefficients in medium temperature of −16°C. This then alters results of curve fitting drastically.

Something also noticeable from figure (49) is change in dispersion of exponents of DFCUs. Dispersion of exponents of all boundaries increase in lower temperatures, which might be a symptom of method to use only two points in curve fitting. On the other hand, similar phenomenon is not noticeable in flow coefficients in figure (48). This suggests that the exponent is harder to predict than flow coefficient, because the behaviour of it seems to alternate more independently between valves.

Last determined parameter was cavitation choking ratio *b*. This was determined only for the pressure side valves. Tank side valves are in cavitation from the start, because the inlet pressure is altered rather than outlet pressure, which is tank pressure of 0 MPa. Cavitation choking was determined for valves of PA-DFCU in all temperatures. Cavitation choking of valves of PB-DFCU were determined in positive temperatures, because the measured point moved out of cavitation choking are in sub-zero temperatures. Results for cavitation choking ratio are in figure (50).

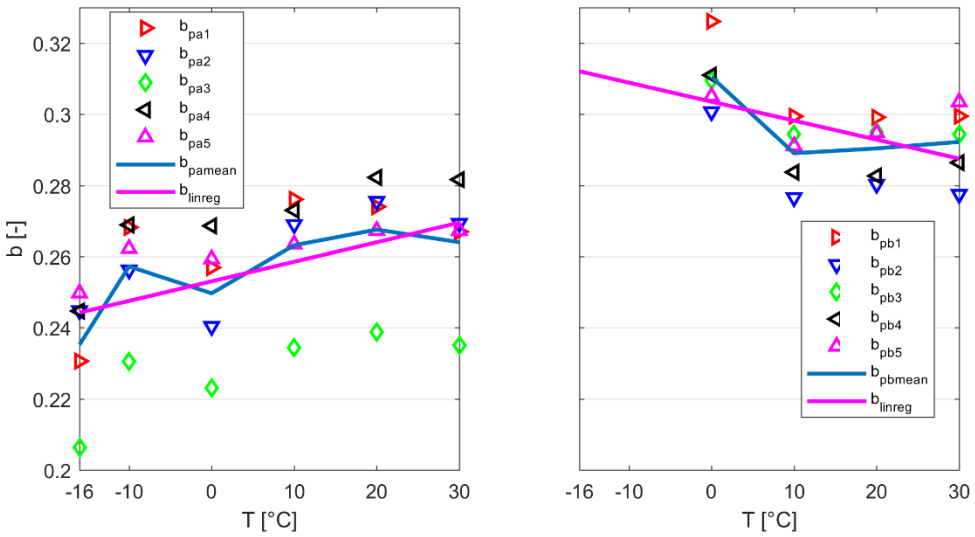

Figure 50. *Cavitation choking ratio as function of temperature.*

Figure (50) show quite clear trend for PA- DFCU valves' cavitation choking ratios. The trend is to decrease when medium temperature decreases. The change is 9.4 % decrease

in regression line, when temperature decreases from 30°C to −16°C. Results for PB-DFCU are little more complicated. From medium temperature 30°C to 10°C trend is decreasing as temperature decreases, which was also the case with PA-DFCU. The trend in that interval can be seen in average value of ratio. At the last interval of medium temperature decrease, the ratio takes sharp increase, which makes the total trend to increase as temperature decreases. Measured cavitation choking sample in medium temperature of 1°C is only barely in the cavitation area, which might distort the determined value and it is likely that the real ratio decreases as medium temperature decreases. Prediction for change of cavitation choking ratio is increase of 8.6 % when temperature decreases from 30°C to −16°C. If the measurement done with 1°C medium temperature is excluded, the prediction would be a decrease of 2.5 %, which is much closer to value determined for the PA-DFCU.

8. MEASUREMENTS OF TRAJECTORIES

Measurements of trajectories were done to prove feasibility of equal coded switching control for slower valves than were used by Paloniitty & Linjama (2018). Results were then compared with results of sum flow control made with similar valves and with the same cylinder bench by Linjama & Vilenius (2005). On the other hand, aim was to examine how the results change in lower temperatures and what is the possible way to improve supposedly degrading results.

Draft for measurements was to measure three different trajectories in three different medium temperatures. Trajectories were strokes of 15 mm, 150 mm and 300 mm with position references of fifth order polynomials. Trajectories were driven back and forth, and one movement time was 2 s, which was used also by Linjama & Vilenius (2005). Although, they used strokes of 15 mm, 50 mm and 200 mm. The results are comparable, when ratio of maximum error to maximum velocity is used as reference value. Extraction trajectory was in time interval 1…3 s and retraction trajectory in time interval 5…7 s in following measurement figures. Trajectories were driven five times in a single temperature to increase reliability of results. One measurement figure for all driven trajectories in all temperatures is given to show characteristic behaviour of the system in corresponding environment. Maximum position error Δx_{max} was used to compare results of different medium temperatures. Used error values were averaged values of different trajectory measurements done in a single temperature. Three different medium temperatures were −18°C, −1°C and 32°C. Temperature varied during measurements but stayed within ±2°C of declared ones.

8.1 Tuning of controller

Tuneable parameters of motion controller are proportional gain K_p and time constant τ for first order low-pass filter of position error. Tuneable parameters of model based-controller are parameters of flow model: flow coefficients K_v, exponents x, cavitation choking ratios b. Switching controller tuneable parameters are minimum pulse width w_v and time compensation parameter t_c. Other parameters to be defined are sample time or period of control cycle, sample time of switching controller, cut-off frequency of pressure filters and threshold tolerance of closed loop velocity reference v_{tol}.

Parameters of controller are collected to table (7). Parameters of model-based controller's flow model are separated to table (8), because parameters differ between different DFCUs. Detailed explanations for parameter values are given afterwards.

Table 7. *Parameters of controllers.*

Parameter	Value
Period of control cycle	10 ms
Sample time of switching controller	1 ms
MWPMW control interval	1.3…3.7
Cut-off frequency of pressure filters	10 Hz
v_{refc} error tolerance v_{tol}	5 mm/s
Proportional controller gain K_p	17 1/s
Time constant of position error filter τ	44 ms
Minimum pulse width w_v	7 ms
Closing time compensation t_c	5 ms

Table 8. *Parameters of model-based controller.*

Parameter	PA-DFCU	PB-DFCU
Flow coefficient K_v(T(°C))	$5.85*10^{-11}$*T(°C) + $5.37*10^{-8}$	$7.13*10^{-11}$*T(°C) + $5.54*10^{-8}$
Exponent x	0.5013/0.5071	0.5104/0.5274
Cavitation choking ratio b	0.27	0.30

Motion controller tuning is based on equations (30), (32) and (33). Hydraulic natural frequency of the system, when medium temperature is 30°C, was measured to be 64.1 rad/s. Using equation (30), desired time constant τ could be defined to be 46.8 ms. Because of miscalculation a value 44 ms was used, but it is still larger than $2/\omega_h$ with a large margin. Setting proportional gain $K_p = 17$, results in closed loop natural frequency $\omega_c = 20$ rad/s and closed loop damping factor $\delta_c = 0.58$. Motion controller tuning was kept constant between measurements, even though increase in hydraulic natural frequency in lower temperatures would have allowed retuning controller to be faster.

Tuning of model-based controller based on measurements of valves' average characteristics. Some adaptivity was integrated to controller. Flow coefficients were adaptive to temperature and regression lines of figure (48) were used. Regression line for PA-DFCU was $K_{v,PA}$(T(°C)) = $5.85*10^{-11}$*T(°C) + $5.37*10^{-8}$ and for PB-DFCU $K_{v,PB}$(T(°C)) = $7.13*10^{-11}$*T(°C) + $5.54*10^{-8}$. Idea to use regression line was considered also for pressure differential exponents. Because, regression line of PB-DFCU exponent in figure (49) did not display measured values of individual valves very well, a compromise was then used. For measurements in 32°C average values of exponents in corresponding temperature was used: $x_{PA} = 0.5013$ and $x_{PB} = 0.5104$. For two other temperatures, average values of all measurements were used: $x_{PA} = 0.5071$ and $x_{PB} = 0.5274$. This was justified by, the measurement results of exponent of PB-DFCU, in which results formed S-shape, therefore average value was good approximation. On the other hand, change in more linearly behaving average results of PA-DFCU was only 1.3 % from maximum temperature to minimum temperature. This fact indicates that the dispersion of exponents of individual valves of PA-DFCU have more significance to results than slight

inaccuracy in average value. Cavitation choking measurements were depicted in figure (50). Used cavitation choking ratios were the measured average values in 30°C: b_{PA} = 0.27 and b_{PB} = 0.30. Usage of only one value for all temperatures was justified by the fact that the pressure levels of chambers were not premised to be in cavitation choking area and the values were still rather good approximations of ratios measured in lower temperatures.

Tuning of switching controller based on the pulsation test. All the valves were determined to be in linear area of volume flow with 7 ms pulse width. Therefore, minimum pulse width w_v = 7 ms. Results of figure (44), indicated that time compensation parameter t_c was most likely 3…5 ms. The right value was verified with open loop tests using trajectory of 150 mm stroke. Best result was with 5 ms compensation, which resulted in maximum error of 11.1 mm. Compensations of 3 ms, 4 ms and 6 ms resulted in maximum errors of 33.1 mm, 19.3 mm and 11.5. Therefore, time compensation was set t_c = 5 ms. These parameters were constant during measurements, except for second round of measurements done in medium temperature of -18°C.

Other parameters were chosen more arbitrarily. Frequency of control cycle was decided to be 100 Hz, which equals to period of 10 ms. Period is suitable, because it is larger than minimum pulse width, but smaller than sum of minimum pulse width and time compensation. Setting period of control cycle, also sets suitable control interval of MVPWM, as were determined in equations (45) and (47). Control interval of MVPWM is $1.3<u_{dec}<3.7$ from maximum interval of 0…5. Sample time of switching controller was set to 1 ms. Smaller value was tested, but CAN was not capable handling such time interval. Cut off frequency of pressure filters were set to 10 Hz. Threshold of closed loop velocity reference was set to prevent too early initial movement, but to not allow error grow too large before initial movement. Good compromise was v_{tol} = 5 mm/s.

8.2 Medium at 32°C

Trajectory measurements done in 32°C were in great interest to prove the feasibility of the control method of MVPWM and MWPFM with slow on/off valves generally. On the other hand, results of measurements in this medium temperature are used as reference to measurements done in lower temperatures.

Typical response for 15 mm stroke when medium temperature is 32°C is in figure (51). Control stays in MVPFM area for entire motion. Movement is rather step-wise and velocity spikes from zero to close of 100 mm/s. This behaviour was not unexpected, because control values $u_{dec} < 1$ means that either one valve is open, or all valves are closed. Position error depicts this rather well with its sawtooth like behaviour. Spiking of velocity, in measurement of figure (51), is greater to positive direction. This is most likely due to pressure levels of chambers, which are lower in positive direction. Pressure differential is higher with lower chamber pressures, which produces more flow through valve, even

though pulse width is same to both directions. Considerable pressure fluctuation is clearly visible, and it was something to expect, because of constant closing of DFCUs. Something also noticeable in figure (51), is the working of fine tuner of position after 3 s mark. Fine tuner works properly in this case.

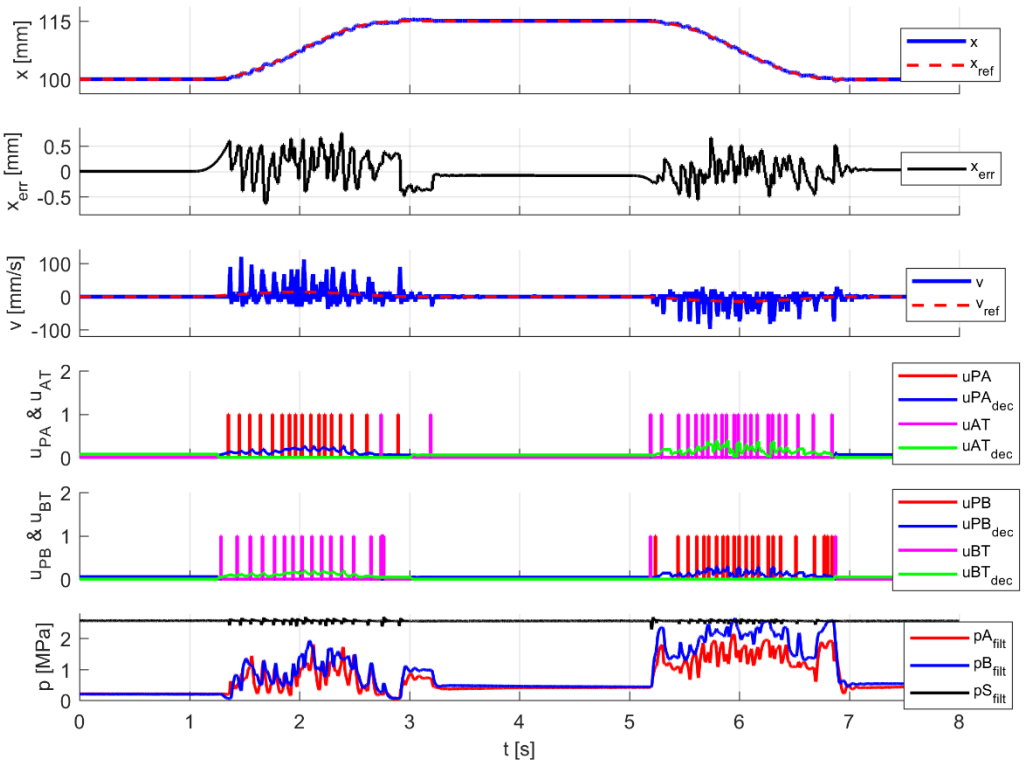

Figure 51. *Measured 15 mm response with medium temperature of 32°C.*

Response for 15 mm stroke was measured five times and results of maximum position errors are in table (9). First measurement has clearly largest position error. This is in fact an example of fine tuner working improperly, because the maximum error was in fact caused by over movement done by fine tuning of position. Without error caused by fine tuning of position, the first measurement would have had lowest maximum error measured.

Table 9. *Measured position errors of 15 mm stroke with medium temperature of 32°C.*

Measurement	Max error [mm]
1	1.097
2	0.762
3	0.895
4	0.801
5	0.841
Average	0.879

Typical measurement for 150 mm stroke when medium temperature is 32°C is in figure (52). The motion is continuous unlike was the case with 15 mm stroke and position error behaves much more linearly. Control switches to MVPWM, when $u_{dec} > 1.3$. Compensation of longer closing time is clearly visible in control values, because floating-point control value u_{dec} surpasses value 1, but control values of integer u_{int} follows only after $u_{dec} > 1.5$. Pressure fluctuation is considerably lower than was the case with 15 mm stroke. Pressure fluctuation can be seen also, in floating point control value u_{dec} which fluctuates as pressure fluctuates.

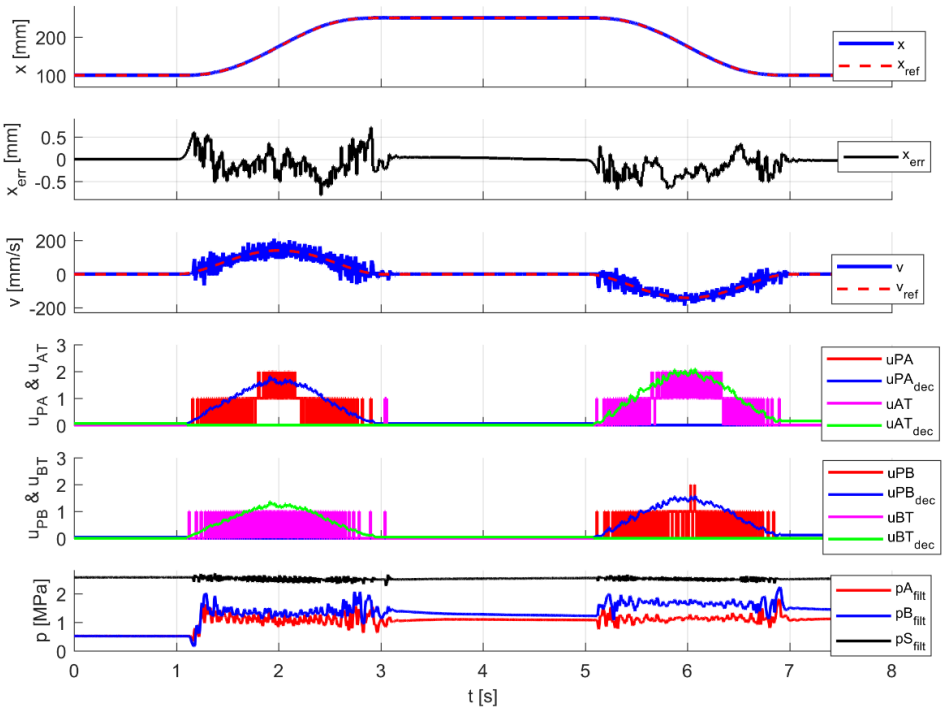

Figure 52. *Measured 150 mm response with medium temperature of 32°C.*

Response for 150 mm stroke was measured five times and results of maximum position errors are in table (10). All maximum errors occurred roughly around 2.5 s mark, in which piston rushes. Around this mark, change from MVPWM to MVPFM happened to PA-DFCU. Change of control method is problematic because of asynchronous clocks. In this case, the effect was too large opening of PA-DFCU.

Table 10. *Measured position errors of 150 mm stroke with medium temperature of 32°C.*

Measurement	Max error [mm]
1	0.915
2	0.811
3	1.168
4	0.978
5	0.769
Average	0.928

Typical measurement for 300 mm stroke when medium temperature is 32°C is in figure (53). Control is mostly in MVPWM, but crosses to MVinvPFM for AT-DFCU. Pressure fluctuation is minimal, when compared to previous strokes. Only exception is during fine tuning of position. Maximum position error occurs during peak velocity of retraction, in around 6 s mark. This was same for all individual measurements. Error in retraction is considerably higher than in extraction, which suggests that parameter tuning was not as successful for PB-DFCU as it was for PA-DFCU.

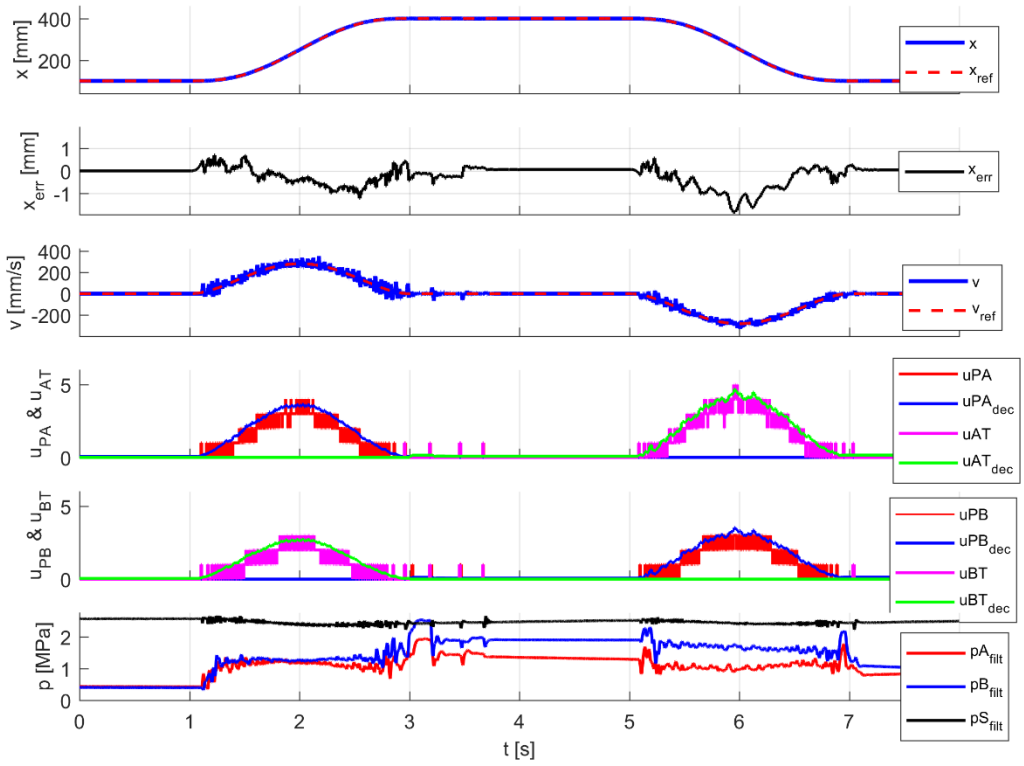

Figure 53. *Measured 300 mm response with medium temperature of 32°C.*

Response for 300 mm stroke was measured five times and results of maximum position errors are in table (11).

Table 11. *Measured position errors of 300 mm stroke with medium temperature of 32°C.*

Measurement	Max error [mm]
1	1.649
2	1.864
3	1.436
4	1.747
5	1.423
Average	1.624

Averaged maximum position errors from tables (9), (10) and (11) are grouped up to figure (54).

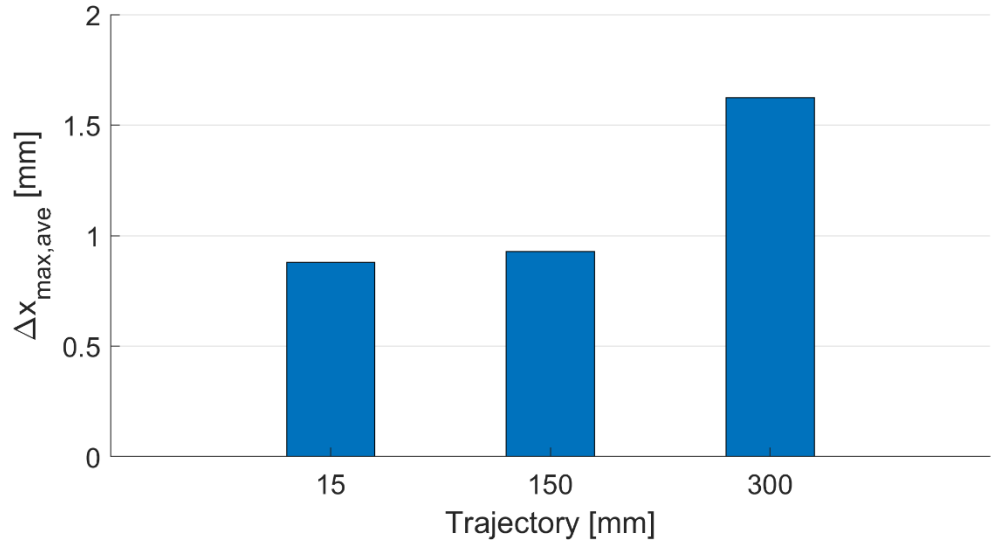

Figure 54. *Average maximum position errors when medium is 32°C.*

Figure (54) shows that maximum error is not sensitive to velocity, when trajectories of 15 mm and 150 mm are compared. Error increases significantly in trajectory of 300 mm, but the error increase is concentrated in retraction and during extraction maximum error is increased only to average of about 1.2 mm. This leaves question open, if this is due to poor tuning of controller for PB-DFCU or is the controller's boundary of performance reached. The error's behaviour is linear and control value is not close to maximum, which indicates that the reason is in tuning of controller. Although, even these results are rather good, resulting in maximum error (1.624 mm) and maximum velocity (280 mm/s) ratio of 5.8 (ms), which is close to 5.3 (ms) attained by Linjama and Vilenius (2005) using sum flow control in binary coded 4x4 DVS.

8.3 Medium at −1°C

Measurements were done in same manner as was earlier. Objective was to research how the results change, when tuning of switching parameters were not changed. Exception was flow coefficient, which change as a function of temperature and exponent, which was set to average.

Typical response for 15 mm stroke when medium temperature is -1°C is in figure (55). Maximum error occurs close to the end of deceleration, which was typical case in these five measurements. This was rather interesting phenomenon as similar did not seem to occur when medium was warmer. Closer look to the measurements reveals that these errors are caused by intersecting pulses of P-side and T-side DFCUs when control value is low and desired velocity is slow. It seems that intersecting pulses causes larger velocity peaks. Reason why this was not revealed already in measurements done in 32°C was not in fact that it did not occur. Reason was that phenomenon occurred but only when error

was significant to other direction. Therefore, peak in error was not noticeable from normal sawtooth like behaviour.

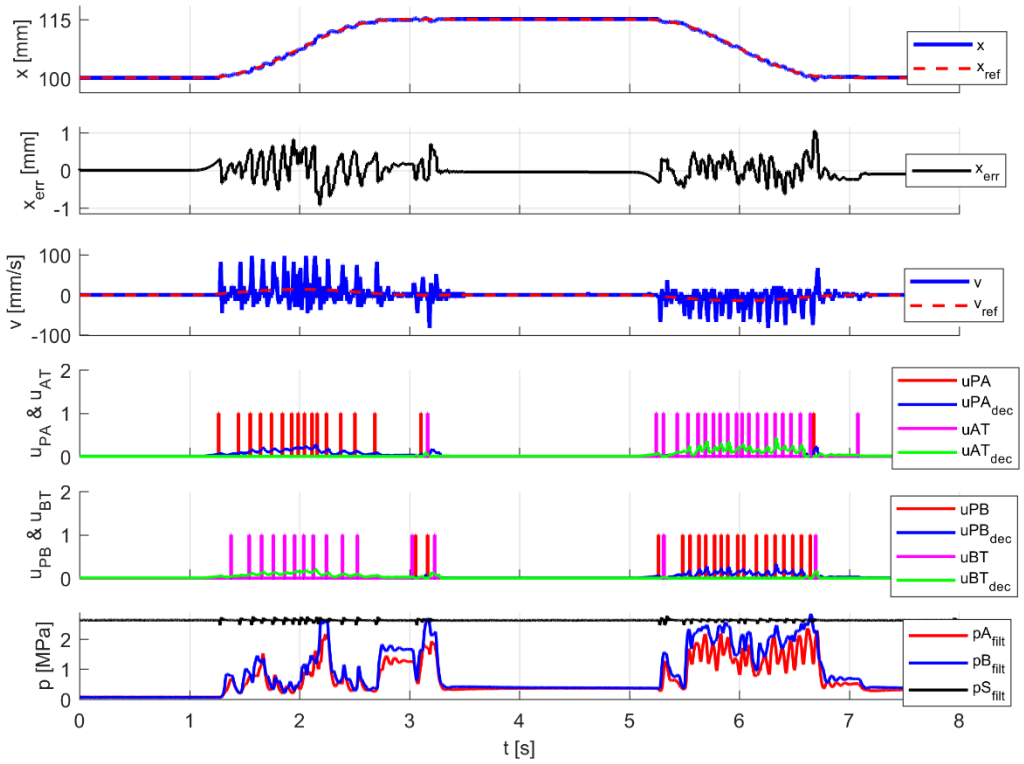

Figure 55. *Measured 15 mm response with medium temperature of −1°C.*

Pressure fluctuation in extraction is clearly smaller in figure (55), but this was not the case in every measurement. Some measured pressures during extraction behaved similarly to figure (51), which depicted typical behaviour of 15 mm stroke with medium temperature of 32°C. Response for 15 mm stroke was measured five times and results of maximum position errors are in table (12).

Table 12. *Measured position errors of 15 mm stroke with medium temperature of −1°C.*

Measurement	Max error [mm]
1	1.089
2	1.048
3	1.027
4	1.582
5	1.444
Average	1.238

Typical response for 150 mm stroke when medium temperature is -1°C is in figure (56). One noticeable phenomenon in the measurement is that the fine tuner is not able to tune position efficiently. This was partly due to poor fine tuner but more, because of drifting of piston. This phenomenon was noticed in lower temperatures. Piston did not steady after

movement, but started to drift, which caused position oscillation, because fine tuner tried to correct the position back to allowed interval. The most probable explanation for the phenomenon is that in lower temperatures seals of piston revert to unbent form slower.

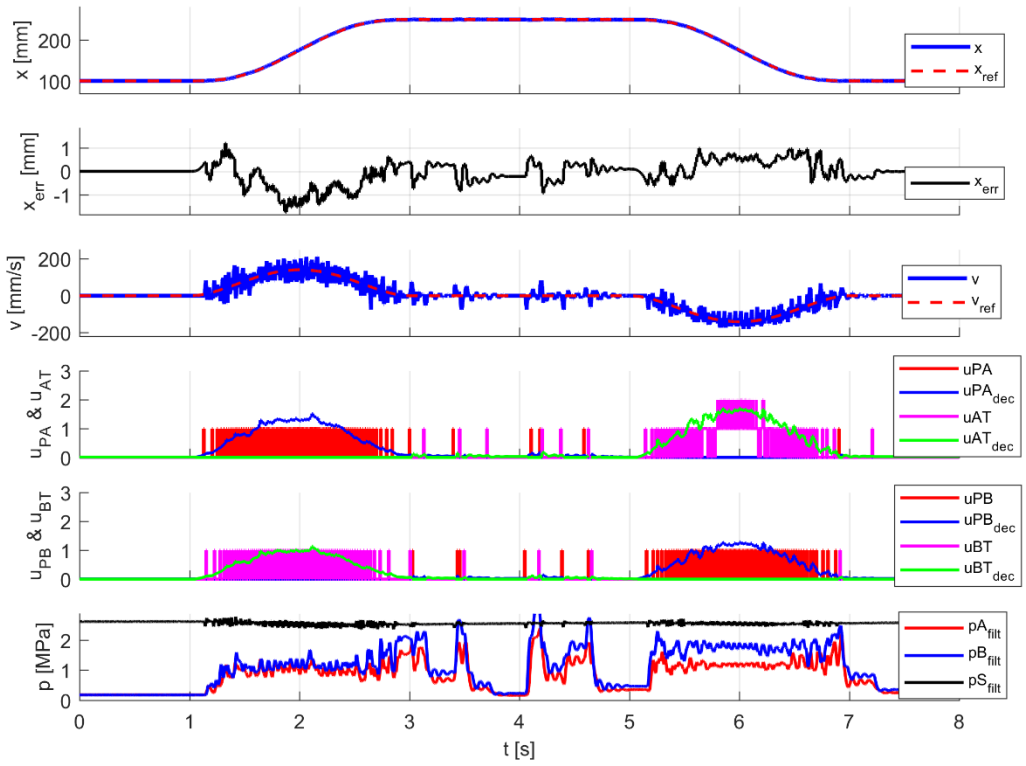

Figure 56. *Measured 150 mm response with medium temperature of −1°C.*

Piston rushes in motions to both directions, which is a symptom of too low closing compensation value. In measurements, maximum errors occurred either on around middle of extraction or then in start of motion or end of motion similarly to measurements of 15 mm stroke. Response for 150 mm stroke was measured five times and results of maximum position errors are in table (13).

Table 13. *Measured position errors of 150 mm stroke with medium temperature of −1°C.*

Measurement	Max error [mm]
1	1.206
2	1.732
3	1.694
4	1.695
5	1.359
Average	1.537

Typical response for 300 mm stroke when medium temperature is -1°C is in figure (57). Position error during retraction shows that unwanted behaviour occurs when control value

of PB-DFCU crosses over value 3. After this piston position suddenly lags from reference. On the other hand, position error during extraction is now about equal but because of rushing. Rushing was something to expect after it was noticed in stroke of 150 mm. Although, rushing can be seen also in retraction in control values below 3, because in measurements done with medium temperature 32°C lag in position is observable from start of motion to end of it.

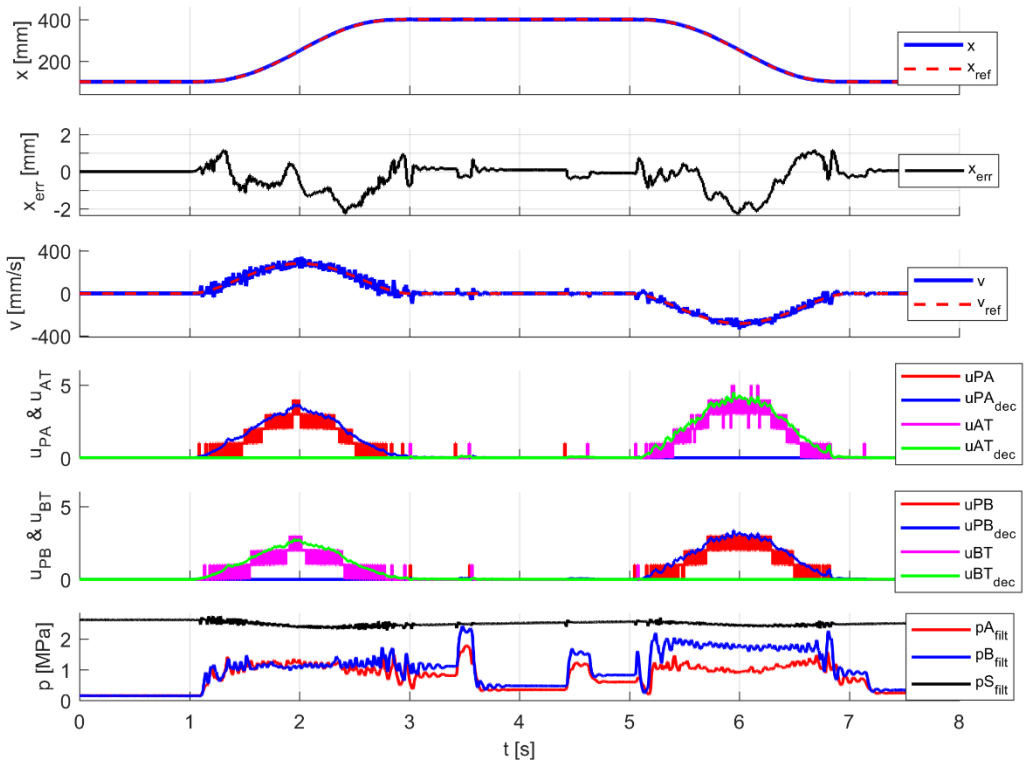

Figure 57. *Measured 300 mm response with medium temperature of −1°C.*

Response for 300 mm stroke was measured five times and results of maximum position errors are in table (14).

Table 14. *Measured position errors of 300 mm stroke with medium temperature of −1°C.*

Measurement	Max error [mm]
1	2.594
2	2.251
3	2.391
4	2.940
5	2.829
Average	2.601

Averaged maximum position errors from tables (12), (13) and (14) are grouped up to figure (58).

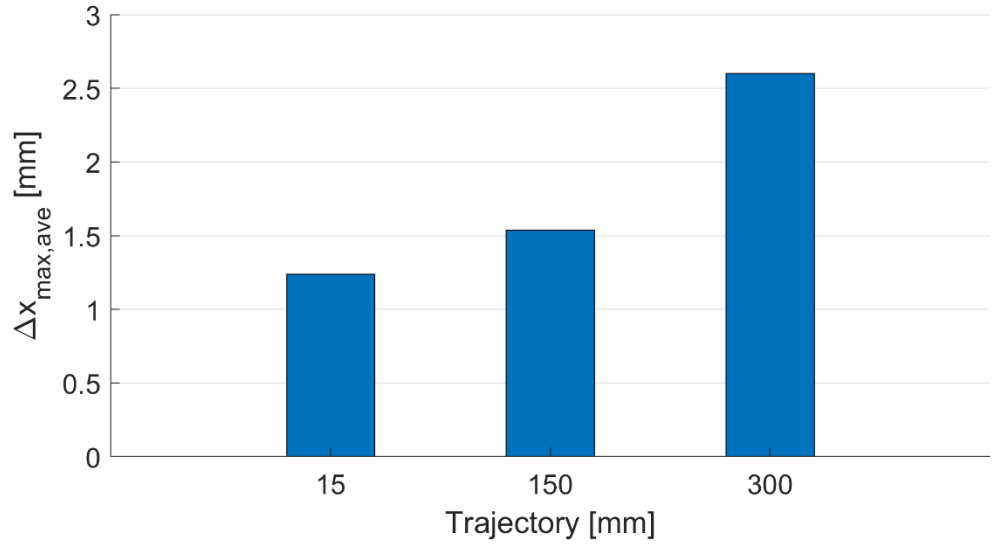

Figure 58. *Average maximum position errors when medium is −1°C.*

Figure (58) shows that maximum position error is more dependent on velocity than was the case with measurements done with medium temperature of 32°C. Although, results have degraded, the maximum position error to maximum velocity ratio is still 9.3 (ms). The result is comparable to reference results of 5.3 (ms) and 5.8 (ms).

8.4 Medium at −18 °C

Initially, the measurements were to be done as earlier with medium temperature of -1°C. Controller parameters were to be kept same as was used with medium temperature of 32°C, except model-based controller's parameters flow coefficient K_v and exponent x. The initially intended set of measurements was executed, but after analysing performance of the system with used parameter values, a decision of a second round of measurements was done. Intend of the second round of measurements was to enhance the performance of the system. Tuning of switching controller parameters was natural way to go forward. Minimum pulse width w_v and closing time compensation parameter t_c were potential tuneable parameters. Tuning was aimed to only t_c, because of time consuming temperature control of medium. On the other hand, this was justifiable, because interest was to find a way to improve performance rather than to get best possible parameter values or response results. Tuning was done with open loop response of 150 mm trajectory. Pulsation tests indicated that desired t_c is between interval of 8...20 ms. Open loop response for t_c= 9 ms was deemed to give best compromise. Piston rushed 31 mm during extraction and 5 mm during retraction. Optimal t_c for extraction would have been 12 ms. This result indicated that the different DFCUs should have been tuned independently also in switching controller and not only in model-based controller. Increase in t_c also narrows the interval of MVPWM control to u_{dec} values 1.6…3.4.

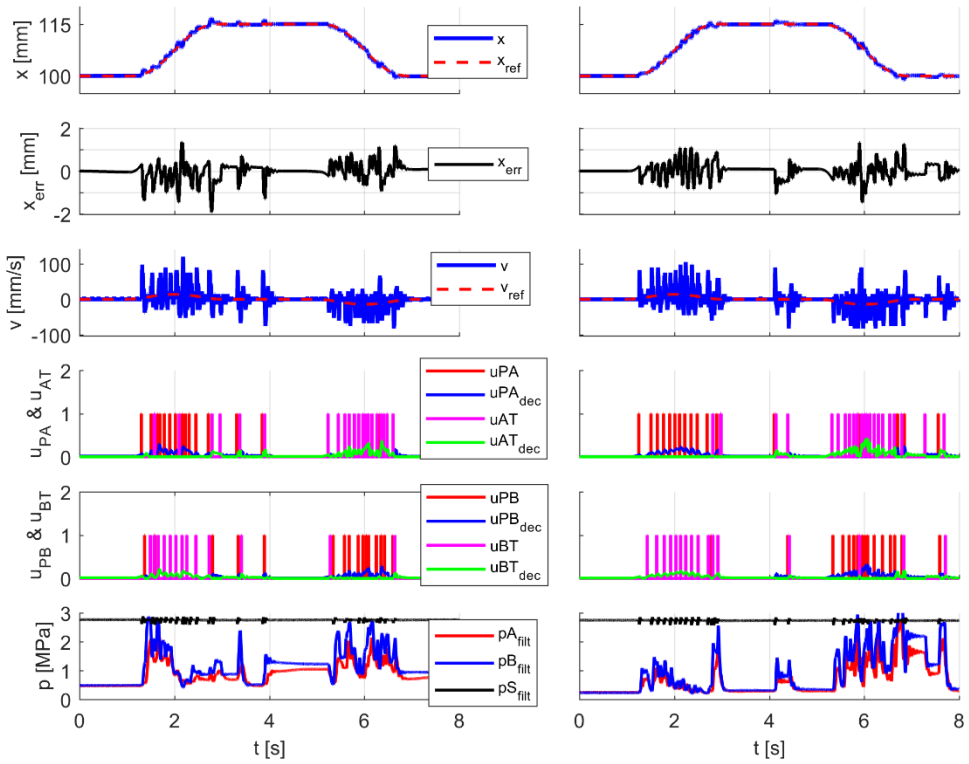

Figure 59. *Measured 15 mm responses with medium temperature of -18°C. Left side using t_c = 5 ms and right side using t_c = 9 ms.*

Typical responses for 15 mm stroke when medium temperature is -18°C are in figure (59). Increase of t_c improves performance mainly in during extraction, which has poorer performance in first place. One reason why the performance is poorer in first place might be that flow happens in area of cavitation choking and cavitation choking parameter was not tuned after measurements done with medium temperature of 32°C. Performance in retraction is better, but pressure fluctuation is more intense compared to extraction or responses with warmer mediums. Responses for 15 mm stroke using t_c = 5 ms (marked using [1]) and t_c = 9 ms (marked using [2]) was measured five times and results of maximum position errors are in table (15).

Table 15. *Measured position errors of 15 mm stroke with medium temperature of -18°C.*

Measurement	Max error [mm][1]	Max error [mm][2]
1	2.076	1.968
2	1.931	1.480
3	1.877	1.358
4	1.546	1.517
5	1.835	1.324
Average	1.853	1.530

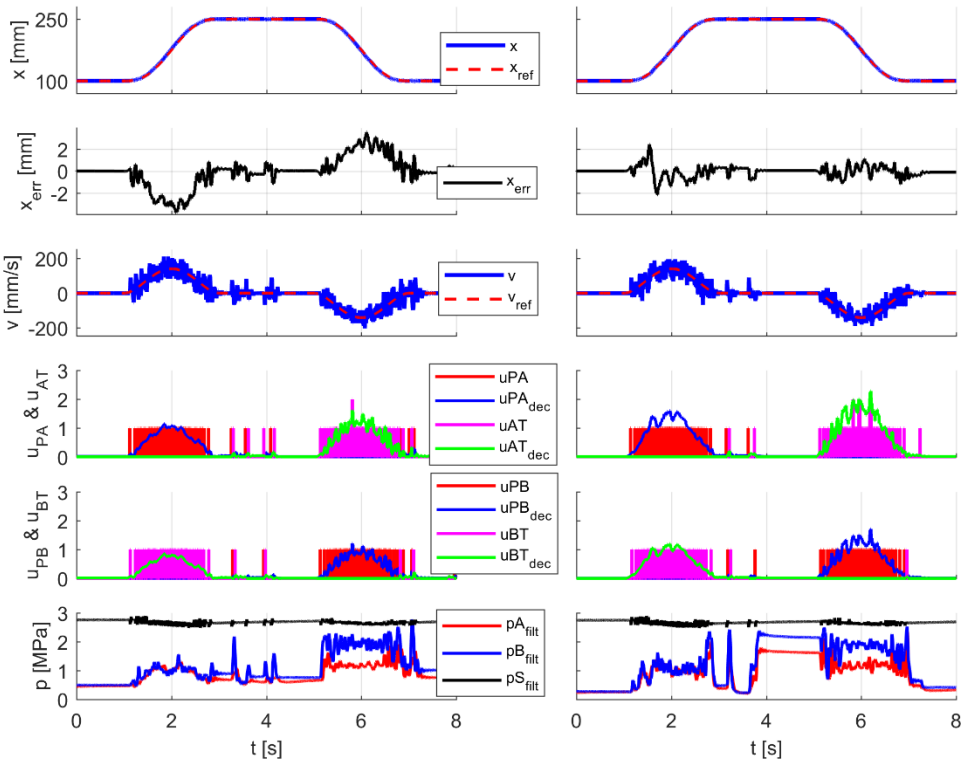

Figure 60. *Measured 150 mm responses with medium temperature of -18°C. Left side using t_c = 5 ms and right side using t_c = 9 ms.*

Typical responses for 150 mm stroke when medium temperature is -18°C are in figure (60). Error behaviour of response using 5 ms closing compensation t_c shows the effect of considerably too low closing compensation t_c as piston rushes during motions of both directions. Increase of closing compensation t_c has drastic improving effect on performance. Responses for 150 mm stroke using t_c = 5 ms (marked using [1]) and t_c = 9 ms (marked using [2]) was measured five times and results of maximum position errors are in table (16). Table not only show that maximum error decreases, when t_c = 9 ms, but also range of variation interval decreases considerably from 3.5 mm to 1.7 mm.

Table 16. *Measured position errors of 150 mm stroke with medium temperature of -18°C.*

Measurement	Max error [mm][1]	Max error [mm][2]
1	5.641	1.855
2	3.748	2.419
3	5.111	3.552
4	7.290	2.614
5	4.572	2.451
Average	5.272	2.578

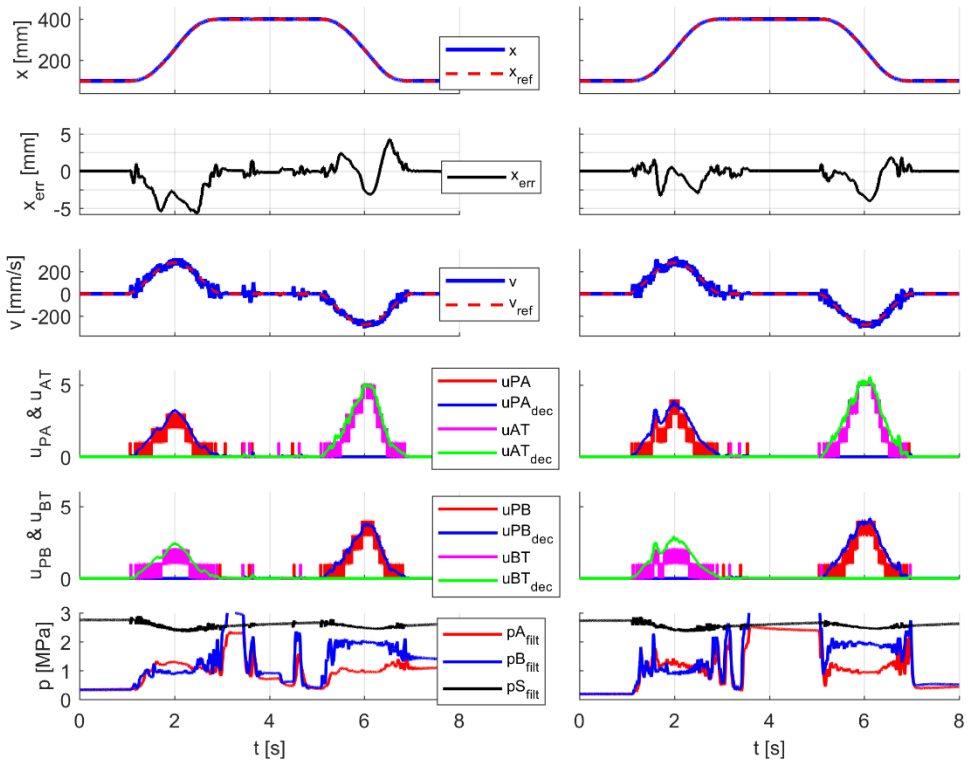

Figure 61. *Measured 300 mm responses with medium temperature of -18°C. Left side using t_c = 5 ms and right side using t_c = 9 ms.*

Typical responses for 300 mm stroke when medium temperature is -18°C are in figure (61). Increase in tc corrects rushing of piston but does not influence on noticeable lagging spike in error around maximum velocity of retraction. This is same phenomenon noticed already with warmer medium temperatures, when control value $u_{dec} > 3$. For higher t_c this phenomenon is even worse, because control of PB-DFCU is in MVinvPFM. Problem emerges, because MVinvPFM control, when $u_{dec} < 4$, was handmade and was intended only for initial control interval of 3.7…4 rather than 3.4…4, which it was used in higher t_c response. Responses for 300 mm stroke using t_c = 5 ms (marked using [1]) and t_c = 9 ms (marked using [2]) was measured five times and results of maximum position errors are in table (17).

Table 17. *Measured position errors of 300 mm stroke with medium temperature of -18°.*

Measurement	Max error [mm][1]	Max error [mm][2]
1	6.310	4.286
2	5.748	4.014
3	5.702	3.423
4	5.956	4.086
5	5.350	3.630
Average	5.813	3.888

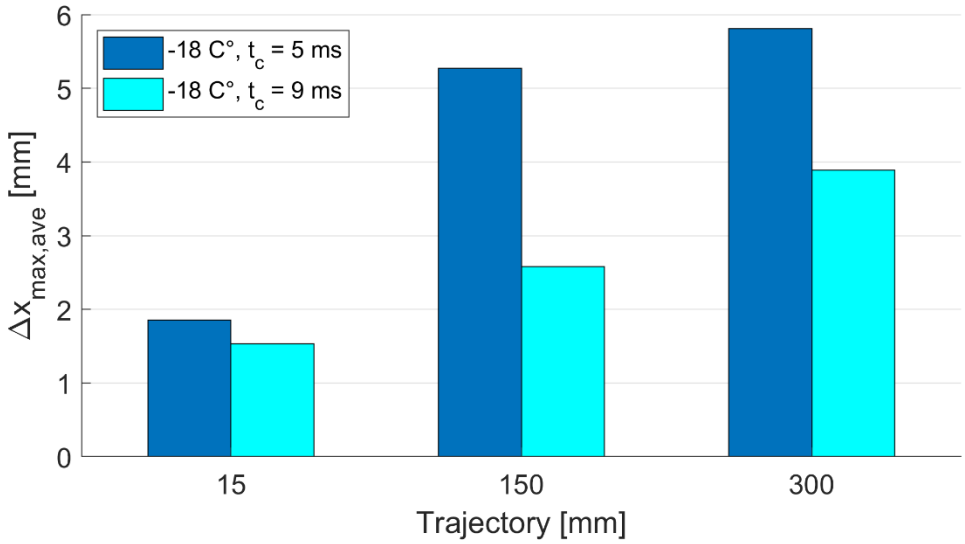

Figure 62. *Average maximum position errors when medium is −18°C*

Figure (62) shows that considerable decrease in maximum errors was achieved, with slight retuning of controller. The maximum position error to maximum velocity ratio of t_c = 5 ms response is 20.8 (ms), which is almost four times the reference values 5.3 (ms) and 5.8 (ms). For response, in which t_c = 9 ms, same ratio is 13.9 (ms). Increase in performance is notable. One must consider that the minimum pulse width was not retuned, because of time consuming temperature control. The point was to show that potential of performance increase lies in switching controller.

8.5 Comparing results in all temperatures

All the measured average maximum position errors of different trajectories with different medium temperatures are in table (18).

Table 18. *All average maximum position errors*

Medium temperature [°C]	Δx_{max} [mm] (Traj. 15 mm)	Δx_{max} [mm] (Traj. 150 mm)	Δx_{max} [mm] (Traj. 300 mm)
-18 (t_c = 5 ms)	1.853	5.272	5.813
-18 (t_c = 9 ms)	1.530	2.578	3.888
-1	1.238	1.537	2.601
32	0.879	0.928	1.624

All the measured average maximum position errors of different trajectories with different medium temperatures are depicted in figure (63).

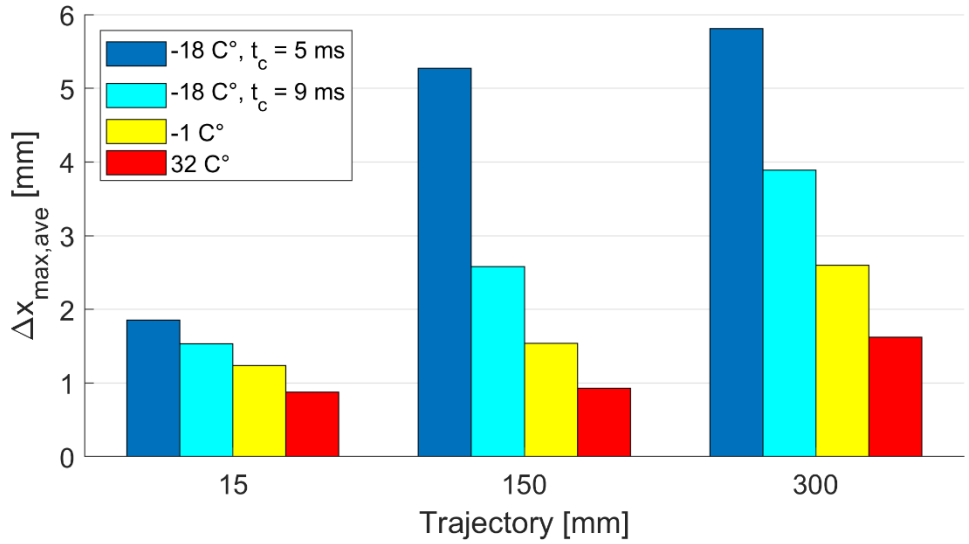

Figure 63. *Average maximum position errors of all measurements.*

Results show that maximum position error increases as medium temperature decreases. Pulsation test showed that decrease in medium temperature makes valves' opening and closing slower, which on other words can be described as decrease in valves' performance. Therefore, increase in maximum position error is something to expect as medium temperature decreases. This would be the case even with optimal controller. Maximum position error increases 60.2 % when medium temperature decreases from 32°C to -1°C. Increase is notable, but still bearable. Increase in maximum position error is 123 % from medium temperature -1°C to -18°C or 358 % from 32°C to -18°C. Performance decrease is unbearable. This indicates that making model-based controller adaptive does not have significant effect on keeping performance, when medium temperatures drops significantly below 0°C. This was perhaps something to expect, because changes in characteristics of flows of valves were quite minor even though fluids viscosity increases considerably. Results, when medium temperature is -18°C, shows that retuning of switching controller with more appropriate parameters increases performance. Performance does not return to level of warmer temperatures, but merely makes the decrease in performance to be about same level as is decrease from 32°C to -1°C. Increase in maximum position error is 49.4 % from medium temperature -1°C or 139 % from medium temperature 32°C.

9. CONCLUSION

This research composed of simulation study and experimental testing using real equipment. Simulation study was conducted to implement and to test the controller. Results of simulations were promising. Although, they proved to be overoptimistic in estimating the independence of error from maximum velocity of a trajectory. Experimental research composed of measurements of characteristics of the test system and measurements of trajectories driven using the MVPWM/MVPFM controller.

Measurements of characteristics were motivated by need of parameters for controller but were conducted also in differing medium temperatures to reveal changes in them. Three different set of measurements were done to reveal characteristics of hydraulic natural frequency ω_h, opening and closing times of valves and steady state flow characteristics. Flow characteristics compose of flow coefficient K_v, exponent x and cavitation choking ratio b. Interest of this research lies in the changes of these characteristics as medium temperature decreases. Changes in characteristics between measurements done with different medium temperatures are combined to tables (19) and (20).

Table 19. *Changes in hydraulic natural frequency and valves' dynamics*

T [°C] change	$\Delta\omega_h$ [%]	Opening time	Closing time
30°C -> 0°C	+10.1	Increase	Unidentified
30°C -> - 20°C	+25.7	Increase	Increase

Table (19) shows clear increase for hydraulic natural frequency. Dynamics of valves also slows down. Closing time change when medium temperature changed from 30 to 0 was left unidentified, because results for measured valves were contradictory.

Table 20. *Average changes in flow characteristics of DFCUs when medium temperature decreases from 30°C to -16°C*

DFCU	ΔK_v [%]	Δx [%]	Δb [%]
PA	-4.9	+1.3	-9.4
PB	-5.3	+4.9	Unidentified
AT	-1.3	-3.5	Unidentified
BT	+1.6/-2.3	-8.4/+2.4	Unidentified

Table (20) shows that flow coefficients of pressure side DFCUs decrease roughly 5 %. For tank side DFCUs decrease is considerably smaller. BT-DFCU has two values: first one considers the measurement done with -16°C medium. The measured flow coefficients differ greatly from the trend of results with other medium temperatures. Therefore, a second value, which does not take it into account is presented also. This value is much closer to value of AT-DFCU and thus more likely to be closer of the real one. Although, this value should also be used with caution, because it is more a prediction of total decrease of K_v, when medium temperature decreases the declared interval, rather than valid value

determined through measurements done to end of the temperature interval. Change in exponents of pressure side DFCUs differ greatly from each other both in level of increase and in behavior. Behavior of PA-DFCU exponent's change was quite linear, while behavior of PB-DFCU was S-shape where exponent increased sharply and then decreased as temperature of medium decreased. Exponent of AT-DFCU decreases and BT-DFCU has similar presentation as was with flow coefficient. If the measurement done with medium temperature -16°C is excluded the exponent increases, which is a contradictory result, when compared to exponent of AT-DFCU. Change in cavitation choking ratio was determined to only PA-DFCU, because PB-DFCU's had sample point in cavitation choking area only in warmer medium temperatures. In colder medium temperatures the sample point moved out of cavitation area. The last sample point measured in medium temperature of 0°C was greatly out of trend of sample points of warmer medium temperatures. On the other hand, using only measurements done in positive temperatures to predict change in negative temperatures is not seen valid. Therefore, change in cavitation choking ratio of PB-DFCU is safest to declare as unidentified. Tank side DFCUs are in area of cavitation choking practically always and therefore, their ratios are declared as unidentified. All in all, changes in flow characteristics of on/off valves seems to be quite minor, when medium of 50/50 water-glycol is used.

Reported problems above in flow parameters were a symptom of used determination method of measuring only couple of sample points of flow and then fitting a curve based on them. This method exposes determined parameters, which depicts quality of valve, to sample points' qualities and to changes in them. Flow coefficient is not constant but changes as function of Reynold's number and Reynold's number changes as function of viscosity. Viscosity then changes as function of medium temperature. This is most probable explanation for differing behaviors of different DFCUs of pressure and tank sides, even though used valves were similar in all of them. Therefore, a more valid measuring method with more sample points would have been an advantage. On the other hand, this would have demanded extra arrangements and valves, because the used test system was not capable to more complex measurements.

Second part of the experimental measurements were driving trajectories with horizontal cylinder to determine feasibility of controller and changes in performance in lower temperatures. Driven trajectories were 15 mm, 150 mm and 300 mm.

Equal coded MVPWM with MVPFM control method for digital hydraulic valve system, introduced by Paloniitty & Linjama (2018), is applicable also with slower, commercially more available on/off valves. Result of ratio of maximum position error to maximum velocity, using medium temperature 32°C, was 5.8 (ms), which is close to reference value of 5.3 (ms) (Linjama & Vilenius 2005). Although, result gained in this research was done with maximum velocity of 280 mm/s compared to 190 mm/s used in reference research. Additionally, maximum position error was encountered in retraction and maximum error

in extraction was somewhat lower. This indicates potential in reduction of maximum position error. One clear way would have been to use separate switching control parameters, minimum pulse width w_v and closing time compensation t_c, for PA- and PB-DFCUs. This method was used in research of Paloniitty & Linjama. Using mutual parameters forced to use compromise, which in this case suited better for PA-DFCU.

For measurements with medium temperatures -1°C and -18°C, controller's model-based controller was altered to use adaptive Kv and average values of x. Average value of x was justifiable for PA-DFCU, because the change was determined to be minimal and for PB-DFCU the behavior was nonlinear and therefore using linear model for it was deemed to be suboptimal. An extra set of measurements was done with medium temperature -18°C, in which parameter of closing time compensation was increased to more valid value. All trajectories were driven five times and average maximum errors are in table (21).

Table 21. *All average maximum position errors*

Medium temperature [°C]	Δx_{max} [mm] (Traj. 15 mm)	Δx_{max} [mm] (Traj. 150 mm)	Δx_{max} [mm] (Traj. 300 mm)
-18 (t_c = 5 ms)	1.853	5.272	5.813
-18 (t_c = 9 ms)	1.530	2.578	3.888
-1	1.238	1.537	2.601
32	0.879	0.928	1.624

Table (21) shows that results decrease with decrease of medium temperature. Error increase is notable with medium temperature -1°C, when compared to measurements done with medium temperature 32°C, but not yet alarmingly bad. Error with medium temperature -18°C using lower closing time compensation on the other hand is very poor. Using more valid closing time compensation increase performance considerably. This indicates that adaptiveness in model-based controller is not capable to keep performance good.

These results with flow characteristics measurements that indicated only minor changes in characteristics lead to the author's suggestion for controller. If performance in lower medium temperature is a concern the adaptivity should not be included in model-based controller, because change in characteristics are minor and model-based controller was not able to keep up the performance in this research. Therefore, defining steady state flow characteristics in normal operation temperature should be good enough approximation even for arctic medium temperatures. Author suggests that adaptivity should be included in switching controller, because performance increase was noted by retuning it in this research when medium with temperature -18°C was used. On the other hand, performance was still good, when medium's temperature was -1°C, which indicates that need for adaptivity, to keep up the performance, rises only when temperature of medium gets closer to arctic temperatures. In addition, increase in hydraulic natural frequency might allow using higher proportional gain K_p when medium temperature is lower. This perhaps interesting option was not examined in this research.

Implemented controller seems to be valid except for MVinvPFM. Used MVinvPFM is only valid when control value is between N-1…N, in which N is maximum control value or maximum control value. In this implementation, MVinvPFM in lower control value was handmade and should not be used ever again. If controller implemented in this research is later used, MVinvPFM should be remade to be usable also in control values under N-1. Other option is to not remake this part of controller but limit the area of MVinvPFM to be over N-1. This can be achieved by setting control cycle duration to be equal or longer than sum of minimum pulse width and compensation of longer closing time ergo $t_{cc} \geq w_v + t_c$.

Water-glycol solution without additives seems to be usable hydraulic medium, when parts intended for water hydraulics are used. The solution allowed successful control of motion in wide area of medium temperatures. Only problem that was encountered was that color of solution changed to lightly yellow, which most likely indicated that bronze from the valve manifold dissolved to solution. This naturally underlines the biggest problem in additive free water-glycol solution, which is that material selection is even more restricted than is the case when used plain water. Although, one must consider that test system was not disassembled before writing of this thesis and therefore all knowledge of the system condition is not clear at this point.

10. REFERENCES

Basniev, K.S., Dmitriev, N.M. & Chilingar, G.V. (2012). Mechanics of Fluid Flow, Wiley, Somerset, 576 p.

Bower, J. (1961), Digital Fluid Control System, US Patent No. 2999482, 6 p.

Bustos, V. (1996). Seal Friction in A Hydraulic Cylinder, Tampere University of Technology, Tampere, 30 p.

C. Canudas de Wit, H. Olsson, K. J. Astrom & P. Lischinsky (1995). A New Model for Control of Systems with Friction, IEEE Transactions on Automatic Control, Vol. 40(3), pp. 419-425.

Conrad, F. (2005). Trends in Design Of Water Hydraulics-Motion Control And Open-Ended Solutions, Proceedings of the JFPS International Symposium on Fluid Power, Vol. 2005(6), pp. 420-431. Available (accessed TI:):

Curme, G.O. (1952). Glycols, Reinhold, New York, 398 p.

Digital Hydraulics (2016). in: Valmet Technical Paper Series, Valmet,

Engineering and Operating Guide, (2008). The DOW Chemical Company, 44 p.

Fischer, H., Laamanen, A., Iso-Heiko, A., Schäfer, O., Karvonen, M., Karhu, O., Huhtala, K., Pulkkinen, V. & Huttunen, A. (2015). Digital Hydraulics on Rails – Pilot Project of Improving Reliability on Railway Rolling Stock by Utilizing Digital Valve System, Proceedings of The Fourteenth Scandinavian International Conference on Fluid Power, SICFP15, pp. 644-654.

Fiume, M.M., Bergfeld, W.F., Belsito, D.V., Hill, R.A., Klaassen, C.D., Liebler, D., Marks, J.G., Shank, R.C., Slaga, T.J., Snyder, P.W. & Andersen, F.A. (2012). Safety Assessment of Propylene Glycol, Tripropylene Glycol, and PPGs as Used in Cosmetics, Int J Toxicol, Vol. 31(5), pp. 245-260.

Fonselius, J., Rinkinen, J. & Vilenius, M. (2006). Koneautomaatio. Hydrauliikka II, 3. p. ed. Tampereen yliopistopaino - Juvenes Print, Tampere, 226 p.

George, J. & Sastry, N.V. (2003). Densities, Dynamic Viscosities, Speeds of Sound, and Relative Permittivities for Water + Alkanediols (Propane-1,2- and -1,3-diol and Butane-1,2-, -1,3-, -1,4-, and -2,3-Diol) at Different Temperatures, Journal of Chemical & Engineering Data, Vol. 48(6), pp. 1529-1539.

Goode, W.J. (1998). Biodegradation of Propylene Glycol-Based MIL-A-8243D Aircraft Deicer, Colorado State University, Department of Chemical and Bioresource Engineering, 53 p.

Guide to Glycols, (2003). The DOW Chemical Company., 58 p.

Heitzig, S., Sgro, S. & Theissen, H. (2012). Energy Efficiency of Hydraulic Systems with Shared Digital Pumps, International Journal of Fluid Power, Vol. 13(3), pp. 49-57.

Huova, M. (2015). Energy Efficient Digital Hydraulic Valve Control, Tampere University of Technology, Tampere,

Huova, M., Laamanen, A. & Linjama, M. (2010). Energy Efficiency of Three-Chamber Cylinder with Digital Valve System, International Journal of Fluid Power, Vol. 11(3), pp. 15-22.

Huova, M. & Plöckinger, A. (2010). Improving Resolution of Digital Hydraulic Valve System by Utilizing Fast Switching Valves, Proceedings of the Third Workshop on Digital Fluid Power, October 13-14 2010, Tampere, Finland, pp. 79-92.

Hyvönen, M. (2015). IHA-2601 Hydraulikomponenttien mallintaminen ja simulointi , Tampere University of Technology, 149 p.

Koskinen, K.T. & Aaltonen, J. (2014). Water Hydraulics Pushes into High-Pressure Systems, Hydraulics & Pneumatics, Vol. 67(2), pp. 84-89.

Koskinen, K.T. (2004). Introduction to Water Hydraulics, Technical University of Tampere, Institute of Hydraulics and Automation,

Laamanen, A., Linjama, M. & Vilenius, M. (2005). Pressure Peak Phenomenon in Digital Hydraulic Systems - S Theoretical Study, Bath Workshop on Power Transmission and Motion Control (PTMC 2005), 7-9 September 2005, pp. 91-104.

Linjama, M. (1996). Aseman säätö hydraulisissa puomeissa, Tampere University of Technology, Tampere, 32 p.

Linjama, M. (2011). Digital Fluid Power - State of The Art, The Twelfth Scandinavian International Conference on Fluid Power, SICFP'11, May 18-20, 2011, Tampere, Finland, Scandinavian International Conference on Fluid Power, pp. 331-354.

Linjama, M. (1998). The Modeling and Actuator Space Control of Flexible Hydraulic Cranes, Finnish Academy of Technology, 110 p.

Linjama, M., Huova, M. & Karvonen, M. (2012). Modelling of Flow Characteristics of On/Off Valves, DFP 12, Proceedings of The Fifth Workshop on Digital Fluid Power, October 24-25, 2012, Tampere, Finland, Tampere University of Technology, Department of Intelligent Hydraulics and Automation, pp. 209-222.

Linjama, M. & Vilenius, M. (2005). Improved Digital Hydraulic Tracking Control of Water Hydraulic Cylinder Drive, International Journal of Fluid Power, Vol. 6(1), pp. 29-39.

Linjama, M., Huova, M., Boström, P., Laamanen, A., Siivonen, L., Morel, L., Walden, M. & Vilenius, M. (2007). Design and Implementation of Energy Saving Digital Hydraulic Control System, The Tenth Scandinavian International Conference on Fluid Power, May 21-23, 2007, Tampere, Finland, SICFP'07, Tampere University of Technology, pp. 341-359.

Linjama, M., Laamanen, A. & Vilenius, M. (2003). Is It Time for Digital Hydraulics? The Eight Scandinavian International Conference on Fluid Power, Proceedings of the Conference, Tampere, Finland, SICFP´03, Tampere University of Technology,

Linjama, M. & Vilenius, M. (2007). Digital Hydraulics - Towards Perfect Valve Technology, The Tenth Scandinavian International Conference on Fluid Power, May 21-23, 2007, Tampere, Finland, SICFP'07, Tampere University of Technology, pp. 181-196.

Paloniitty, M. (2016). Water Hydraulic Control Valves, Tampere University of Technology, 15 p.

Paloniitty, M. & Linjama, M. (2018). High-linear digital hydraulic valve control by an equal coded valve system and novel switching schemes, Proceedings of the Institution of Mechanical Engineers, Part I: Journal of Systems and Control Engineering, Vol. 232(3), pp. 258-269.

Paloniitty, M., Linjama, M. & Huhtala, K. (2014). Concept of Digital Microhydraulic Valve System Utilising Lamination Technology, Conference Proceedings, 9th International Fluid Power Conference, 24th - 26th March, 2014, Aachen, Germany, Modern Fluid Power - Challenges, Responsibilities, Markets, Vol. 1, Hp - Fördervereinigung Fluidtechnik E.v, pp. 303-313.

Paloniitty, M., Linjama, M. & Huhtala, K. (2015). Equal Coded Digital Hydraulic Valve System – Improving Tracking Control with Pulse Frequency Modulation, Procedia Engineering, Vol. 106 pp. 83-91.

Pan, M. & Plummer, A. (2018). Digital switched hydraulics, Frontiers of Mechanical Engineering, Vol. 13(2), pp. 225-231.

Pollard, F.H. (1963). Reasearch Investigation of Hydraulic Pulsation Concepts , Farmingdale, New York, 38 p.

Rampen, W. (1992). The Digital Displacement Pump, The University of Edinburgh, 180 p.

Scheidl, R., Kogler, H. & Winkler, B. (2013). Hydraulic Switching Control - Objectives, Concepts, Challenges and Potential Applications, Hidraulica, (1), pp. 7-18.

Scheidl, R., Manhartsgruber, B., Mikota, G. & Winkler, B. (2005). State of The Art in Hydraulic Switching Control – Components, Systems, Applications, The Ninth Scandinavian International Conference on Fluid Power, SICFP'05, June 1-3, 2005, Linköping, Sweden,

Schepers, I., Schmitz, D., Weiler, D., Cochoy, O. & Neumann, U. (2011). A Novel Model for Optimized Development and Application of Switching Valves in Closed Loop Control, International Journal of Fluid Power, Vol. 12(3), pp. 31-40.

Schepers, I., Weber, J. & Weiler, D. (2012). Comparison and evaluation of digital control methods for on/off valves
, DFP 12, Proceedings of The Fifth Workshop on Digital Fluid Power, October 24-25, 2012, Tampere, Finland, pp. 19.

Shell Tellus S3 M 32 - Tuotetiedot, Royal Dutch Shell plc, 3 p. Available: https://hyvamaa.fi/application/files/1414/3030/8673/GPCDOC_Local_TDS_Finland_Shell_Tellus_S3_M_32_en_TDS_v1.pdf. (Read: 25.9.2018)

Siivonen, L., Linjama, M. & Vilenius, M. (2005). The Effect of Fluid Viscosity on Performance of Proportional Directional Valve and Digital Flow Control Unit, The Ninth Scandinavian International Conference on Fluid Power, SICFP'05, Linköping Sweden, pp. 13.

Skoog, P. (2016). Maintaining Water Glycol Fluids: Follow the Formula for Success, Plant Engineering, Vol. 70(5), pp. 30-32.

Toscano, G., Cavalca, L., Letizia Colarieti, M., Scelza, R., Scotti, R., Rao, M.A., Andreoni, V., Ciccazzo, S. & Greco, G. (2013). Aerobic Biodegradation of propylene Glycol by Soil Bacteria, Biodegradation, Vol. 24(5), pp. 603-613.

Toscano, G., Colarieti, M.L., Anton, A., Greco, G. & Biró, B. (2014). Natural and Enhanced Biodegradation of Propylene Glycol in Airport Soil, Environmental Science and Pollution Research, Vol. 21(15), pp. 9028-9035.

Totten, G.E. (2012). Handbook of Hydraulic Fluid Technology, 2nd Edition ed. CRC Press, Boca Raton, 982 p.

Trostmann, E. (1996). Water Hydraulics Control Technology, Dekker, New York, 180 p.

Veltman, S., Schoenberg, T. & Switzenbaum, M.S. (1998). Alcohol and Acid Formation During the Anaerobic Decomposition of Propylene Glycol Under Methanogenic Conditions, Biodegradation, Vol. 9(2), pp. 113-118.

APPENDIX A: M-CODES OF FUNCTIONS USED IN CONTROLLER

```
function [u, viceVersa_flag] = fcn(time,t_i, n_s, t_c, t_sample)

    ti = t_i-t_sample/2; %Time for pulse without compensation
    ns = n_s; %High value of open valves
    tc = t_c; %Compensation for differing opening and closing times for valves
    u1 = 0; %Number of valves open of a DFCU (output)
    viceVersa_flag = 0; %Flag to open a valve and close another at the same
time
    t_compensated = ti-tc; %Compensated time that used to determine pulse time.
If negative then negative pulse, if positive then positive pulse compared to
u_floor value.

    if t_compensated < 0

        t_compensatedNeg = t_compensated + t_sample; % Adding value to fix
issues with negative pulse time and positive control time to create pulse with
right width. Whitout this the pulse is too wide

        if t_compensatedNeg >= 0 && time == 0 %Desired u_dec comes with simul-
taneous opening and closing
            viceVersa_flag = 1;
            u1 = n_s-1;
        else
            if abs(t_compensatedNeg) > time %Time for negative pulse
                u1 = ns-2;
            else %Time for negative pulse is over
                u1 = ns-1;
            end

        end
    elseif t_compensated >= 0

        if t_compensated > time %Time for positive pulse
                u1 = ns;
            else %Time for positive pulse is over
                u1 = ns-1;
        end
    end

u = u1;
```

Program 1. *MWPWM control function or PWM1 function.*

```
function [u,viceVersa] = fcn(u_initial, start_pulse, end_pulse1, end_pulse2)

    u_temp = 0;
    viceVersaTemp = 0;

    %Checks what event has happened and changes signal value accordingly or
    %calls for simultaneous switching. If no event is occurring then keeps
    %control signal immutable.
    if start_pulse == true && end_pulse1 == false && end_pulse2 == false
        u_temp = u_initial-1;
        viceVersaTemp = 0;
    elseif start_pulse == false && (end_pulse1 == true || end_pulse2 == true)
```

```
        u_temp = u_initial+1;
        viceVersaTemp = 0;
    elseif start_pulse == true && (end_pulse1 == true || end_pulse2 == true)
        u_temp = u_initial;
        viceVersaTemp = 1;
    elseif start_pulse == false && end_pulse1 == false && end_pulse2 == false
        u_temp = u_initial;
        viceVersaTemp = 0;
    end

    %Prevent control signal from going over limits.
    if u_temp > 5
        u_temp = 5;
    elseif u_temp < 3
        u_temp= 3;
    end

viceVersa = viceVersaTemp;
u = u_temp;
```

Program 2. *MVinvPFM control function or inverse PFM function.*